Localization of Secretases Involved in the Processing of β-Amyloid Precursor Protein related to Alzheimer's Disease

Anna V. Pliássova

2013

DEPARTAMENTO DE CIÊNCIAS DA VIDA

FACULDADE DE CIÊNCIAS E TECNOLOGIA
UNIVERSIDADE DE COIMBRA

Localization of Secretases Involved in the Processing of β-Amyloid Precursor Protein related to Alzheimer's Disease

Anna Vladímirovna Pliássova

2013

DEPARTAMENTO DE CIÊNCIAS DA VIDA

FACULDADE DE CIÊNCIAS E TECNOLOGIA
UNIVERSIDADE DE COIMBRA

Localization of Secretases Involved in the Processing of β-Amyloid Precursor Protein related to Alzheimer's Disease

Dissertação apresentada à Universidade de Coimbra para cumprimento dos requisitos necessários à obtenção do grau de Mestre em Bioquímica, realizada sob a orientação científica da Professora Doutora Paula Agostinho (Universidade de Coimbra) e do Professor Doutor Ângelo Tomé (Universidade de Coimbra

Anna Vladímirovna Pliássova

2013

Este trabalho foi realizado no Centro de Neurociências e Biologia Celular, em Coimbra, no Grupo "Neuromodulation" ("Purines at CNC")

Agradecimentos

À Doutora Paula Agostinho, orientadora científica, pela orientação, disponibilidade, paciência e compreensão, desde que me aceitou como aluna de mestrado.

Ao Doutor Ângelo Tomé, co-orientador, pela ajuda e por me ter primeiramente indicado este grupo de investigação.

Ao Doutor Rodrigo Cunha, líder do grupo "Purines at CNC", pela oportunidade concedida de me inserir no seu grupo e por sempre me ter incentivado.

A todos os colegas do grupo, sem excepção, pelas amizades criadas e pela plena disponibilidade e vontade de ajudar.

À Doutora Paula Canas, por toda a ajuda.

Ao Rui, ao Gonçalo e ao Tiago por todos os momentos partilhados ao longo deste ano. Ao Tiago também pelo contributo essencial para o trabalho.

Aos meus Pais e Irmã, pelo apoio incondicional, reconhecimento e afecto.

A todos os bons amigos, que por serem muitos, não referirei todos, mas, em especial, à Teresinha, à Ana e à Cláudia.

A todos os que, ao longo do meu percurso académico, contribuíram para a minha formação.

Table of Contents

LIST OF ABBREVIATIONS

Aβ - β-amyloid peptide

AD-Alzheimer´disease

AP - Alkaline phosphatase

APLP1 - Amyloid precursor-like protein 1

APLP2 - Amyloid precursor-like protein 2

APP - Amyloid precursor protein

APS - Ammonium persulphate

BCA - Bicinchoninic acid

BSA - Bovine serum albumin

CLAP - Cocktail of proteases inhibitors

DTT - Dithiothreitol

ER - Endoplasmic reticulum

ECF - Enhanced chemifluorescence

EDTA - Ethylenediaminetetraacetic acid

GABA - γ-Aminobutyric acid

HBM - HEPES buffered medium

HEPES - 4-(2-hydroxyethyl)-1-piperazineethanesulfonic acid

IB - Isolation buffer

NHS - Normal horse serum

PFA - Paraformaldehyde

PBS - Phosphate buffer saline

PSD-95 -postsynaptic density protein 95

PVDF - Polyvinilidene fluoride

RT - Room temperature

SDS - Sodium dodecyl sulfate

SDS-PAGE - Sodium dodecyl sulfate-polyacrylamide gel electrophoresis

SEM - Standard error of the mean

SNAP-25 - Synaptosome-associated protein of 25000 daltons

Syn - Synaptophysin

TGN - Trans-Golgi-network

TEMED - Tris(hydroxymethyl)aminomethane

TBS - Trizma buffered saline

TBS-T - Trizma buffered saline with tween

vGAT - Vesicular GABA transporter

vGLUT1 - Vesicular glutamate transporter 1

vGLUT2 – Vesicular glutamate transporter 2

RESUMO

As fases iniciais da doença de Alzheimer são caracterizadas por alterações na eficiência sináptica, que se pensa serem causadas por oligómeros solúveis dos peptídeos β-amilóide (Aβ). Estes peptídeos são formados a partir da clivagem proteolítica da proteína precursora β-amilóide (APP), através da ação de secretases (α- e β-). Apesar de se saber que a formação de Aβ a nível sináptico é provavelmente crucial para o dano inicialmente verificado na doença de Alzheimer, a distribuição da APP e das secretases (α- β- e γ-) envolvidas no seu processamento proteolítico, em diferentes terminais nervosos, permanece desconhecida. Não se sabe ainda por que razão apenas alguns tipos específicos de sinapses sofrem degeneração nas fases iniciais da doença. É ainda mais surpreendente o facto de não ser conhecida a distribuição a nível sináptico e sub-sináptico da APP e das secretases, em diferentes tipos de terminais nervosos, em diversas regiões cerebrais, bem como o facto de se desconhecer se esta distribuição sofre alterações em modelos animais da patologia de Alzheimer.

Os principais objetivos deste trabalho eram: i) investigar a distribuição sináptica e sub-sináptica (zonas pré-, pós- e extra-sinápticas) da APP e das secretases (α- β- e γ-), com particular foco no hipocampo, ii) definir a presença de APP e das secretases, bem como a sua co-localização em diferentes tipos de terminais nervosos, principalmente glutamatérgicos e GABAérgicos e iii) investigar se a idade e condições de doença de Alzheimer afectam a distribuição da APP e das secretases em terminais nervosos. A distribuição sináptica e a densidade da APP, da BACE1 (β-secretase), da ADAM-10 (α-secretase) e da presenilina -1 (PS1, um componente da γ-secretase) foram avaliadas por Western blot e imunocitoquímica, em preparações sinápticas de hipocampo (sinaptossomas e terminais nervosos purificados), que foram obtidas a partir de murganhos machos adultos C57/Bl6, com 2-3 meses de idade, a partir de murganhos do mesmo tipo, com 9 meses de idade, e também a partir de murganhos triplos transgénicos modelos da doença de Alzheimer. Recorrendo a um protocolo de fracionamento sináptico, que permite a separação das fracções pré-, pós- e extra-sinápticas, avaliámos ainda a distribuição sub-sináptica relativa da APP e das secretases.

Além disso, fizemos também um estudo preliminar para determinar os níveis de APP em amostras de cérebro humano de indivíduos com diferentes idades.

No hipocampo de murganhos jovens adultos (2-3 meses), através da comparação das imunoreactividades da APP e das secretases em sinaptossomas (terminais nervosos) e membranas totais, verificámos que a APP, a α- e a β-secretases se encontram presentes em terminais nervosos, apesar de não estarem enriquecidas nos sinaptossomas. Também observámos que a APP está localizada preferencialmente a nível pré-sináptico, a α-secretase (ADAM10) se encontra distribuída pré- e extra-sinapticamente, ao passo que a β-secretase (BACE1) se encontra principalmente na fração extra-sináptica. Através de análise imunocitoquímica, em terminais pré-sinápticos do hipocampo, purificados e plaqueados, verificamos que a APP é mais abundante do que as secretases (ADAM10, BACE1 e presenilina1, PS1), que a APP e a BACE1 estão parcialmente co-localizadas em cerca de 40% e ainda que esta secretase se encontra mais presente nos terminais glutamatérgicos do que nos GABAérgicos. Inesperadamente, não observamos diferenças significativas na densidade da APP e das α- e β-secretases, nos sinaptossomas de hipocampo de murganhos adultos (9 meses de idade), em comparação com murganhos jovens adultos (2-3 meses de idade). Por outro lado, em amostras de cérebro humano verificámos uma clara diminuição da densidade da APP com o aumento da idade (resultados preliminares). Em murganhos triplos transgénicos modelos da doença Alzheimer, observámos uma clara diminuição da imunoreactividade da ADAM10, bem como um aumento da PS1, por análise de imunocitoquímica.

Os resultados apresentados neste estudo representam a primeira análise comparativa das distribuições sináptica e sub-sináptica da APP e das secretases, em regiões corticais (principalmente do hipocampo) do cérebro de murganhos, bem como da avaliação da abundância relativa da APP e das secretases e da sua co-localização, em diferentes terminais nervosos de hipocampo. Foi também avaliada a existência de alterações relacionadas com a idade e com a doença de Alzheimer no que diz respeito à densidade da APP e das secretases. Este projeto constitui o primeiro passo para a compreensão da particular susceptibilidade para a disfunção e degeneração de sinapses glutamatérgicas e GABAérgicas, em etapas iniciais da doença de Alzheimer, e pode vir a ser útil para o desenvolvimento de novas estratégias terapêuticas.

Palavras-chave: Sinapses, Doença de Alzheimer, BACE1, ADAM10, Presenilina 1

ABSTRACT

The early stages of Alzheimer´s disease (AD) are associated with alterations in synaptic efficiency, which are thought to be caused by oligomeric assemblies of soluble β-amyloid peptides (Aβ). Aβ are derived from the proteolytic cleavage of the amyloid precursor protein (APP) through the action of secretases Although it is widely accepted that synaptic Aβ formation is likely crucial for AD initial damage, the distribution of APP and secretases which mediate APP proteolytic processing (α- and β-) in different nerve terminals remains to be clarified. It is still not known why only some particular synapses begin degenerating in early AD. In fact, it is surprising to note that the synaptic and subsynaptic distribution of APP and secretases across different types of nerve terminals in different brain regions is unknown, nor is it known if their distribution changes in animal models of AD.

The main goals of this study were: to i) to investigate the synaptic and subsynaptic (pre-, post- and extra-synaptic zones) distribution of APP and secretases (α- β- and γ-) with a particular focus on the hippocampus, ii) to define the presence of APP and secretases and their co-localization in different types of nerve terminals, mainly glutamatergic and GABAergic terminals and iii) to investigate whether the age and AD condition affect the distribution of APP and secretases in nerve terminals. The synaptic distribution and density of APP, BACE1 (β-secretase), ADAM-10 (α-secretase) and presenilin -1 (PS1, a component of γ-secretase) were assessed through Western blot and immunocytochemical analyses in hippocampal synaptic preparations (synaptosomes and purified presynaptic terminals) obtained from adult male C57/Bl6 mice with 2-3 months old or 9 months old, and in a triple transgenic mice model of AD (3xTg-AD). Using a procedure of synaptic fractioning, which allows the separation of pre-, post- and non-synaptic (extrasynaptic) fractions we have also evaluated the relative subsynaptic distribution of APP and secretases. Moreover, we also perform a preliminary study to determine the levels of APP in cortical human samples from individuals with different ages.

In hippocampus of young adult mice (2-3 months), by comparing the immunoreactivities of APP and secretases in synaptosomes (nerve terminals) and total membranes, it was found that APP, α- and β-secretases are present in nerve terminals,

albeit they were not enriched in synaptosomes. It was also observed that APP was mainly located presynaptically, the α-secretase (ADAM10) was distributed pre- and extrasynaptically, whereas β-secretase (BACE1) was preferentially located in the extrasynaptic fraction. Through immunocytochemistry analysis, in platted purified hippocampal presynaptic nerve terminals, we observed that APP was more abundant than secretases (ADAM10, BACE1 and Presenilin1) in nerve terminals and also that APP and BACE 1 are partially co-localized by about 40%, and this secretase is present in higher levels in glutamatergic than in GABAergic terminals. Unexpectedly, no significant differences were observed in the density of APP and α- and β-secretases in hippocampal synaptosomes of adult mice (9 months old as compared to young adult mice (2 months old), whereas in cortical human brain it seems to occur a reduction of APP density with the advance of age (preliminary data). In triple transgenic AD model mice, we observed a clear decrease in ADAM 10 immunoreactivity, as well as an increase of PS1 in immunocytochemical analysis.

The results present in this study provide the first comparative analysis of synaptic and subsynaptic distribution of APP and secretases in cortical brain regions of mice mainly in hippocampus; and the assessment of the relative abundance of APP and secretases and their co-localization in different hippocampal nerve terminals. Age- and AD pathology-related changes in APP and secretases were also investigated. This provides a first step to understand the particular susceptibility to dysfunction and degeneration of glutamatergic and GABAergic synapses in early AD, and might be useful to the development of novel therapeutic strategies.

Keywords: Synapses, Alzheimer's Disease, BACE1, ADAM10, Presenilin

1. INTRODUCTION

1.1. Alzheimer's Disease: a loss of synaptic function

Alzheimer's disease (AD) is the most common of all dementia disorders in the elderly people and is characterized by a progressive decline in cognitive functions, involving mainly memory deterioration (Belousov et al., 2009). Nowadays, more than 35 million people live with dementia and this number is estimated to double in the next 20 years. Large amounts of resources and money are spent in caring for this type of patients and, therefore, new therapeutics and treatment are urgently needed (Wimo et al., 2013).

AD may be categorized into two types. The inherited form (familial AD) is the rarest one and is due to autosomal genetic mutations that exist in the genes encoding the Amyloid-β Precursor Protein (APP) and presenilins 1 and 2 (PS1 and PS2) (Götz et al., 2011). The causes of the sporadic AD form are not completely clear, but several risk factors have been identified, such as aging and specific cardiovascular diseases (Götz et al., 2011). However, histopathologically both AD familial and sporadic forms are identical, as they are characterized by brain atrophy and by the presence of amyloid plaques. Those plaques are extracellular deposits that are composed mainly by amyloid-β (Aβ) peptides, which are formed by 38 to 43 amino acid residues. The Aβ peptides are formed via the sequential proteolytic cleavage of APP, and accumulate in particular brain regions, like the hippocampus, which is particularly important in the formation and/or retrieval of some forms of memory, and the cortex (Zhang et al., 2011).

Although AD brains display cortical atrophy, the general loss of brain volume appears to be a consequence of shrinkage and damage of neuronal processes (synapses and dendrites), which are particularly vulnerable to Aβ peptides (Huang and Mucke, 2012). Indeed, the hippocampal synaptic loss is an AD early event and the major structural correlates of cognitive dysfunction. Several studies suggest that lower levels of synaptic proteins are directly related to AD cognitive impairment and its severity (Arendt, 2009).

For the last twenty years, the idea that AD development depends on Aβ peptide formation and its deposition has dominated and it is usually called the "Amyloid cascade hypothesis" (Hardy and Higgins, 1992). According to this theory, the main event in the pathogenesis of AD is the formation of $A\beta_{40-42}$, through the processing of the Amyloid Precursor Protein (APP). This form of Aβ is highly neurotoxic and is

considered to be the primary causative agent of neuropathological changes occurring in AD brains including: i) the early disruption of synaptic function, ii) Aβ aggregation and the subsequent formation of amyloid plaques, iii) tau protein hyperphosphorylation and neurofibrillary tangles (NFT) formation, and iv) neuronal death. However, in the last years, this hypothesis has been reappraised. First of all, the principal toxic agent is now considered to be the oligomeric forms of Aβ. Furthermore, several therapeutic approaches, based solely on this hypothesis, have not reached clinical trials (Nalivaeva and Turner, 2013).

Brain dysfunction in this pathology seems to occur in a staged biological sequence: neuronal injury, synaptic failure and neuronal death (Coleman et al., 2004). Therefore, prior to neuronal loss, the early phases of AD are associated to alterations in synaptic efficiency. Since defects in synaptic transmission occur before the formation of amyloid plaques, the neuroplasticity alterations are thought to be caused by oligomeric assemblies of soluble Aβ peptides (Cleary et al. 2005). The oligomers of Aβ peptides are thus considered to be the toxic agent, as they are directly involved in synaptic damage and subsequent neurodegeneration (Cleary et al. 2005, Arendt, 2009). Several evidence suggest that Aβ oligomers have a more potent effect in disrupting synaptic function than Aβ fibrils and amyloid deposits. In fact, *in vitro* and *in vivo* studies have shown that elevated levels of Aβ oligomers affect the glutamatergic synaptic transmission and cause synaptic loss, which is one of the pathological hallmarks of AD that directly correlates with cognitive decline (Palop and Mucke, 2010).

The accumulation of Aβ peptides in the brain is a consequence of an altered balance between its synthesis, clearance and aggregation rate. Although in normal conditions the human brain produces considerable amounts of Aβ peptides, those quantities are much higher in AD patients, and they are approximately equivalent to 7 years of total Aβ production in healthy individuals (Karran et al., 2011). It has been recently hypothesized that the pathogenic mutations that occur in genes encoding APP affect its dimerization at the membrane, changing its conformation and/or its stability. This may be a probable reason for an alternative proteolysis by γ-secretase and the enhancement of the production of $A\beta_{1-42}$ rather than $A\beta_{1-40}$ (Nadezhdin et al., 2011).

1.2. APP

The APP, which gives rise to Aβ peptides, belongs to a protein family that includes also amyloid precursor-like proteins, such as APLP1 and APLP2 in mammals. All the elements of the family are type 1 transmembrane proteins, resemble cell-surface receptors, have large extracellular domains (that constitute ~88% of the total protein mass) and short cytoplasmic regions, and are processed in similar ways (O'Brien and Wong, 2011). In addition to that, they share some regions, conserved among the family members, but the Aβ domain is unique to the APP (Zhang et al., 2011). One of the most conserved regions among the family to which APP belongs is located at the N-terminal, immediately after the signal sequence (Gralle and Ferreira, 2007).

APP has been widely studied, but its exact functions are still unclear. The protein members of the APP family seem to be involved in a diversity of cellular processes, related to the development of the nervous system. Quite a few roles have been proposed and, among others, it is thought that APP participates in synaptogenesis, spine formation, synaptic vesicle release, axonal transport, cell adhesion, transmembrane signal transduction. Like APP, also the other family members protein APLP1 and APLP2 play an important role in synaptogenesis, during some important periods of brain development (Octave et al., 2013). Besides the crucial role of APP in synaptic formation and intracellular signalling, it also regulates intracellular calcium homeostasis, which is crucial for synaptic transmission; thus APP is currently considered to have a key modulator of synaptic plasticity and neuronal viability (Kedikian et al., 2010; Zhang et al., 2011; Octave et al., 2013). For these reasons, it is thought that the loss of APP function might contribute to disturbed neuronal communication and consequently to memory impairment.

Moreover, a lot of similarities between APP and the Notch receptor have been reported, suggesting that APP may function as a cell surface receptor (Zhang et al., 2011). Some studies also revealed that Aβ can bind to APP and thus act as a potential ligand. Besides the Aβ peptide, other compounds have been found to interact with APP, such as F-spondin, a neuronal secreted glycoprotein, as well as Nogo-66 receptor, whose binding regulates Aβ production and downstream signaling (Zheng and Koo, 2011).

1.3. APP production and proteolytic processing

APP production is particularly elevated in neurons and, in humans, APP is encoded by a gene located on chromosome 21 that was identified for the first time in 1987 (for review see Thinakaran and Koo, 2008).

Several important steps in APP formation occur at the cell surface and in the *trans*-Golgi Network (TGN). It is processed in the constitutive secretory pathway and, like other proteins; this peptide is produced in the endoplasmatic reticulum (ER) and then transported through the TGN to the plasmatic membrane. After reaching the cell membrane, APP seems to be re-internalized and trafficked by endocytic and recycling compartments or processed in lysosomes (O'Brien and Wong, 2011) (Figure 1).

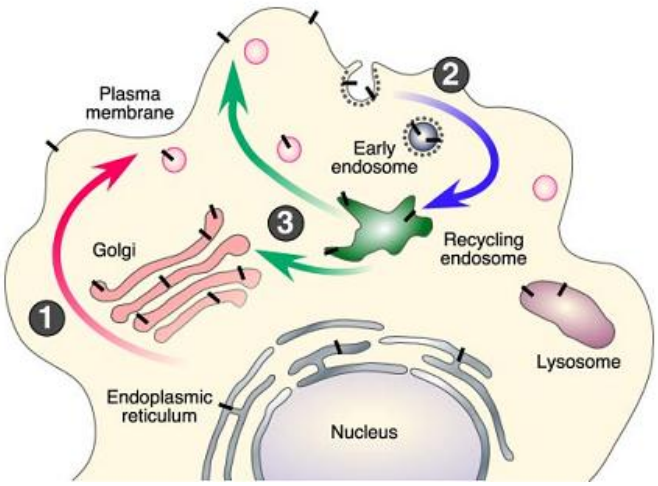

Figure 1. Intracellular trafficking of APP. The APP nascent molecules are represented by black bars. They mature through the constitutive secretory pathway (step 1). Once APP reaches the cell surface, it is re-internalized (step 2) and trafficked through endocytic and recycling compartments back to the cell surface (step 3) or degraded in the lysosome (adapted from Thinakaran and Koo, 2008)

APP has at least three isoforms that result from alternative splicing of its pre-mRNA, APP_{695}, APP_{751} and APP_{770}. The APP_{695} is the most abundant in the brain, in normal conditions, and is the most commonly expressed by neurons. However, in AD brains the amount of APP_{695} mRNA is reduced, while the mRNA of APP_{770} is augmented (Davis and Laroche, 2003). The two longer APP isoforms (APP_{751} and APP_{770}) are mostly present in glial cells, such as astrocytes (Revett et al., 2013).

APP can suffer proteolysis via two major pathways. One of those pathways leads to Aβ formation, while the other originates different products. It can be proteolyzed directly by α-secretase and then by γ-secretase. Due to the fact that the α-secretase's cleavage point is located within the Aβ sequence, the process does not lead to Aβ production and so it is called the non-amyloidogenic pathway. This processing occurs mainly at the cell surface (Chow et al., 2010; O'Brien and Wong, 2011;).

On the other hand, the amyloidogenic pathway leads to Aβ production. This peptide is generated from endoproteolysis of APP, performed by β- and γ-secretases (Mangialasche et al., 2010). β-secretase cleaves the APP in a specific site located in the extracellular domain (N-terminal), whereas γ-secretase's cleavage point is in the transmembrane region (C-terminal) (Tabaton and Tamagno, 2007; Thinakaran and Koo, 2008). The resulting peptides vary in length: $A\beta_{40}$ is the most common form, but $A\beta_{42}$ is more prone to aggregate and, thus, it is present in large quantities in amyloid plaques (Mangialasche et al., 2010). This processing occurs in endosomal compartments that contain the required proteases (secretases) and is a consequence of the re-internalization of APP (O'Brien and Wong, 2011). It is interesting to point out that Aβ peptides are formed only by the cleavage of APP and not by the cleavage of other APP protein family members (Priller et al., 2006).

Both the non-amyloidogenic and the amyloidogenic pathways are crucial to guarantee normal brain function. If the homeostasis between them is disrupted, the non –amyloidogenic APP processing is affected and quite a few metabolic routes become compromised. Example of this is the switch to the amyloidogenic pathway in AD, leading to overproduction of Aβ (Epis et al., 2012).

The understanding of the mechanisms involved in APP trafficking and proteolytic processing are, therefore, essential to delineate the pathogenesis of AD (Tan and Evin, 2011).

1.4. Secretases involved in the proteolytic processing of APP

1.4.1. α-secretase

The cleavage of APP by the α-secretase occurs within the Aβ sequence, preventing the Aβ peptide formation. The enzyme's action results in the production of a soluble ectodomain, called sAPPα, and of a membrane-bound 83-amino acid C-terminal fragment (C83), also known as α-Carboxyl-terminal fragments (α-CTF) (Tan and Evin, 2011). The sAPPα acts as a proliferative factor, has a protective role against excitotoxic and ischemic injuries and is essential to neuroplasticity (Zhang et al., 2011).

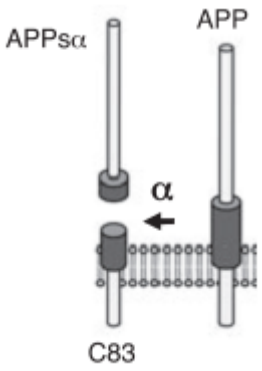

Figure 2. The α-secretase-mediated cleavage of APP, which leads to the release of sAPPα and of a C-terminal fragment (C83) (adapted from Lichtenthaler, 2011)

It is known that quite a few elements of the ADAM (a disintegrin and metalloproteinase) family exhibit α-secretase-like activity. In fact, ADAM9, ADAM10 and ADAM17, which are type I transmembrane proteins, have been suggested to act as α-secretases. Among these proteases, ADAM10 is considered a key protease in the processing of APP and it is also thought to be necessary for the secretion of enough sAPPα *in vivo.* On the other hand, several studies have confirmed that ADAM17, also named TACE (*tumor necrosis factor-α-converting enzyme*) likely affects regulated, but not constitutive, APP α-cleavage (Zhang et al., 2011).

ADAM10 belongs to the zinc proteinase family and its typical structure consists of a prodomain, a catalytical domain with a zinc binding sequence, a disintegrin-like domain

rich in cysteines, a transmembrane domain and a short cytoplasmic domain (Figure 3) (Endres and Fahrenholz, 2010).

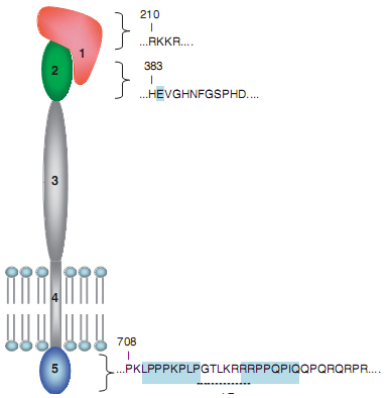

Figure 3. Multidomain structure of ADAM10. This enzyme is composed of 5 different domains: 1-prodomain, 2-zinc-binding motif, 3-cystein-rich disintegrin domain, 4-transmembrane region and 5-short cytoplasmic domain (adapted from Endres and Fahrenholz, 2010)

The ADAM family is formed by proteins, which have both features from cell adhesion molecules and proteases. Among different important roles, they are involved in fertilization, neurogenesis, angiogenesis and also in the proteolysis of some substrates, such as the Notch receptor and APP (Reiss et al., 2005).

ADAM10, which is considered to be the major α-secretase, is found mainly in the Golgi, where it is supposed to be inactive, as a pro-enzyme. After the cleavage of the signal peptide, ADAM10 enters the secretory pathway and suffers N-glycosilation, thus becoming an active protease. This activated form is mainly localized at the plasma membrane, therefore supporting the idea that the α-secretase mediated APP cleavage occurs at the cell surface. On the other hand, ADAM10 is also found in the TGN, so APP may also be proteolyzed there (Epis et al., 2012).

1.4.2. β-secretase

The Aβ peptide formation is initiated by β-site APP-cleaving enzyme 1 (BACE1) also known as aspartyl protease 2 (Asp2), which was identified as the major β-secretase. This enzyme cleaves the APP to the formation of a large soluble APP N-terminal portion (sAPPβ) and of a 99-amino acid C-terminal fragment (C99, also known as β-CTF), that contains the Aβ peptide and does not dissociate from the membrane. The C99 fragment is further processed by γ-secretase to release Aβ peptides (Figure 4). While Aβ is neurotoxic, sAPPβ is thought to be neuroprotective (Evin et al., 2010; Zhang et al., 2011).

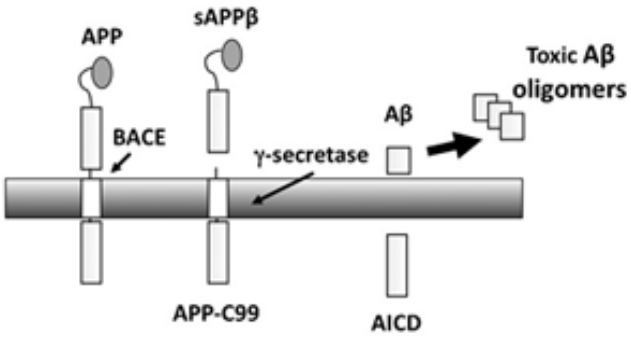

Figure 4. The amyloidogenic processing of APP by BACE1. The cleavage by BACE1 leads to the release of sAPPβ and of a C-terminal fragment (C99). C99 is then processed by γ-secretase to release Aβ and the APP intracellular domain (AICD). Aβ peptides aggregate to form toxic oligomers that trigger neurodegeneration. Aβ further self-associates to form fibrils and amyloid deposits (adapted from Evin et al. 2010)

BACE1 was identified more than 10 years ago as a membrane-anchored aspartyl protease and it is expressed mainly in the brain and pancreas (R. Vassar, 1999). The highest levels of BACE1 mRNA are found in the brain cortex region. Under normal conditions, the BACE1 expression is almost exclusive to neurons, but there also has been observed an increase of its distribution in astrocytes with age and following stress, trauma, hypoxia or ischemia in transgenic mice. Also, during inflammation, glial cells may produce significant amounts of this enzyme. On the other hand, in the brain of AD patients, the levels of BACE1 are quite elevated in 50% of the cases and could, therefore, provide an early biomarker of this disease (Tan and Evin, 2011; Epis et al., 2012).

BACE1 is a type I membrane protease and has two active site motifs, both necessary to its correct function. The enzyme has a luminal active site, which provides a correct topological orientation for APP cleavage, while near the C-terminus there is a single transmembrane domain (Cole and Vassar, 2008). Several studies suggest that BACE1 has maximal activity at acidic pH and, thus, it is more active in the acidic subcellular compartments of the secretory pathway, such as in the TGN and endosomes (Vassar, 2004). The β-secretase activity is primarily neuronal, thus it is logical to postulate that BACE1 can be upregulated by synaptic activity (Kamenetz et al., 2003). In normal conditions, BACE1 has important physiological functions in synaptic transmission and plasticity and it is found in CA1 and CA3 regions of the hippocampus. It also seems to play an unspecific role in the regulation of presynaptic activity (Wang et al., 2012). BACE1, like any of the other secretases involved in APP processing, is not APP-specific, as it also cleaves some substrates that include neuregulin and the β2 subunit of voltage-gated sodium channels, which are both essential elements for the normal brain development (Epis et al. 2012). Moreover, this protein, which is transported throughout the axons, seems to have an essential role in axonal outgrowth and brain development, and it was reported that the elevated expression of this enzyme in axons, mainly at birth, may be related to the myelinization onset by Schwann cells (Epis et al., 2012)

In addition to BACE1, there is a BACE2 homolog capable of cleaving the APP; however, it does not seem to be involved in Aβ production, as the enzyme cleaves near the same site as α-secretase (Zheng and Koo, 2011). Besides, the levels of BACE2 in the brain are approximately 10-fold lower when compared to BACE1 expression (Stockley and O'Neill, 2007).

Since BACE1 expression is increased in the brain cortex of most patients with sporadic AD, the control of this enzyme's activity, without affecting its interaction with other substrates, may constitute a potential therapeutic strategy (Evin et al., 2010).

1.4.3. γ-secretase

After α- or β-cleavage, the APP carboxyl terminal fragments are cleaved by γ-secretase, leading to the production of p3 (a 3 kDa product) or Aβ, respectively. The p3 does not appear to play any important role and is degraded, while the cleavage of Aβ, mediated by β and γ-secretase, can lead to the production of two peptides that vary in length: $A\beta_{40}$, which is the most abundant form, and $A\beta_{42}$, which is largely present in amyloid deposits.

Although it is usually considered that APP cleavage by α-secretase leads to the inhibition of Aβ protein formation, it is interesting to point out that it has been observed p3 deposition in the brain of AD patients, so it is possible to conclude that shorter Aβ peptides may contribute to some aspects of AD-associated pathology, as well (Gralle and Ferreira, 2007; Zheng and Koo, 2011).

Figure 5 is a schematic representation of the two possible pathways for APP cleavage.

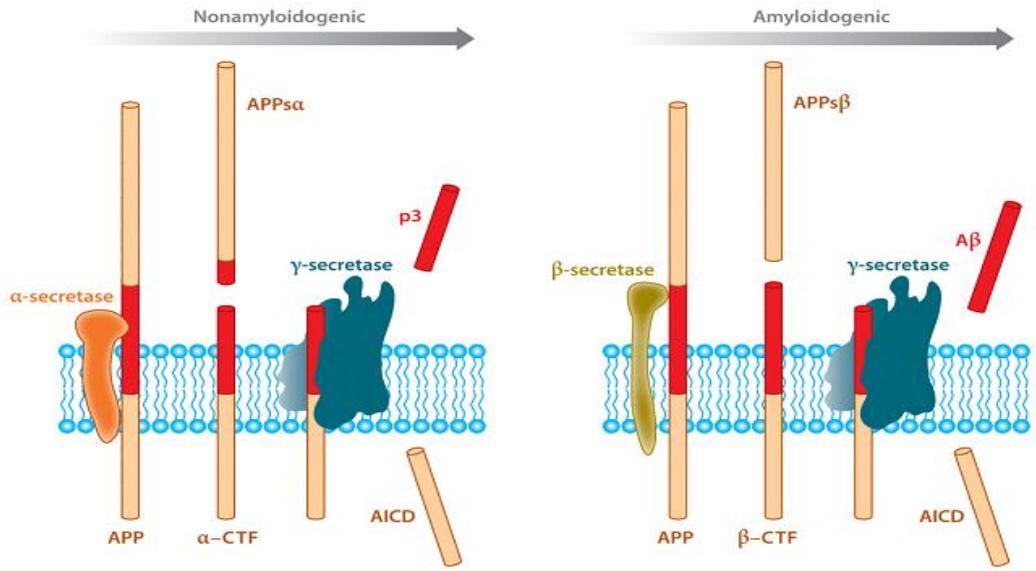

Figure 5. APP processing through two different pathways. On the left image, the Non-amyloidogenic processing of APP is shown, involving the cleavage by α-secretase, followed by γ-secretase. On the right image, is shown the Amyloidogenic processing of APP, involving β- and γ-secretase cleavages. In both pathways, besides their final products (p3 and Aβ), there are also formed soluble ectodomains (sAPPα and sAPPβ), C-terminal fragments (α-CTF and β-CTF) and the APP intracellular domain (AICD) (adapted from O'Brien and Wong, 2011)

γ-secretase is a high molecular weight multisubunit protease complex, composed of at least four integral membrane proteins: presenilin (PS), nicastrin (NCT), presenilin-enhancer 2 (PEN-2) and anterior pharynx defective 1 (APH-1) (Figure 6). Presenilin is the catalytic component, functioning as an aspartyl protease, while the other three elements are cofactors and/or scaffold proteins. NCT is thought to be involved in the recognition and binding of substrates and PEN-2 initiates the proteolysis of PS, during the activation of the complex (Fraering, 2007).

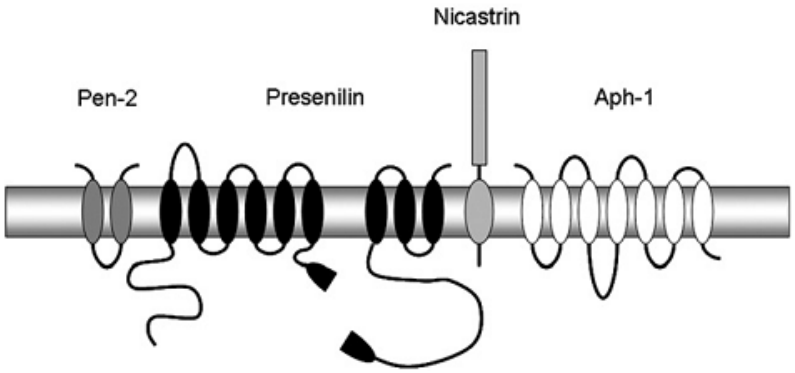

Figure 6. Schematic representation of the four known components of the γ-secretase complex: Pen-2, PS1, NCT and APH-1 (adapted from Laudon et al., 2007)

In most genomes studied, the PS family comprises two homologous proteins: PS1 and PS2. They share more than a half of the amino acid sequence, but they are not redundant (Smolarkiewicz et al., 2013). Interestingly, autosomal mutations in PS1 and PS2 genes have been suggested as one of the possible causes for AD, as the proteins they codify for are involved in the γ-secretase catalytic sites (Karran et al., 2011)

The γ-secretase also does not have unique specificity towards APP and it has been proved to cleave more than 50 other type I transmembrane proteins. However, the neuronal compartments in which γ-secretase processing occurs have not been identified yet (Lazarov et al.,2005). Furthermore, this enzyme is a mediator in multiple signaling pathways. In addition to its role in the formation of the Aβ peptide, this enzyme is also involved in proteolysis of the intracellular domains of Notch receptor, which is known to be responsible for the regulation of some genes crucial to the development (Zhang et

al., 2011). The presenilins might also play an important role in synaptic transmission and plasticity, the molecular basis for cognitive functions. One of the possible mechanisms through which neuronal activity and APP processing correlate is by the enhancement and/or depression of APP to γ-secretase cleavage. In fact, it has been demonstrated that PS1 is necessary to improve excitatory synaptic transmission, after a decrease in neuronal activity (Wang et al., 2012).

To sum up, since the Aβ peptide oligomers are now known to act and trigger synaptotoxicity and the subsequent development of AD and because of the pivotal role of APP in AD pathogenesis, it is important to assess whether APP and the secretases involved in its metabolism are located at synaptic fractions. The definition of the specific localization of these proteins would undoubtedly be of crucial importance for the development of novel therapeutical approaches.

2. AIMS

This work will focus on three main objectives:

- **to define the synaptic and subsynaptic localization of APP and of the secretases responsible both for the amyloidogenic and non-amyloidogenic processing of APP;**

- **to define the presence of APP and secretases and their co-localization in different types of nerve terminals, mainly glutamatergic and GABAergic;**

- **to investigate whether the age and AD condition affect the distribution of APP and secretases in nerve terminals**

3. MATERIAL AND METHODS

3. 1. Material

3.1.1. Reagents

Table 1: Reagents used

Reagent	Supplier
30% Acrylamide/Bis solution	Bio Rad (Portugal)
Ammonium persulfate (APS)	Sigma-Aldrich (Portugal)
BCA Kit	Thermo scientific (USA)
Bovine serum albumin (BSA)	Sigma-Aldrich (Portugal)
Bromophenol blue	Sigma-Aldrich (Portugal)
Calcium chloride ($CaCl_2$)	Sigma-Aldrich (Portugal)
CAPS ([3-(cyclohexylamino)-1-propane-sulfonic acid)	Sigma-Aldrich (Portugal)
CLAP (cocktail of proteases inhibitors)	Sigma-Aldrich (Portugal)
Dithiothreitol (DTT)	Sigma-Aldrich (Portugal)
ECF	GE Healthcare (United Kingdom)
Ethylenediaminetetraacetic acid (EDTA)	Sigma-Aldrich (Portugal)
Glucose	Sigma-Aldrich (Portugal)
Glycerol	Sigma-Aldrich (Portugal)
Halothane	Sigma-Aldrich (Portugal)
HEPES	Sigma-Aldrich (Portugal)
Hydrochloric acid (HCl)	Sigma-Aldrich (Portugal)
Magnesium Chloride ($MgCl_2$)	Sigma-Aldrich (Portugal)
Methanol	Sigma-Aldrich (Portugal)
Normal Horse Serum (NHS)	Invitrogen (United Kingdom)
Paraformaldehyde	Sigma-Aldrich (Portugal)
Percoll	GE Healthcare (United Kingdom)
Penylmethanesulfonylfluoride (PMSF)	Sigma-Aldrich (Portugal)
Poli-D-Lysine	Sigma-Aldrich (Portugal
Potassium chloride (KCl)	Sigma-Aldrich (Portugal)
ProLong Gold Antifade	Invitrogen (United Kingdom)
Sodium dodecyl sulfate (SDS)	Bio Rad (Portugal)
Sodium azide	Sigma-Aldrich (Portugal)
Sodium Bicarbonate ($NaHCO_3$)	Sigma-Aldrich (Portugal)
Sodium Chloride (NaCl)	Sigma-Aldrich (Portugal)
Sodium phosphate monobasic (NaH_2PO_4)	Sigma-Aldrich (Portugal)
Sucrose	Sigma-Aldrich (Portugal)
TEMED	Sigma-Aldrich (Portugal)
Triton -X-100	Sigma-Aldrich (Portugal)
Trizma base	Sigma-Aldrich (Portugal)
Tween	Sigma-Aldrich (Portugal

3.1.2. Antibodies

Table 2: Primary and secondary antibodies for Western blot

Antibodies	Supplier	Host	Type	Dilution
ADAM10 C-terminal	Millipore	Rabbit	Polyclonal	1:1000
APP C-terminal	Sigma	Rabbit	Polyclonal	1:1000
BACE	Millipore	Mouse	Monoclonal	1:1000
Presenilin-1	Abcam	Mouse	Monoclonal	1:500
PSD-95	Sigma	Mouse	Monoclonal	1:20000
SNAP-25	Sigma	Mouse	Monoclonal	1:40000
Synaptophysin	Millipore	Rabbit	Polyclonal	1:20000
Syntaxin	Sigma	Mouse	Monoclonal	1:40000
β-actin	Sigma	Mouse	Monoclonal	1:20000
Rabbit- alkaline phosphatase conjugate (AP)	GE Healthcare	Goat	IgG + IgM (H+L)	1:20000
Mouse-AP	GE Healthcare	Goat	IgG (H+L)	1:20000

Table 3: Primary and secondary antibodies for immunocytochemistry

Antibodies	Supplier	Host	Type	Dilution
APP C-terminal	Sigma	Rabbit	Polyclonal	1:500
APP N-terminal	Millipore	Mouse	Monoclonal	1:500
ADAM10 C-terminal	Millipore	Rabbit	Polyclonal	1:100
BACE C-terminal	Millipore	Mouse	Monoclonal	1:300
PS1	Abcam	Mouse	Monoclonal	1:100
PSD-95	Sigma	Mouse	Monoclonal	1:200
vGLUT1	Synaptic Systems	Guinea Pig	Polyclonal	1:1000
vGAT	Synaptic Systems	Guinea Pig	Polyclonal	1:1000
Synaptophysin	Millipore	Rabbit	Polyclonal	1:200
Synaptophysin	Sigma	Mouse	Monoclonal	1:200
Anti–Mouse Alexa Fluor 488	Invitrogen	Donkey	IgG (H+L)	1:1000
Anti–Mouse Alexa Fluor 594	Invitrogen	Donkey	IgG (H+L)	1:1000
Anti-Rabbit Alexa Fluor 488	Invitrogen	Donkey	IgG (H+L)	1:1000
Anti-Rabbit Alexa Fluor 594	Invitrogen	Donkey	IgG (H+L)	1:1000
Anti–Guinea pig Alexa Fluor 488	Invitrogen	Donkey	IgG (H+L)	1:1000

3.1.3. Animals

In our study, three types of mice were used:

1- male C57/Bl6 mice with 2-3 months old
2- male C57/Bl6 mice with 9 months old
3- male triple transgenic AD mice (3xTg-AD), and the respective control mice (Wild –type) mice15 months old.

Male C57 Black 6 mice were obtained from Charles River (Barcelona, Spain). The 3xTg-AD transgenic mice and the wild-type littermates were obtained from a colony of these animals that exist at the CNC animal facilities. These animals were obtained from Frank La Ferla group (University of California, Irvine, CA, USA). The animals were housed under controlled temperature (23 ± 2 ºC), subject to a fixed 12 h light/dark cycle, with free access to food and water. All efforts were made to reduce the number of animals used and to minimize their stress and discomfort. The animals were sacrificed by under anesthesia with halothane (no reaction to handling or tail pinch, while still breathing).

3.1.4. Human samples

Brain samples were obtained at autopsy from the Instituto de Medicina Legal (Coimbra), thanks to collaboration between Beatriz da Silva and our group, namely Rodrigo A. Cunha and Paula Canas. The samples used were prepared and kindly provided by Paula Canas.

3.2. Methods

3.2.1. Synaptosomal Preparations

Synaptosomes are re-sealed nerve terminals, which enclose all the typical neuronal contents, including cytoplasm, synaptic vesicles and mitochondria, and present several advantages that make them one of the best models to study the physiological properties of synapses. Their functions closely resemble nerve terminals *in vivo*: they can produce ATP, they have functional ion channels, carriers and receptors on their plasma membranes and also functional proteins, enzymes and synaptic vesicles, capable of taking up and releasing neurotransmitters (Dunkley et al., 2008). The synaptosomal preparations we used are pure enough to study physiological aspects of synaptic function. The isolation of synaptosomes can be done using two different procedures:

3.2.1.1. Rapid isolation of synaptosomes and total membranes

The animals were anesthetized under halothane atmosphere before being sacrificed by decapitation. Membranes from Percoll-purified synaptosomes were prepared as previously described by our group (Rebola et al., 2005). The two hippocampi from one mouse were homogenized at 4º C in sucrose solution (0.32 M), containing 1 mM EDTA, 10 mM HEPES, 1 mg/ml bovine serum albumin (BSA, pH 7.4). The homogenate was centrifuged at 3000 x*g* for 10 min (Sigma 3-18K centrifuge, rotor 12-158H), the supernatant was collected and centrifuged at 14000 x*g* for 20 min at 4º C (Sigma 3-18K centrifuge, rotor 12-158H). The supernatant was discarded and the pellet was either taken as total membrane fraction, resuspended in RIPA buffer (supplemented with 2 μM PMSF and 1% CLAP) for Western blot analysis and stored at -20ºC or it was resuspended in 1 ml of a 45% (v/v) Percoll solution made up in a Krebs solution (composition: 140 mM NaCl, 5 mM KCl, 25 mM HEPES, 1 mM EDTA, 10 mM glucose, pH 7.4). After centrifugation at 14,000 x*g* for 2 min at 4 °C, the top layer was collected (synaptosomal fraction), washed in 1 ml Krebs solution and resuspended in Krebs solution. This mixture was centrifuged at 14,000 x*g* for 20 min at 4 °C (eppendorf centrifuge). The resulting pellet corresponded to the nerve terminal membranes and was resuspended in RIPA buffer (50 mM Tris HCl pH 8; 150 mM

NaCl, 1% NP-40, 0.5% sodium deoxycholate, 0.1% SDS)supplemented with 2 μM PMSF and 1% CLAP) for Western blot analysis and stored at -20ºC.

3.2.1.2.Isolation of synaptosomes with a discontinuous Percoll gradient

First of all, gradients with Percoll solutions were prepared and maintained on ice. The Percoll solutions were prepared in a 0.32 M sucrose solution with 1 mM EDTA and 0.25 mM DTT, pH 7.4 at 4ºC. In each tube, the gradient was built as follows (from bottom to top): 3 ml of a 23% (v/v) Percoll solution, 4 ml of a 10% (v/v) Percoll solution and 3 ml of a 3% (v/v) Percoll solution (Figure 7).

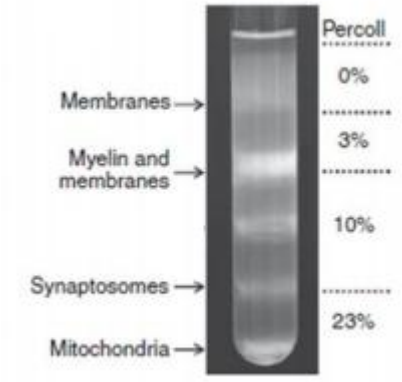

Figure 7. Representation of the discontinuous Percoll gradient (adapted from Dunkley et al., 2008)

Hippocampi were removed from the sacrificed mice and homogenized in a medium containing 0.32 M sucrose and 10mM HEPES (pH 7.4). The homogenates were centrifuged at 2000 x*g* for 5 min at 4º C (Sigma 3-18K centrifuge, rotor 12-158H), the supernatants collected and further centrifuged at 9500 x*g* for 13 min at 4ºC (Sigma 3-18K centrifuge, rotor 12-158H). The supernatants were discarded and the pellets re-suspended in 2 ml of 0.32 M sucrose and 10 mM HEPES (pH 7.4). This suspension was slowly and carefully placed over the top 3% layer in each tube containing the Percoll discontinuous gradients prepared before. These gradients were centrifuged at 25000 x*g* for 11 min at 4ºC, without deceleration (Avanti J-26X centrifuge, rotor JA-22-50). Synaptosomes were collected between the 10% (v/v) and 23% (v/v) Percoll bands and diluted in 15 ml of HEPES buffered medium (HBM, containing: 140 mM NaCl, 5 mM

KCl, 5 mM $NaHCO_3$, 1.2 mM NaH_2PO_4, 1 mM $MgCl_2$, 10 mM glucose and 10 mM HEPES, pH 7.4). Then, a centrifugation at 22000 x*g* for 11min at 4º C was performed, and the synaptosomal freely-moving pellets were carefully removed and resuspended in HBM.

3.2.2. Subsynaptic fractionation

The separation of the presynaptic active zone, postsynaptic density and extrasynaptic fractions from cortex nerve terminals was performed using a methodology previously described by our group (Rebola et al., 2005). For synaptosomes preparation, in order to obtain a good yield, it is advisable to use at least three mice cortex per procedure. The cortices were homogenized in Isolation Buffer (IB, containing: 0.32 M sucrose, 0.1 mM $CaCl_2$, 1 mM $MgCl_2$, 1% CLAP and 1 mM PMSF). The homogenate was resuspended in 2 M sucrose and 0.1 mM $CaCl_2$ and the obtained mixture (1.25 M sucrose) gently agitated. This solution was separated into tubes Ultraclear™ and 1 M sucrose solution, containing 0.1 mM $CaCl_2$, was carefully added in order to allow the formation of a gradient. The tubes were equilibrated with IB solution and centrifuged at 100000 x*g* at 4º C, for 3 h (Beckman Coulter – Optima CL – 100XP DU ultracentrifuge, rotor SW41Ti). The IB and the myelin layer present at the interface IB/1M sucrose were aspirated and the synaptosomes were collected at the interface 1.25 M/1 M sucrose. They were diluted 10 times in IB and centrifuged at 15000x*g*, during 30 min (Avanti J-26x centrifuge, rotor JA-22-50). Part of the obtained supernatant was centrifuged at 12400 x*g* (eppendorf centrifuge) and the obtained pellet resuspended with 5% SDS and stored for control analysis, at -80ºC. The pellet was re-suspended in IB and diluted 1:10 in pre-cooled 0.1 mM $CaCl_2$. An equal volume of 2 x solubilisation buffer (2% Triton X-100, 40 mM Tris, pH 6.0) was added to the suspension. The mixture was incubated for 30min on ice with mild agitation and then centrifuged at 40000 x*g* for 30 min, at 4º C (Avanti J-26x centrifuge, rotor JA-22-50). The pellet corresponds to synaptic junctions and the supernatant to the extrasynaptic fraction. The extrasynaptic fraction was decanted and proteins precipitated with six volumes acetone at -20º C, overnight. The synaptic junctions pellet was washed in 1x solubilization buffer (20mM Tris, 1% Triton X-100, pH 6.0) and resuspended in 10 volumes of another 1x solubilization buffer (20mM Tris, 1% Triton X-100, pH 8.0). This mixture was incubated for 30 min

on ice, with mild agitation, and then centrifuged at 40000 x*g* for 30 min at 4º C (Avanti J-26x centrifuge, rotor JA-22-50). The obtained supernatant corresponds to the presynaptic fraction and was processed as described for the extrasynaptic fraction. The insoluble pellet corresponds to the postsynaptic density, which was resuspended in a minimal volume of 5% SDS with 0.1 mM PMSF and stored overnight at -20ºC. The extra and presynaptic fractions were pelleted by centrifugation at 18000 x*g* for 30 min at -15º C (Sorvall RC6, rotor SS34) and also solubilized in 5% SDS with 0.1 mM PMSF, before storing at -20º C.

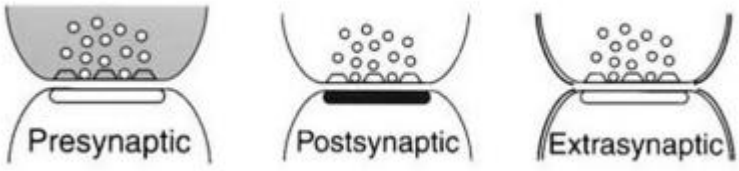

Figure 8. Schematic representation of the subsynaptic components that are expected to be enriched in each of the fractions isolated in this procedure (adapted from Phillips et al., 2001)

3.2.3. Human brain total extracts preparation

Human brain cortex, obtained from individuals with different years old that died from unknown causes, were homogenized in RIPA buffer, supplemented with 2 μM PMSF and 1% CLAP, and then sonicated for 20 min.

The post mortem interval (PMI) average was 40.1 h. The quality of the samples used was taken into account: the average pH value was 6.4 and the average RNA integrity number (RIN) was 6.1.

3.2.4. Protein quantification by the BCA method

Protein determination was performed using the BCA protein assay reagent kit. In this method, BSA is used as a protein standard. Therefore, a standard curve was drawn, by preparation of several dilutions of BSA in miliQ water, using: 2, 1, 0.5, 0.25, 0.125, 0.0625 and 0 μg/μl of BSA. The samples and the solution in which the samples had been resuspended before storage were diluted 10 times. In a 96 well dish, the standard curve was prepared in triplicate, by adding lysis buffer and BCA reagent to each well containing different BSA concentrations. Also, the samples were added to several wells, in triplicates, as well as miliQ water and the BCA reagent. The multi-well dish was incubated at 37º C, during 30 min, and, after that, the absorbance was read at 570 nm in a spectrophotometer.

The standard curve was then used to calculate the protein concentration in μg/μL.

3.2.5. Western blot

After determining the protein concentration using the BCA method , the protein were denatured in sample buffer (500 mM Tris, 600 mM DTT, 10.3% SDS, 30% glycerol and 0.012% bromophenol; usually it was used 1/6 of a 6x concentrated sample buffer) at 95ºC for min. Protein samples (concentration normalized) were separated by SDS-PAGE electrophoresis, using a 10% polyacrylamide resolving gel with 4% polyacrylamide stacking gel. Then, the proteins were then electrotransferred to previously activated polyvinylidene difluoride (PVDF) membranes for 2 h, at 4º C. After that, the membranes were incubated for 1 h, at room temperature, with 5% low-fat milk or with 3% bovine serum albumin, depending on the antibodies used, in Tris buffer with Tween (TBS-T, 150 mM NaCl, 25 mM Tris-HCl pH 7.6; 0.1% Tween 20) to block unspecific binding The membranes were then incubated with primary antibodies diluted in TBS-T with 5% milk or 3% BSA, overnight, at 4ºC. After washing with TBS-T, the membranes were incubated with secondary antibodies, also diluted in TBS-T with 5% milk or 3% BSA, for 2 hours, at RT. Then the membranes were washed in TBS-T, revealed by an enhanced chemifluorescence (ECF) kit and visualized in a VersaDoc system.

Table 4: Gel Formulation

Gel Formulation (1 Gel)	10% - Resolving Gel	4% - Stacking Gel
Tris-buffer, 1.5 M, pH 8.8 (Resolving gel)	2.5 ml	-
Tris-buffer, 0.5 M, pH 6.8 (Stacking gel)	-	2.5 ml
Acrylamide 30 %	3.3 ml	1.3 ml
Water	4.1 ml	6.1 ml
TEMED	5 µl	10 µl
APS 20% (freshly prepared, diluted in water)	50 µl	50 µl

3.2.6. Immunocytochemistry in synaptosomes

Hippocampal nerve terminals from mice were purified through a discontinuous Percoll gradient (Dunkley et al., 2008). The obtained synaptosomes were placed on coverslips coated with poly-D-lysine, fixed with 4% paraformaldehyde for 15 min and washed twice with PBS medium. The synaptosomes were permeabilized using a PBS 0.2% Triton X-100 solution, for 10 min at RT, and then blocked with PBS 3% BSA and 5% normal horse serum for 1 h. The synaptosomes were then washed twice with PBS in the presence of 3% BSA and incubated with primary antibodies for 1 h at RT. They were then washed three times with PBS with 3% BSA and incubated for 1h with secondary antibodies labelled with a fluorescent dye. The synaptosomes were then washed three times in PBS medium, mounted on slides with Prolong Antifade and left to dry overnight. The preparations were then visualized by fluorescence microscopy (Zeiss Axiovert 200 microscope with a 63 x oil objective), under a total magnification of 630 times. For co-localization purposes, the fluorescence in each coverslip was analysed by counting five different fields using Image J software, classifying synaptosomes as particles between 4 and 25 pixel resolution. Only pixel intensities above background (measured in structures labelled only with secondary antibodies) were considered.

3.3. Data Presentation

Results are presented as means ± S.E.M. values of the number of experiments (n) indicated in figure legends. To test the significance of the difference between two independent groups, an unpaired Student's *t* test was used considering a statistical difference for a $p<0.05$. In experiments with more than two groups it was used one-way analysis of variance (ANOVA), followed by Tukey's multiple comparison test. A value of $p<0.05$ was considered to represent a significant difference.

4. RESULTS AND DISCUSSION

Rationale

The parameters that correlate better with cognitive impairment in the early phases of AD are the loss of synapses and the increased levels of soluble β-amyloid peptides (Aβ), namely $A\beta_{1-42}$ (Walsh et al., 2002), which are formed from amyloid precursor protein (APP) through the action of particular secretases (α-and β- secretases). Since Aβ can disrupt synaptic function and cause synaptotoxicity, it is proposed that Aβ may be a causative factor in AD, which begins with an insidious loss of synaptic contacts before evolving into overt loss of particular neurons in limbic cortical regions such as the hippocampus (Coleman et al., 2004). Surprisingly, little is known about the synaptic and subsynaptic distribution of APP and secretases in different types of nerve terminals (i.e. glutamatergic and GABAergic terminals), nor it is known if the distribution of APP and secretases changes with aging and in AD conditions. Therefore, in the present study we investigate the synaptic and subsynaptic localization of APP, BACE1, ADAM10 and Presenilin1 in young adult mice (2-3 months) and in mice with 9 months old, in triple transgenic mice model of AD (3xTg-AD) and also in human cortical brain tissue samples obtained from individuals of different ages.

The present study was focused on cortical regions, mainly in the hippocampus, because it is one of the most affected brain regions in AD. This region typically suffers a dramatic decrease in the number and density of synapses, an event associated with early cognitive decline in AD. The synaptoxicity may be explained due to high energetic demand of synapses that become impaired as a result of mitochondrial dysfunction: (Yaxno and Preobrazhenskaya, 2006; Reddy et al, 2010; Wang et al., 2012). Synapses represent about 1-2% of total hippocampal volume and have high protein abundance because of their adhesion and cytoskeletal proteins responsible for maintaining their structure (Phillips et al., 2001). As the study of synapses in native brain preparations is limited, quantitative Western blot analysis was performed in synaptosomes and in total membranes from the hippocampus of healthy adult male mice. Synaptosomes correspond to purified synapses and are considered to be the best model to study biochemical and neurochemical properties of synapses (Cunha, 1998). Moreover, the subsynaptic localization of APP and secretases was also evaluated in order to test their relative abundance in the presynaptic active zone, extrasynaptic fractions and in postsynaptic density, using a fractionation method that our group has previously validated (Rodrigues et al., 2005) .

4.1 Synaptic and subsynaptic distribution of APP and secretases in mice hippocampus

4.1.1. Amyloid precursor Protein (APP)

4.1.1.1. Synaptic distribution of APP

APP is widely expressed in the mammalian brain, but it seems to be quite abundant in both peripheral and central synapses (Wang et al., 2005). However, endogenous APP is expressed at very low levels in both rat and mouse neurons and, therefore, the quantifications of this protein is not easy (Groemer et al., 2011; Hoe et al., 2012;). The presence of APP at synapses was demonstrated by Sanbrink and colleagues in 1997, by co-localization with synaptophysin. Moreover, the importance of APP in synapse maturation was suggested by Kirazov and colleagues in a study in which an increase in the levels of APP was observed during the periods of most intense synapse formation (Sandbrink et al., 1997; Kirazov et al. 2001). Furthermore, it has been demonstrated in cultured neurons that the absence of APP inevitably affects synaptic formation, maintenance and transmission, thereby confirming the essential role of this protein in neuronal development (Priller et al., 2006).

4.1.1.1.1. APP in synaptosomes and total membranes

The interactions of APP and its proteolytic fragments with synaptic systems are complex and involve subtle changes in the levels of APP (Hunter and Brayne, 2012). In this part of our study, the relative abundance of APP was compared in synaptosomes and in total membranes of hippocampi of the same animal by quantitative Western blot analysis. It was used an antibody against the APP carboxyl-terminal (APP C-Term), since previous data from our group showed that the antibody against APP amino-terminal (APP N-term) had a pattern of APP labeling similar to that of antibody against APP C-term (unpublished data). Furthermore, it has been shown that the extracellular domain (C-terminal) of APP is especially important for the promotion of synapse formation. The APP is trafficked trough anterograde transport to the presynaptic

terminal in transport vesicles, and further recruited to the plasma membrane by exocytosis (Groemer et al. 2011). Thus, it is viable to infer that the C-terminal should be more accessible to antibody labeling than the N-terminal, which would be oriented towards the lumen of the vesicle (Groemer et al. 2011; Hoe et al., 2012; Claeysen et al., 2012).

The anti-APP antibody (APP C-term) used recognized a double well-defined band with an apparent molecular weight of approximately 120 kDa. In the same immunoblot we have loaded three amounts of protein (10, 20 and 40 μg) of synaptosomes and total membranes, which were obtained from the same hippocampal samples (see material and methods), in order to detect the APP immunoreactivity for non-saturating amounts of protein (Figure 9.B). The relative amount of APP immunoreactivity was achieved for 20 μg of loaded protein and it was observed that the density of APP in synaptosomes was lower (59.1% ± 11.7%, n=4) than in total membranes (86.3% ± 8.5%, n=4, Figure 9.A). The ratio between APP immunoreactivity in synaptosomes and in total membranes, was 0.7 ± 1.4 (n=4), indicating that APP, albeit present, is not enriched in hippocampal nerve terminals as compared with the bulk of total membranes.

Although there are evidences that APP is a synaptic protein (Kim et al., 1995), it is also known that APP is co-translationally inserted into the endoplasmic reticulum (ER), trafficked through the Golgi apparatus, and further transported in secretory vesicles to the plasma membrane, from where can be internalized and delivered to endosomes (Thinakaran and Koo, 2008; Groemer et al., 2011). This could explain why in our preparations it was not observed an enrichment of APP in synaptic membranes as compared with the bulk of whole membranes, since it is likely that a large amount of APP are in intracellular vesicles.

A

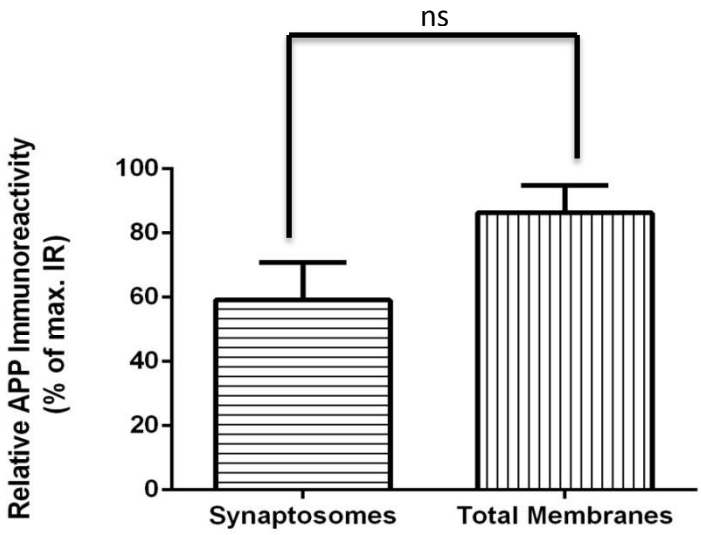

B

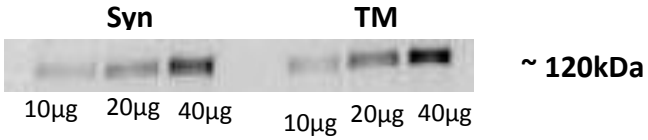

Figure 9. APP is not enriched in synaptic nerve terminals as compared with its density in total membranes. (A) The graphic represents the percentage of immunoreactivity for 20 µg of loaded protein, which was calculated considering the maximal immunoreactivity value obtained as 100%. The results are presented as mean ± SEM of 4 independent experiments. n.s. –non-significant ($p>0.05$). **(B)** Representative Western blot of the APP levels in synaptosomes (Syn) and total membranes (TM) for different amounts of loaded protein.

4.1.1.2. Subsynaptic distribution of APP

In this part of the study, it was analyzed if APP is differently distributed in the different subsynaptic fractions. Therefore, we used a fractionation procedure, previously validated by our group, which allows an effective separation (over 90% efficiency) of the presynaptic active zone, postsynaptic and extrasynaptic (non-synaptic) (fractions. With this technique, the accessibility of antibodies to epitopes located at synapses is enhanced by the solubilization of different subsynaptic components (Rebola et al., 2005; Phillips et al., 2001).

The data presented in Figure 10 (A and B) show that APP is mainly located in the presynaptic fraction of nerve terminals, although it is also present in the postsynaptic density. By quantifying the relative abundance of APP immunoreactivity in the three fractions (in three different preparations from different groups of mice) it was determined that APP immunoreactivity is most abundant in the presynaptic fraction (53.1% ± 5.5%, n=3), but it is also present in the postsynaptic density (37.1% ± 2.6%, n=3), and the lowest density was observed extrasynaptically (9.8% ± 7.7%, n=3). In accordance to the higher presence of APP at presynaptic fractions it was hinted that APP undergoes transport along axons, rather than dendrites (Brunholz et al., 2012). Moreover, the previous reported presence of APP into synaptic vesicles (Groemer et al., 2011) is also in consonance with our findings that APP is localized mainly in presynaptic fractions. The validation of the subsynaptic fractionation procedures used in this study was verified by Western blot analysis, using antibodies against presynaptic (synaptosomal-associated protein 25, SNAP-25), postsynaptic (postsynaptic density protein 95, PSD-95) and extrasynaptic (synaptophysin) protein markers. In these controls, it is expected an enrichment of the subsynaptic proteins in the corresponding subsynaptic fractions. Therefore, SNAP-25 should be preferentially located in the presynaptic fraction, PSD-95 should have a high density in the postsynaptic fraction and synaptophysin should be enriched in the extrasynaptic fraction. The immunoblots done to verify the purity of subsynaptic fractions used in this study showed that it was obtained an effective subsynaptic fractionation (Figure 10.C).

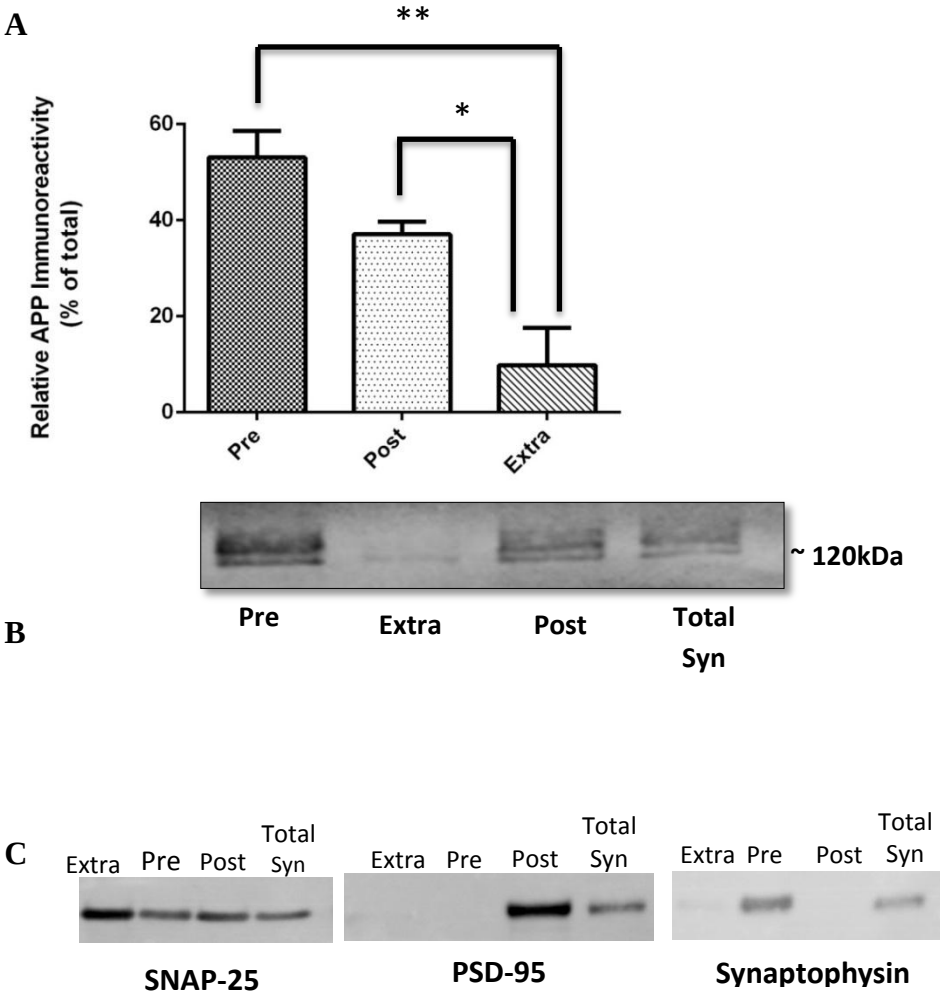

Figure 10. Cortical subsynaptic levels of APP. (**A**) The percentage of APP immunoreactivity for each subsynaptic fraction was calculated considering the sum of the pre- (Pre), post- (Post) and extrasynaptic (Extra) immunoreactivities. The total synaptosomes (Total Syn) were analyzed as an internal control of the experiment. The results are presented as mean ± SEM of 3 independent experiments. * $p < 0.05$; ** $p < 0.01$. (**B**) Representative Western blot of the APP levels in subsynaptic fractions and total synaptosomes. 20 μg of protein were loaded in each lane of the gel. (**C**) Representative Western blot of the control purity of subsynaptic preparations, where it is expected an enrichment of subsynaptic proteins in the respective membrane fractions: in presynaptic (SNAP-25, with 25 kDa), in postsynaptic (PSD-95, with 95 kDa) and extrasynapic (synaptophysin with 38kDa).

Our results suggest that APP is restricted to a specific part of the nerve terminals and not randomly located in the axons and dendrites. It's evident presence at the presynaptic zone, specifically, and at the synapses, in general, supports the well-known theory that

APP has several crucial roles in the development and maintenance of synapses (Kirazov et al. 2001). Furthermore, our data are in accordance to some studies describing APP as a protein that is preferentially localized to presynaptic ending in the cortical synapses (Kim et al., 1995). APP processing is also referred as a phenomenon that occurs mainly presynaptically and it is claimed that APP derivatives remain bound to the membrane and accumulate at the nerve terminals in the CNS (Lazarov et al., 2005). Recent data obtained using techniques that allow the direct access to presynaptic mechanisms, showed that small amounts of APP are present in synaptic vesicles at the presynaptic terminals (Groemer et al., 2011). Nevertheless, this protein has also been located in the postsynaptic density (Marcello et al., 2007).

4.1.2. β-secretase (BACE1)

4.1.2.1. Synaptic distribution of BACE1

BACE1 is known to be highly expressed in neurons and, in both rodents and humans, typically forms homodimers, which have higher enzymatic activity than the monomeric form. This beta-secretase has important physiological functions in synaptic transmission and plasticity and it is found in CA1 and CA3 regions of the hippocampus, where it seems to play a role in the regulation of presynaptic activity (Wang et al., 2012), being postulated that BACE1can be upregulated by synaptic activity (Kamenetz et al., 2003). In our study, we focused on BACE1, as it seems to be the only enzyme with physiological APP β-secretase activity in the brain (Kamenetz et al., 2003).

4.1.2.1.1. BACE1 in synaptosomes and in total membranes

Considering the presumably high neuronal levels of BACE1, even in healthy individuals, we decided to investigate the relative abundance of this protein in both synaptic membranes and in total membranes, in order to determine whether BACE1 is preferentially synaptic or not. The density of BACE1 was analyzed, by Western blot, using healthy mice hippocampi of the same animal, in the same gel. The antibody used was against the C-terminal of BACE1, and recognized a well-defined band with an apparent molecular weight of approximately 70 kDa. It is notable that, during its trafficking through the cell, BACE1 suffers several post-translational modifications. In fact, its immature form has approximately 65kDa, but then the protein is subjected to extensive glycosylation, giving rise to a protein with 75kDa (Epis et al., 2012). Depending on experimental conditions and individual cell lines' glycosylation machinery, the molecular weight of BACE1 has been reported to be between 70 and 75 kDa for the mature protein and between 60 and 70 kDa for its immature forms (Capell et al. 2000).

Figure 11 shows that the immunoreactivity of the bands for BACE1 in synaptosomes was 37.1% ± 10.7% (n=3), while in the total membranes was 85.2% ± 10.7% (n=3). Besides, the ratio of BACE1 immunoreactivity in the synaptosomal fraction *versus* the whole membranes fraction was 0.4 ± 1.3 (n=3), suggesting that BACE1 is less localized in nerve terminals than in total membranes. Indeed, there are evidences that BACE1,

like APP, can be transported through the TGN to the nerve terminals into synaptic vesicles (Groemer et al., 2011).

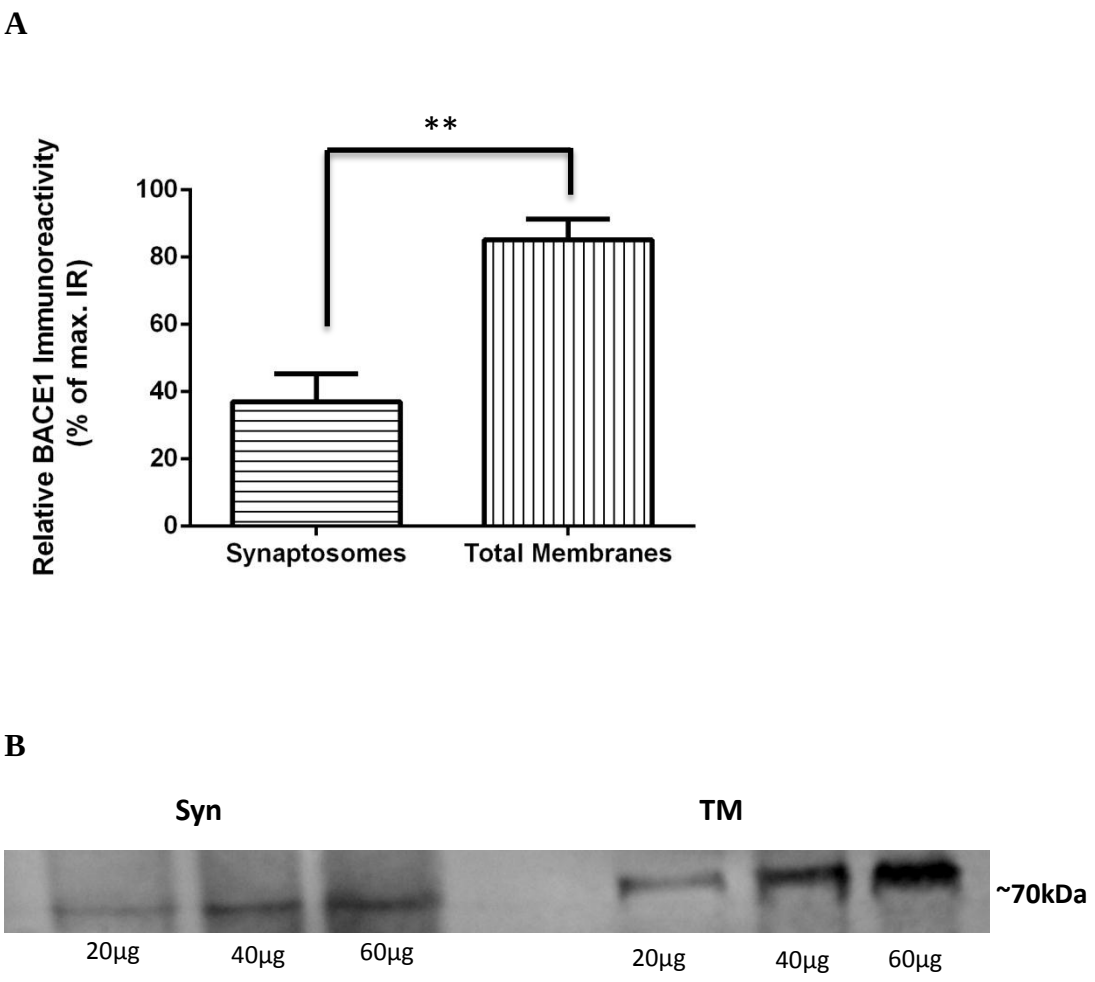

Figure 11. BACE1 is not enriched in synaptic nerve terminals as compared with its density in total membranes. (A) The graphic represents the percentage of immunoreactivity for 20 µg of loaded protein, which was calculated considering the maximal immunoreactivity value obtained as 100%. The results are presented as mean ± SEM of 3 independent experiments. **p<0.01 **(B)** Representative Western blot of the BACE1 levels in synaptosomes (Syn) and total membranes (TM) for different amounts of loaded protein.

4.1.2.2. Subsynaptic distribution of BACE1

Although a number of studies outline the importance of BACE1 at the synaptic level, little is known about it subsynaptic distribution. Therefore, in this part of the study, it was analyzed if BACE1 was differently distributed across the different synapse zones. As it can be seen in Figure 12 (A and B), BACE1 immunoreactivity was located preferentially in the extrasynaptic fraction of nerve terminals, although it was also present in both the presynaptic and postsynaptic zones. When quantifying the relative abundance of BACE1 immunoreactivity in the three subsynaptic fractions (in t 3 independent preparations) it was observed that BACE1 immunoreactivity is most abundant in the extrasynaptic density (72.5% ± 4.9%, n=3), but it is also present in the presynaptic fraction (15.8% ± 3.9%, n=3) and also in the postsynaptic compartment (11.7% ± 2.1%, n=3). The purity of the subsynaptic fractions was verified by Western Blot analysis, using antibodies against presynaptic (SNAP-25), postsynaptic (PSD-95) and extrasynaptic (synaptophysin) protein markers (Figure 12.C).

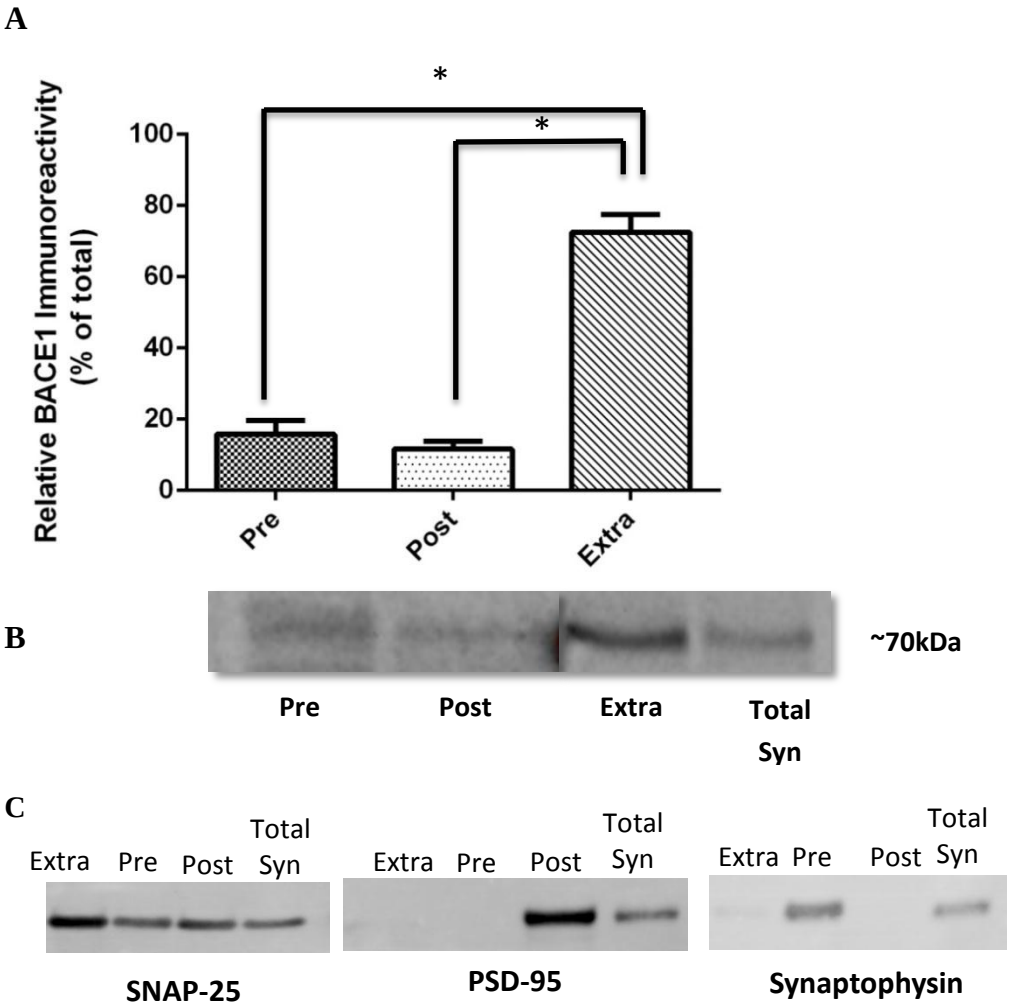

Figure 12. Cortical subsynaptic levels of BACE1. **(A)** The percentage of immunoreactivity was calculated considering the sum of the pre- (Pre), post- (Post) and extrasynaptic (Extra) immunoreactivities. The total synaptosomes (Total Syn) were analyzed as an internal control of the experiment. The results are presented as mean ± SEM of 3 independent experiments. * $p < 0.05$. (**B**) Representative Western blot of the BACE1 levels in subsynaptic fractions and total synaptosomes. 20 μg of protein were loaded in each lane of the gel (**C**) Representative Western blot of the controls of subsynaptic preparations, where it is expected an enrichment of subsynaptic proteins in the respective membrane fractions, as described in captions of Figure10. C.

The importance of BACE1 is pointed out in some recent studies, that emphasize the idea that β-secretase mediated cleavage of APP might act positively on normal brain functions, enhancing some of them (Marcello et al., 2008). There are *in vivo* evidences that β-secretase mediated cleavage might be able to facilitate some cognitive processes, like learning and memory, thus BACE1 might be important in the regulation of presynaptic function (Wang et al., 2012). Moreover, BACE1 was found in the synaptic vesicle fraction, suggesting that this β-secretase is trafficked to the synaptic nerve terminals in transport vesicles (Groemer et al., 2011).

Giving the supposed role of BACE1 in the modulation of presynaptic function, higher levels of this enzyme would be expectable in the presynaptic compartment. Also, given the high levels observed in the extrasynaptic fraction, it might be speculated that BACE1 acts, in fact, through synaptic vesicles.

4.1.3. α-secretase (ADAM10)

4.1.3.1. Synaptic distribution of ADAM10

Quite a few elements of the ADAM family of proteins exhibit α-secretase-like activity. Among these proteases, ADAM10 is considered a key protease in the processing of APP. The ADAM10's expression in the human brain appears to coordinate with APP, which is less seen for ADAM17 (Reiss et al., 2005). It is known that ADAM10 is widely distributed in adult brain and is expressed mainly in neurons, but is also present in astrocytes and microglia (Reiss et al., 2005). This ubiquity may be explained by the variety of processes in which ADAM10 is involved, such as: embryonic development, cell adhesion, signal transduction and axon outgrowth (Vingtdeux and Marambaud, 2012).

4.1.3.1.1. ADAM10 in Synaptosomes and Total Membranes

In this part of the study, ADAM10 hippocampal synaptic distribution was evaluated and the levels of this enzyme were compared in total membranes and in synaptic membranes by Western blot analysis. The anti-ADAM 10 antibody recognized a band with an apparent molecular weight of approximately 80 kDa. The ADAM10 immunoreactivity was lower in synaptosomes (41.2% ± 8.6%, n=4) than in total membranes (88.6% ± 5.2%, n=4), which suggests that ADAM10 is more abundant in the bulk of total membranes than in purified presynaptic terminals (Figure 13 A and B).

A

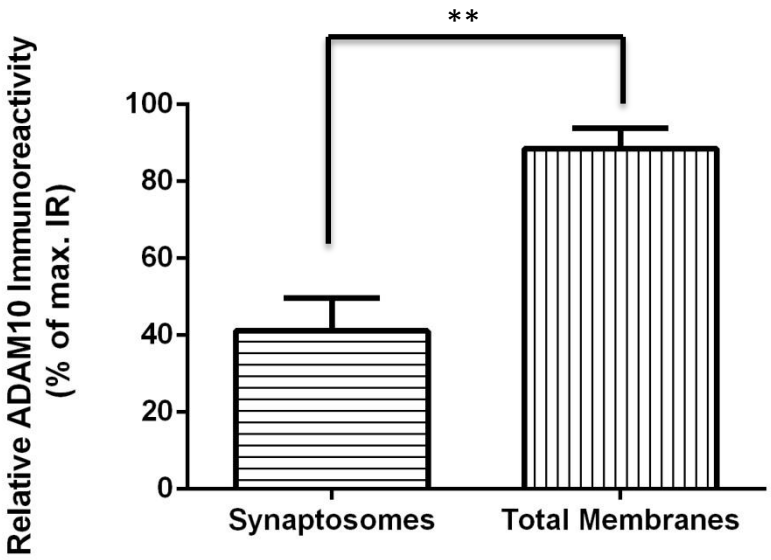

B

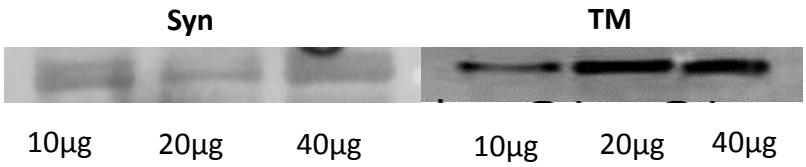

Figure 13. ADAM10 is not enriched in synaptic nerve terminals as compared with its density in total membranes. (A) The graphic represents the percentage of immunoreactivity for 20 µg of loaded protein, which was calculated considering the maximal immunoreactivity value obtained as 100%. The results are presented as mean ± SEM of 4 independent experiments. ** $p<0.01$ **(B)** Representative Western blot of the APP levels in synaptosomes (Syn) and total membranes (TM) for different amounts of loaded protein

4.1.3.2. Subsynaptic distribution of ADAM10

In this part of the study, it was analyzed if ADAM10 distribution was different at a subsynaptic level. In mice cortex, ADAM10 immunoreactivity was located almost exclusively in the postsynaptic fraction of nerve terminals, although it was also present in the presynaptic zone (Figure 14). When quantifying the relative abundance of ADAM10 immunoreactivity in the three fractions, it was observed that ADAM10

immunoreactivity is most abundant in the postsynaptic density (61.3% ± 4.3%, n=3), but it is also present in the presynaptic compartment (38.7% ± 4.3%, n=3). The validation of subsynaptic fraction was verified by Western Blot analysis (Figure 14.C).

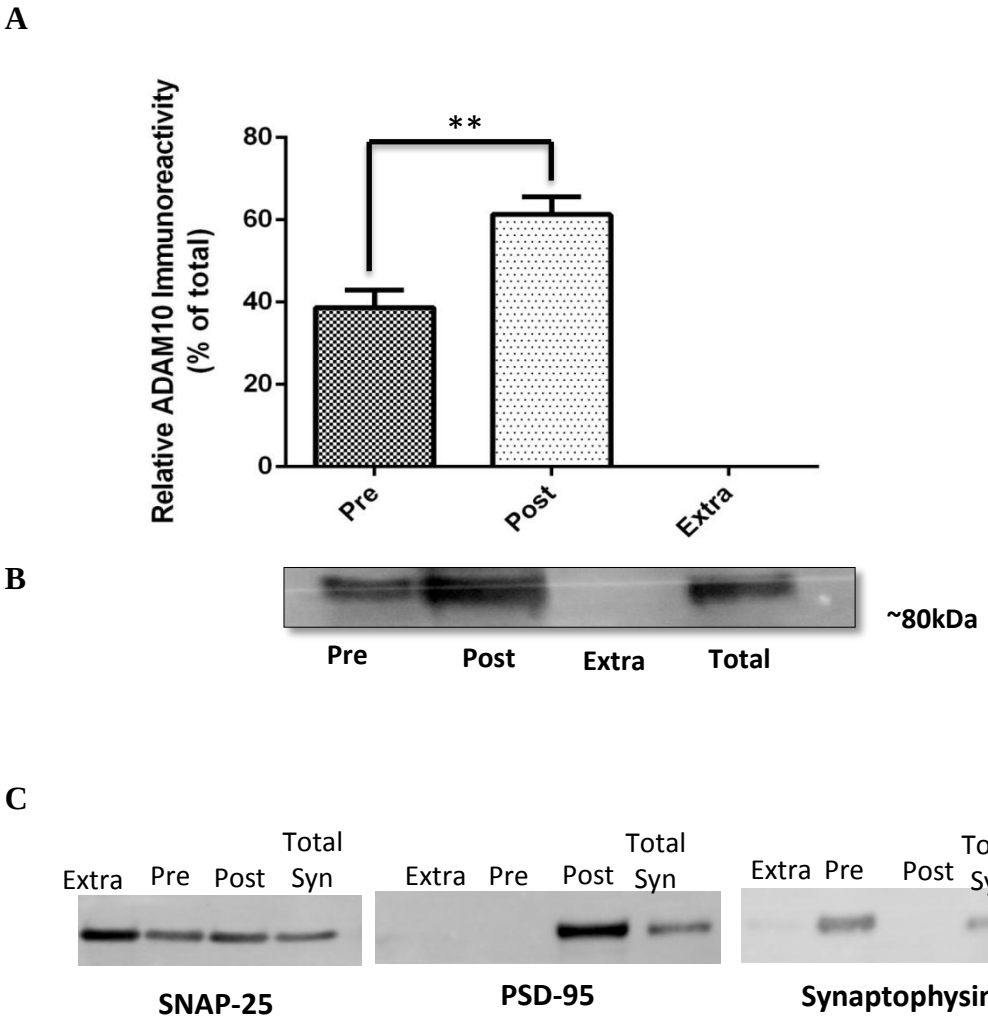

Figure 14. Cortical subsynaptic levels of ADAM10. (**A**) The percentage of immunoreactivity was calculated considering the sum of the pre- (Pre), post- (Post) and extrasynaptic (Extra) immunoreactivities. The total synaptosomes (Total Syn) were analyzed as an internal control of the experiment. The results are presented as mean ± SEM of 3 independent experiments. **p< 0.01. (**B**) Representative Western blot of the ADAM10 levels in subsynaptic fractions and total synaptosomes. 20 μg of protein were loaded in each lane of the gel (**C**) Representative Western blot of the controls of subsynaptic preparations, where it is expected an enrichment of subsynaptic proteins in the respective membrane fractions, , as described in captions of Figure10. C.

Our results showing an enrichment of ADAM10 in postsynaptic fractions are consistent with recent findings indicating that α-secretase activity is affected when the

transport of ADAM10 to the postsynaptic membrane is blocked (Prox et al., 2012). In fact, some studies suggest that ADAM10 is mostly localized at the postsynaptic density of excitatory synapses and it is thought to act on several substrates with postsynaptic distribution (Marcello et al., 2013). This is particularly important from the functional point of view, since the postsynaptic location of ADAM10 correlates with APP metabolism at glutamatergic synapses. This process involves the synapse-associated protein-97 (SAP97), which binds to the cytosolic domain of ADAM10 and drives the enzyme to the postsynaptic membrane, thereby enhancing APP cleavage mediated by α-secretase (Marcello et al., 2007). Thus, ADAM10 activity seems to depend on NMDA receptors activation at the postsynaptic membrane, and APP metabolism can be potentiated towards a non-amyloidogenic pathway. Furthermore, the localization of ADAM10 to the postsynaptic density correlates with APP metabolism. In addition to that, this enzyme has been described to interact with several substrates characteristic of the postsynaptic density. This may constitute a potential regulatory mechanism, which can be altered during AD pathogenesis (Marcello et al., 2007; Lichtenthaler 2011; Reiss et al., 2005).

4.1.4. γ-secretase (Presenilin1)

4.1.4.1. Synaptic distribution of Presenilin1

Presenilin 1 (PS1) has been described as the probable catalytic subunit of the γ-secretase complex, and requires the other members of the enzymatic complex to have a protease activity. Apart from its proteolytic activity in both the amyloidogenic and non-amyloidogenic pathways of APP metabolism, this enzyme is involved in the regulation of neurotransmitter release and calcium homeostasis. There is also evidence that presenilins participate in the intracellular mechanisms underlying cognitive functions (Wang et al., 2012).

4.1.4.1.1. Presenilin1 in Total Membranes

The density of Presenilin1 (PS1) was analyzed, by Western blot, using mice hippocampi of the same animal, in the same gel. The antibody used was against the N-terminus cleavage product of the protein and should recognize a 28 kDa protein. However, we had several difficulties in obtaining observable bands, despite we tried a variety of conditions in the Western blot analysis and also using different samples. In fact, the only blot we were able to obtain was the one represented in Figure 15 and it should be referred that we did not get PS1 immunoreactivity in synaptosomes

It was observed that the density of PS1in total membranes was 92.6% ± 7.5% (n=2).

A

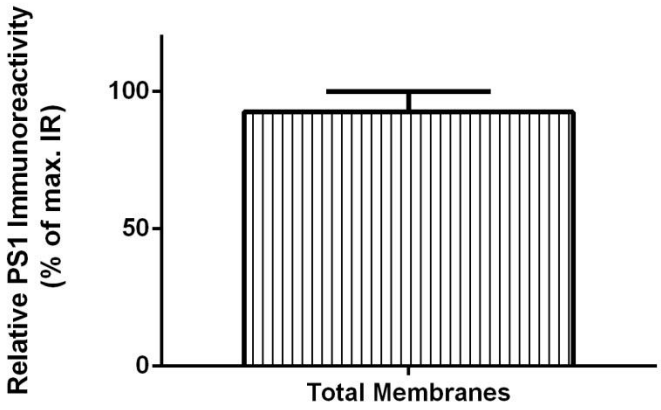

B

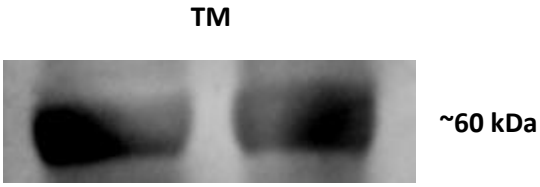

Figure 15. PS1 is present in total membranes (A) The graphic represents the percentage of immunoreactivity for 80 μg of loaded protein, which was calculated considering the maximal immunoreactivity value obtained as 100%. The results are presented as mean ± SEM of 2 independent experiments. **(B)** Representative Western blot of the PS1 levels hippocampal total membranes (TM).

The represented bands have approximately 60 kDa, which corresponds to almost the twice of the molecular weight expected.

Although surprising, this result can be explained by a study performed in 1996, in which Sahara and colleagues showed that this protein can have several isoforms, whose molecular weight varies, as a result of alternative splicing that the PS1-encoding gene suffers. One of the presenilin isoforms is commonly known as I-467 and is ubiquitously

expressed in the organism. The authors of the study obtained, by immunoprecipitation followed by Western blot analysis, bands with approximately 52 and 42 kDa and with 74 and 65 kDa, when the same samples were heat-treated (Sahara et al., 1996).

The absence of PS1 in synaptosomes is a little surprising, because PS1 has already been found to be concentrated at the synapses of both cerebellar and hippocampal neurons, where it was distributed mainly in the synaptic compartments, suggesting that this secretase may have important synaptic functions (Ribaut-Barassin et al. 2000). Nevertheless, it is undoubtedly present in total membranes and this is quite logical, as γ-secretase activity has been localized in different cell body compartments, like endosomes, and also in synaptic vesicles and membranes in rat brain (Frykman et al., 2010).

Overall, it is noteworthy that albeit exist some studies that reported the presence of APP and of secretases (α-, β- and ɣ-) in synapses or in subsynaptic components, none study of our knowledge had compared the relative abundance of these proteins in nerve terminals (synaptosomes) relatively to total membranes nor their relative abundance in the pre-, post and extrasynaptic fractions.

4.1.5. Distribution of APP and Secretases in Glutamatergic and GABAergic nerve terminals in young adult mice

Due to the crucial role in synaptotoxicity suggested for Aβ peptides, it is surprising to verify that the distribution of APP and of secretases (α-, β-, γ-secretases) involved in APP processing, across different types of nerve terminals, is unknown, nor is it known if their distribution changes in animal models of AD. Therefore, in this part of the study we aimed to investigate the distribution of APP and secretases in glutamatergic and GABAergic nerve terminals and whether this precursor protein is co-localized with different secretases. This was achieved by double immunocytochemistry studies in platted purified nerve terminals, mainly presynaptic terminals, that consist on the simultaneous labeling of specific markers of different types of nerve terminals and of one of the proteins involved in APP metabolism, in order to define in which type of terminals (glutamatergic or GABAergic) APP and secretases exist.

In order to differentiate the glutamatergic terminals from the GABAergic ones, there were used antibodies against: i) the vesicular glutamate transporter 1 (vGLUT1), which is a specific protein marker of neurons that use glutamate as a neurotransmitter, and ii) the vesicular GABA transporter (vGAT) that is present only in neurons that release GABA. These vesicular transporters are responsible for the packing of glutamate and GABA into synaptic vesicles of glutamatergic and GABAergic neurons, respectively (McIntire et al., 1997 ; Takamori et al., 2000). It is crucial to notice that glutamate is the major excitatory neurotransmitter in the CNS and has important roles in processes like synaptic transmission and plasticity, learning and memory. Impairment in the glutamatergic neurotransmission seems to occur in AD, leading to an increase in the levels of glutamate at the synapse (Revett et al., 2013).

Prior to the main experiments, the purity of platted nerve terminals preparations was assessed. For this purpose, the nerve terminals were double-labeled with synaptophysin (a presynaptic marker) and with PSD-95 (a postsynaptic marker) and the percentage of their co-localization was determined. The co-localization value obtained was about 10%, indicating that our preparations were enriched in presynaptic nerve terminals (data not shown).

The overall abundance of glutamatergic and GABAergic nerve terminals in our preparations was also investigated, by assessing the percentage of synaptophysin-immunopositive terminals that co-localized with vGLUT1 and vGAT. As illustrated in Figure 16, 69.1% ± 1.7% (n=3) of the synaptophysin-immunopositive elements were endowed with vGLUT1 immunoreactivity, while GABAergic terminals represented 30.9% ± 0.4% (n=3) of hippocampal nerve terminals.

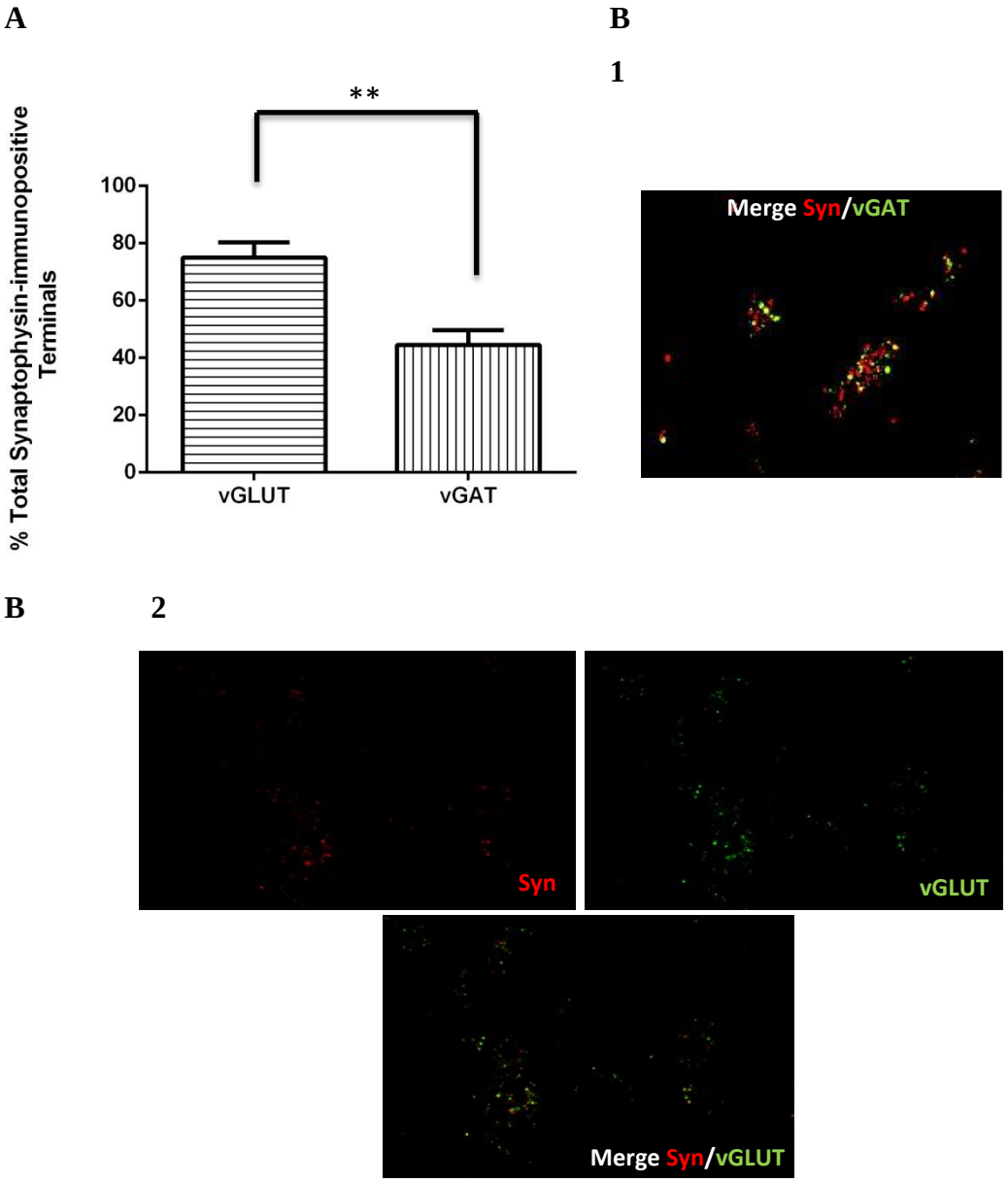

Figure 16. Relative Glutamatergic and GABAergic nerve terminals abundance in presynaptic nerve terminals. (A) The graphic represents the percentage of co-localization between markers of glutamatergic (vGLUT) and GABAergic (vGAT) nerve terminals and synaptophysin-immunopositive elements (Syn). The total population was considered to be the overall number of synaptophysin-immunopositive elements. The results are presented as mean ± SEM of 3 independent experiments. ***p<0.001. **(B.1.)** Representative merge image obtained for synaptophysin-immunopositive elements (red) and vGAT-immunopositve elements (green). The yellow labeling corresponds to the co-localizaton of synaptophysin and vGAT co-localization. **(B.2.)** Representation of the images taken for synaptophysin (Alexa Fluor 594, red) and vGLUT (Alexa Fluor 488 green) immunolabbeling, and of the merge images that represent the co-localization of synaptophysin and vGLUT labelling (yellow). The magnification used to obtain the images was 630x.

After the characterization of our preparations of purified nerve terminals, it was investigated the relative abundance of APP and secretases in the overall population of nerve terminals. As illustrated in Figure 17, the synaptophysin-immunopositive elements were endowed with: 24.5% ± 7.9% (n=3) of APP, 10.1% ± 2.2% (n=3) of BACE1, 11.9% ± 6.2% of ADAM10 and 0.4% ± 0.3% (n=2) of PS1 immunoreactivities.

A

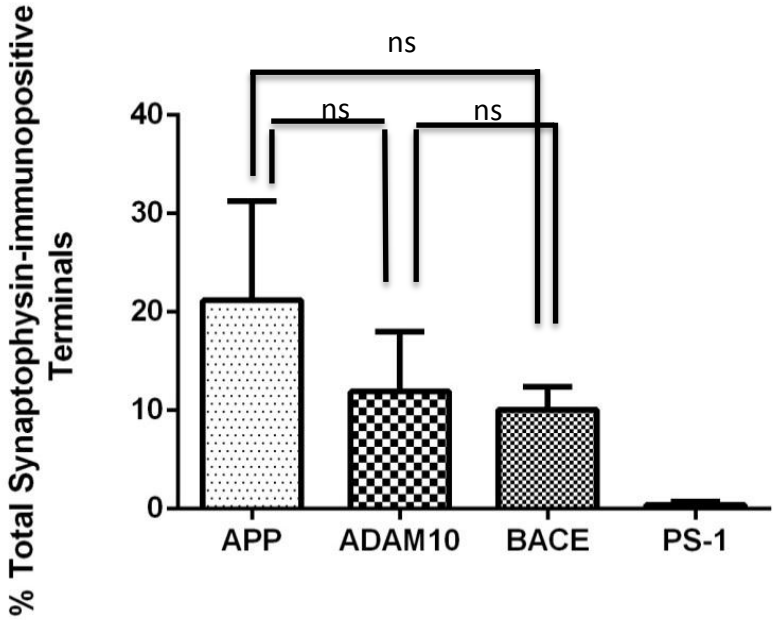

B

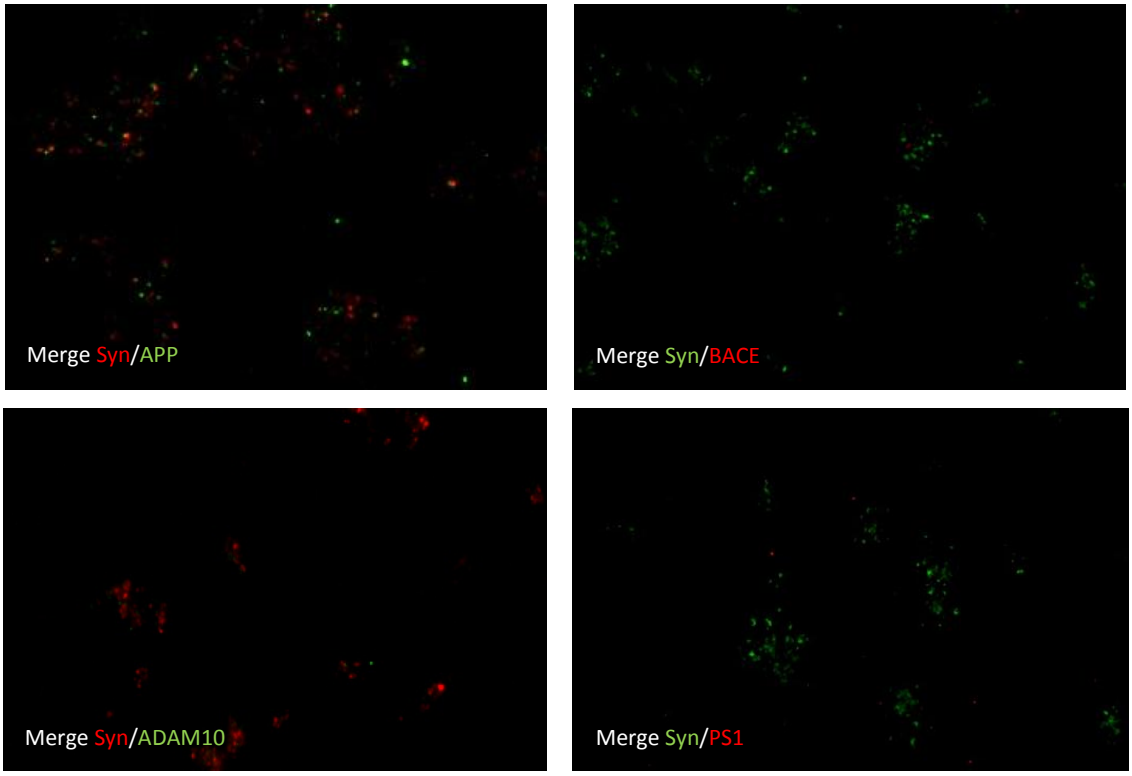

Figure 17. Relative abundance of APP, α- (ADAM10), β- (BACE) and γ- (PS1) secretases in presynaptic nerve terminals. (A) The graphic represents the percentage of co-localization between each protein and synaptophysin-immunopositive elements. The total population was considered to be the overall number of synaptophysin-immunopositive elements. The results are presented as mean ± SEM of 3 and 2 (for PS1) independent experiments. n.s.–non-significant ($p>0.05$) **(B)** Representative merge images of the co-localization between synaptophysin-immunopositive elements (Syn) and APP-, ADAM-10-, BACE1- and PS1- immunopositive elements. The yellow labeling corresponds to co-localized or red and green elements (see color in images). The magnification used to obtain the images was 630x.

The oligomeric Aβ is known to affect the glutamatergic system, mainly glutamate receptors (Crimins et al., 2013), thus it pertinent to speculate if the APP is present in large quantities in glutamatergic neurons. Likewise, APP seems to have a functional role in GABAergic transmission, as it has already been described that lack of APP disrupts GABAergic synapses, but they may be rescued by the re-introduction of the protein (Zheng et al., 2010). Also, since β-secretase is the main enzyme involved in the amyloidogenic pathway and glutamatergic neurons are known to suffer a disruption in AD pathology, it is logical to wonder whether BACE1 is equally distributed in different types of nerve terminals. Therefore, we investigated the co-localization of APP and BACE1 with different markers for nerve terminals (vGLUT1 and vGAT). As illustrated in Figure 18, 31.0% ± 6.5% of glutamatergic terminals and 23.9% ± 1.3% (n=3) of GABAergic terminals were labeled for APP. Likewise, it was observed that 60.6% ± 5.1% (n=3) of glutamatergic terminals and 29.1% ± 10.5% (n=3) of GABAergic terminals were endowed with BACE1.

A

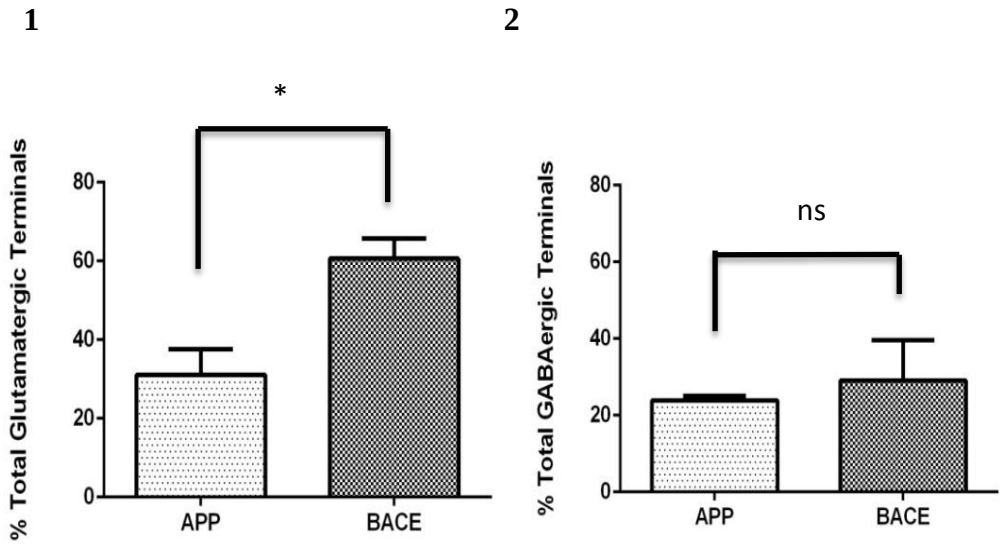

B

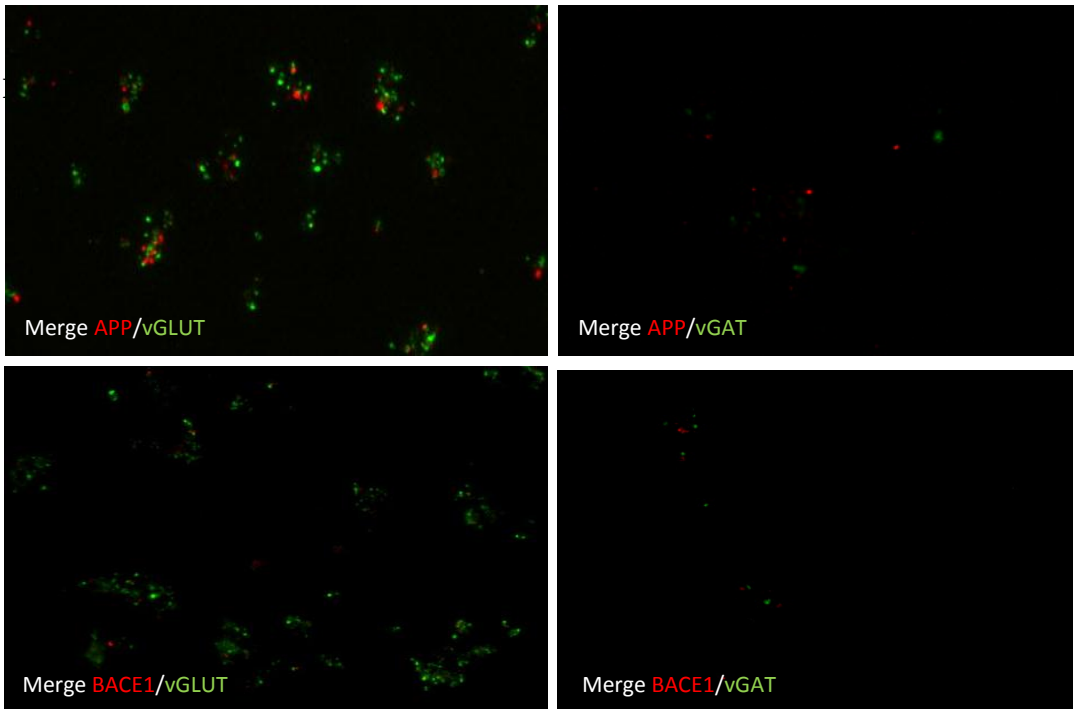

Figure 18. APP and BACE are present in both glutamatergic and GABAergic presynaptic nerve terminals. Double immunocytochemistry analysis of APP and BACE1 with markers of glutamatergic (vGLUT) and GABAergic (vGAT) nerve terminals. **(A.1.)** The graphic represents the percentage of co-localization between APP- or BACE1-immunopositive elements and vGLUT-immunopositive elements. The total population was considered to be the overall number of vGLUT-immunopositive elements. **(A.2.)** The graphic represents the percentage of co-localization between APP- or BACE1-immunopositive elements and vGAT-immunopositive elements. The total population was considered to be the overall number of vGAT-immunopositive elements. The results are presented as mean ± SEM of 3 independent experiments. n.s. $p>0.05$; *$p<0.05$). **(B)** Representative merge images obtained for APP-immunopositive elements (APP, red) or BACE1-immunopositive elements (BACE1, red) and markers of glutamatergic (vGLUT, green) and GABAergic (vGAT, green) nerve terminals. The yellow labeling corresponds to the co-localization of green and red elements. The magnification used to obtain the images was 630x.

4.1.6. Co-localization of APP with β-secretase in hippocampal nerve terminals of young adult mice

In order to investigate whether APP co-localized with β-secretase in hippocampal nerve terminals, we further performed immunocytochemistry studies co-labeling the APP and BACE1 in platted purified presynaptic terminals. The data obtained showed that 41.6% ± 3.9% (n=3) of APP-immunopositive nerve terminals were also labeled with BACE1 (Figure 19).

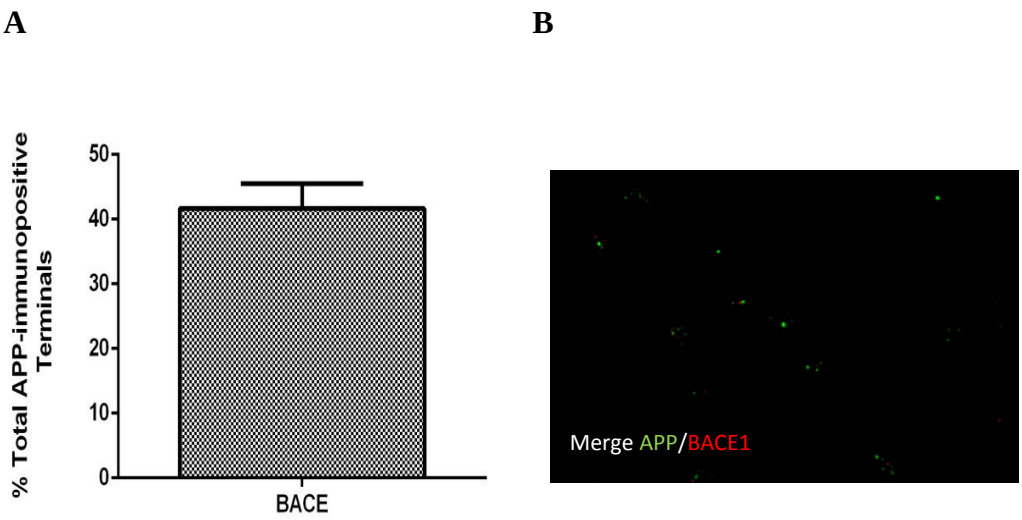

Figure 19. APP and BACE1 co-localized in presynaptic nerve terminals. Double immunocytochemistry analysis of APP and BACE1 **(A)** The graphic represents the percentage of co-localization between BACE1-immunopositive elements and APP-immunopositive elements. The total population was considered to be the overall number of APP-immunopositive elements. The results are presented as mean ± SEM of 3 independent experiments **(B)** Representative merge image obtained for APP-immunopositive elements (APP, green) and BACE1-immunopositive elements (BACE1, red). The yellow labeling corresponds to the co-localization of green and red elements. The magnification used to obtain the images was 630x.

Our data show that APP and BACE1 were to some degree co-localized in presynaptic nerve terminals; however only of 41.6% of APP immunopositive elements co-labeled with BACE1. This means that in some hippocampal terminals both APP and BACE1 are present, whereas in other terminals these two proteins are not together. The observed co-localization between APP and BACE1 is somewhat expectable, since there are evidences demonstrating a physical association between sAPP-β (a large secreted N-terminal soluble fragment, resulting from the β-secretase-mediated cleavage of APP) and BACE1 (Obregon et al., 2012). However, it was also stated that, in healthy animals and humans, the encounter of APP and BACE1 is expected to be limited, as there is evidence supporting the theory that these two proteins suffer different cellular trafficking (Tan and Evin, 2011).

.

4.2. The impact of age on the distribution of APP and secretases hippocampal nerve terminals

In order to investigate if there are age-related modifications in the distribution and density of APP and secretases, we next compared the levels of these proteins in two groups of mice with different ages. For this purpose, synaptosomes and total membranes were prepared from the hippocampus of 9 months old mice, in order to evaluate the relative abundance of APP and of the secretases involved in its metabolism by Western blot analysis, in comparison to the same type of preparations from 2-3 months old mice.

4.2.1. APP in synaptosomes and in total membranes

The relative abundance of APP in both synaptosomes and total membranes from a group of different animals, in comparison to samples form a group of control younger mice, was assessed by quantitative Western blot analysis. The immunoreactivity of each band was normalized with β-actin.

In hippocampal synaptosomes, the APP immunoreactivity in the control group (2 months old) was slightly lower (87.2% ± 1.0%, n=3) than in the 9 months old group (91.7% ± 4.8%, n=3). In hippocampal total membranes, the difference in APP abundance was a little more evident than in synaptosomal fractions. In the control group, the APP immunoreactivity was 83.9% ± 7.6 % (n=2), while, in the group of 9 months old mice, it was 57.1% ± 23.2% (n=3).

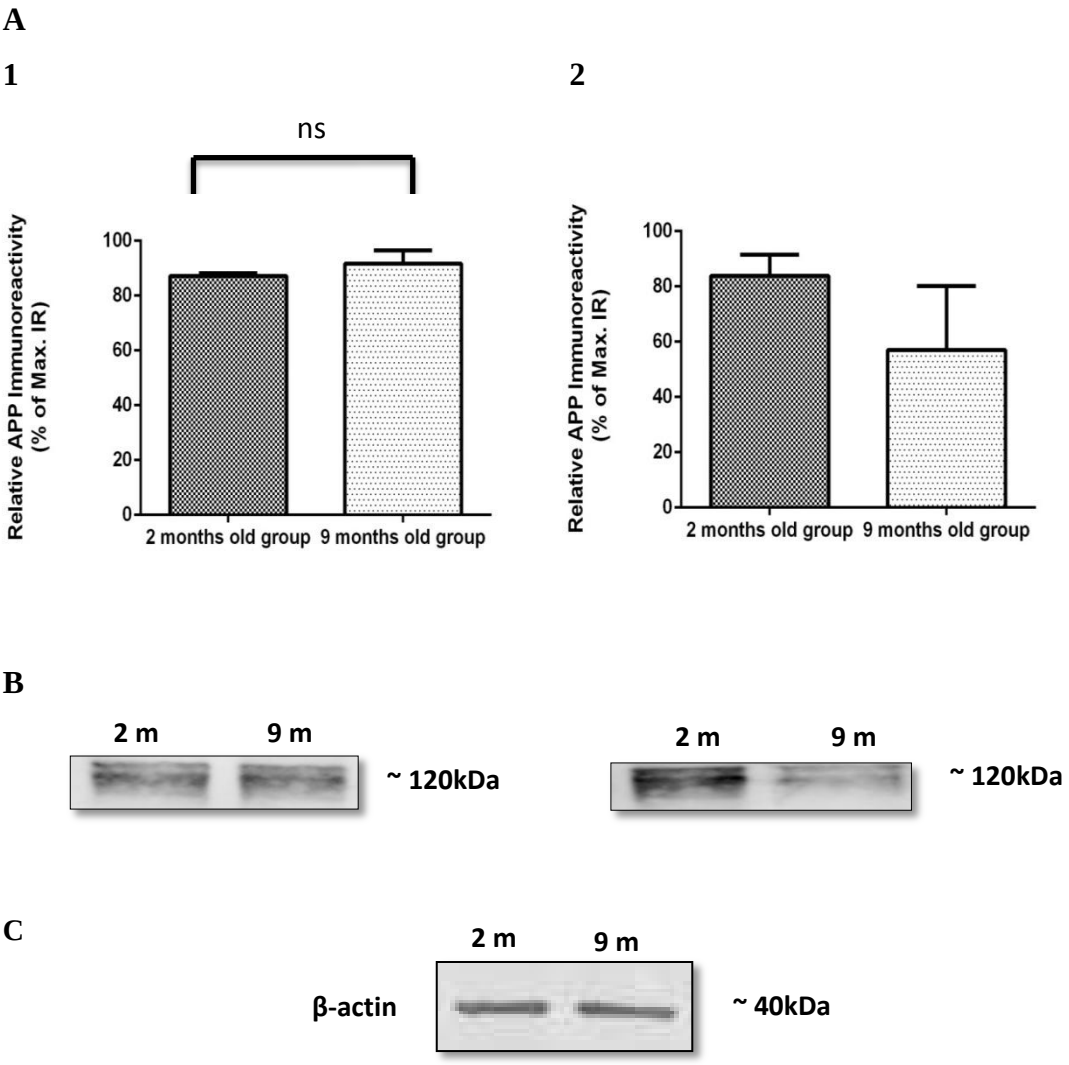

Figure 20. Hippocampal levels of APP in synaptosomes and in total membranes of 2 months old mice, in comparison to 9 months old mice. (A) The graphic represents the percentage of immunoreactivity for 20 µg of loaded protein, which was calculated considering the maximal immunoreactivity value obtained as 100% for 40ug (an amount of loaded protein that was previously defined as close to saturating levels). The results are presented as mean ± SEM of 3 and 2 independent experiments. ns – non significant **(B)** Representative Western blot of the APP levels in the 2 months old group (2 m) and in the 9 months old group (9 m) of mice. **(C)** Representative Western blot of the β-actin density (control for protein loading).

Studies concerning the levels of APP and Aβ in aging brains are controversial. In 1995, Carroll and colleagues studied the levels of these proteins in a group of people with an ample range of ages and did not find any alterations in the cerebrospinal fluid (Carroll et al., 1995). However, studies performed in transgenic mice models of AD (Tg2576) showed an age-dependent increase in total membrane-bound APP (Mustafiz et al., 2011).

4.2.2. BACE1 in synaptosomes and in total membranes

The relative abundance of BACE1 in both synaptosomes and total membranes from the two groups of mice was evaluated by quantitative Western blot analysis. The immunoreactivity of each band was normalized with β-actin.

In hippocampal synaptosomes, the BACE1 immunoreactivity in the control group was 44.9% ± 22.8% (n=3), while in the 9 months old group tends to be higher, although not statistically significant: 78.8% ± 13.1% (n=3). These results suggest a tendency towards an increase in the levels of BACE1 with the progression of age, in synaptic fractions. On the contrary, in hippocampal total membranes, the BACE1 immunoreactivity in the control group was lower (53.7% ± 9.4%, n=3) than in the 9 months old group: 82.6% ± 15.6% (n=3). These results suggest a tendency to an increase in the intracellular levels of BACE1 in ageing brains.

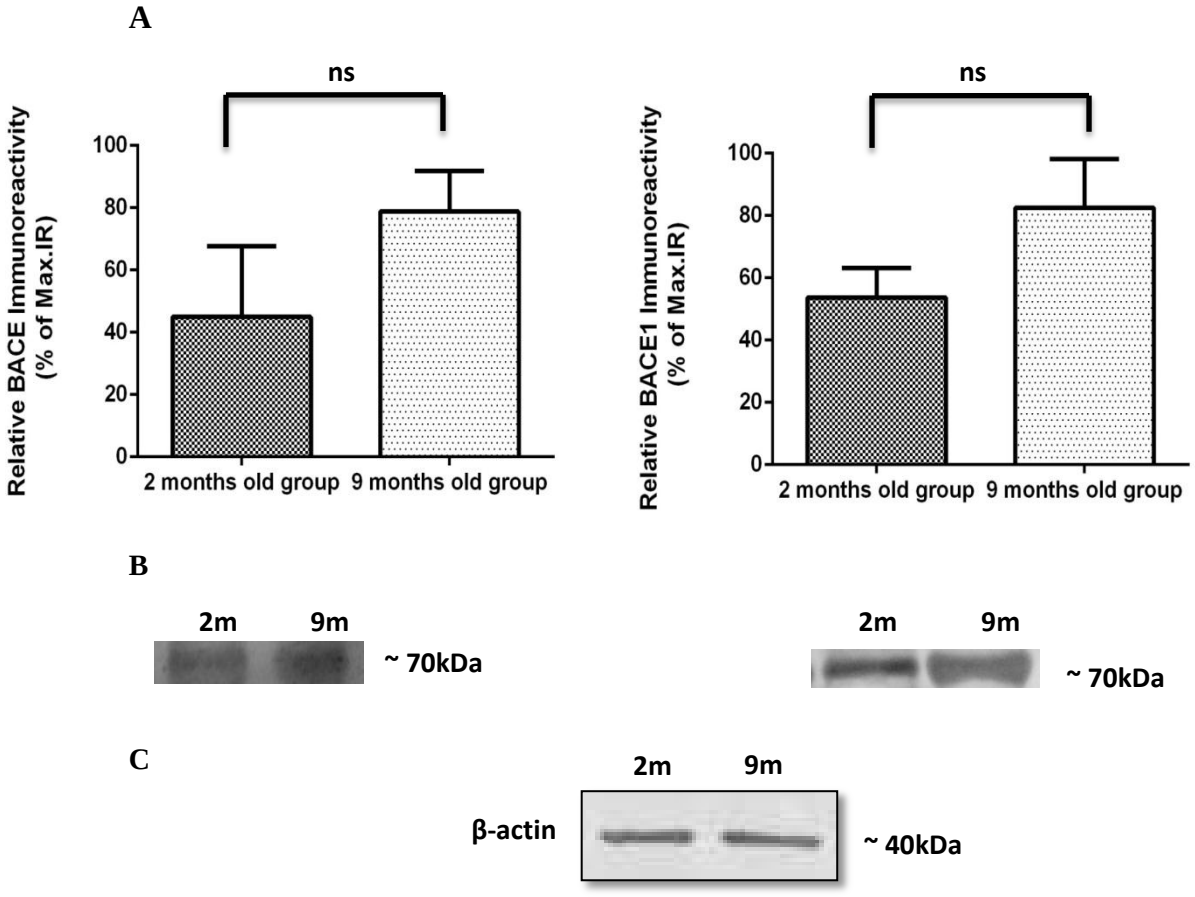

Figure 21. Hippocampal levels of BACE1 in synaptosomes and in total membranes of 2 months old mice, in comparison to 9 months old mice. (A) The graphic represents the percentage of immunoreactivity for 20 μg of loaded protein, which was calculated considering the maximal immunoreactivity value obtained as 100% for 40ug (an amount of loaded protein that was previously defined as close to saturating levels). The results are presented as mean ± SEM of 3 independent experiments. ns – non significant. **(B)** Representative Western blot of the BACE1 levels in the 2 months old group (2 m) and in the 9 months old group (9 m) of mice. **(C**Representative Western blot of the β-actin density (control for protein loading).

Whether BACE1 levels suffer or not an increase with the progression of age remains controversial. In the study performed by Kögel and colleagues using a human cell line, the authors obserevd and increase in the levels of this β-secretase with the progression of age (IMR-90, see Kögel et al., 2012), which is some way in accordance with our results. However, Fukumoto and colleagues did not observe significant changes in BACE1 levels with aging, but demonstrated an increase in the enzyme activity, suggesting that this secretase can suffer some post-translational modifications, involving allosteric modulation or even co-factor association (Fukumoto et al., 2004).

4.2.3. ADAM10 in synaptosomes and in total membranes

There are evidences suggesting a decrease in neuronal ADAM10 levels in both ageing and disease-affected brains. In addition to that, when comparing healthy and aged brains, the co-localization between ADAM10 and nardilysin (an enzyme's regulator) was also decreased, too (Endres and Fahrenholz, 2010).

The relative abundance of ADAM10 in both synaptosomes and total membranes from three different animals, in comparison to samples from three control younger mice, was assessed by quantitative Western Blot analysis. The immunoreactivity of each band was normalized with β-actin. In hippocampal synaptosomes, the ADAM10 immunoreactivity in the control group was 36.8% ± 13.7%, (n=3), while in the 9 months old group was 47.1% ± 26.5% (n=3). These results suggest a tendency to an increase in the levels of ADAM10 with the progression of age, in synaptic fractions. In hippocampal total membranes, the difference in ADAM10 abundance was a little more evident, although not statistically significant, than in synaptosomal fractions. In the control group, the ADAM10 immunoreactivity was 49.7% ± 23.8% (n=3), while, in the group of 9 months old mice, it was 73.3% ± 15.6% (n=3).

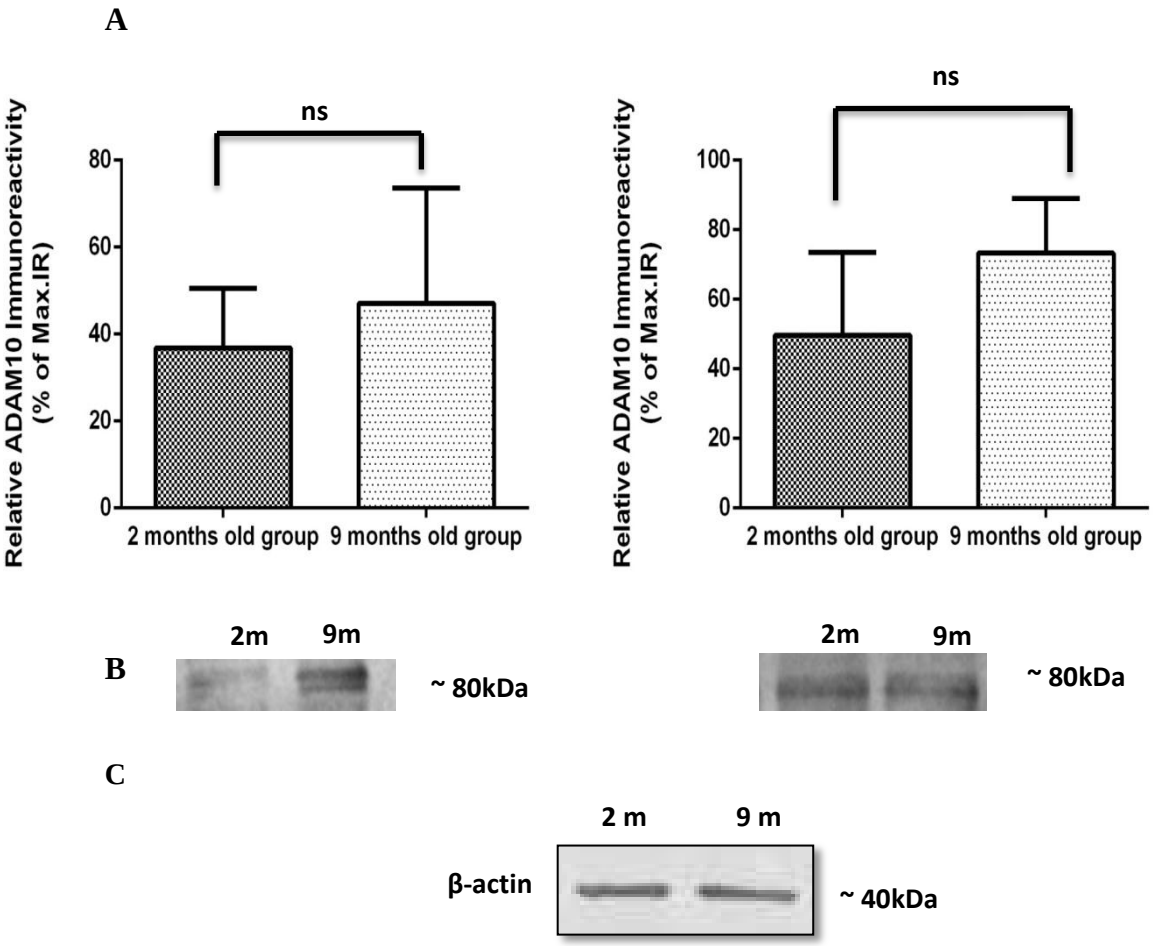

Figure 22. Hippocampal levels of ADAM10 in synaptosomes and in total membranes of 2 months old mice, in comparison to 9 months old mice. The graphic represents the percentage of immunoreactivity for 20 μg of loaded protein, which was calculated considering the maximal immunoreactivity value obtained as 100% for 40ug (an amount of loaded protein that was previously defined as close to saturating levels). The results are presented as mean ± SEM of 3 independent experiments. ns – non significant **(B)** Representative Western blot of the ADAM10 levels in the 2 months old group (2 m) and in the 9 months old group (9 m) of mice. **(C)** Representative Western blot of the β-actin density (control for protein loading).

These data are in accordance with a recent study, in which Kögel and colleagues showedthat this α-secretease did not exhibit an age-associated regulation in a human cell line (IMR-90, see Kögel et al., 2012).

4.3. Synaptic levels and distribution of APP and secretases in a transgenic AD mice model (3xTg-AD)

Transgenic mice models of AD provide the chance to better understand how the deposition of several pathology biomarkers is related to the progression of dementia in AD. Several animal models have been developed, characterized by at least one neuropathological change related to AD. The most common feature of these rodent models is the overexpression of mutated APP that inevitably leads to the overaccumulation of Aβ peptides and its subsequent deposition, forming amyloid plaques. Often a mutant PS1 allele is also included, in order to accelerate the deposition rate of Aβ, as well as to enhance the severity of the pathology (Oddo et al., 2003, Manaye et al., 2013; 3).

In our study, we used triple-transgenic models of AD (3xTg-AD) 15 months old, which have the advantage to express 3 dementia-related transgenes: APP_{SWE}, $PS1_{M146V}$ and tau_{P301L}, and are described to demonstrate an age-dependent onset of the pathology. This model offers also the possibility to study, in the same animal, both Aβ and tau-associated pathologies, which are hallmarks in the clinical expression of the disease (Oddo et al. 2003; Sterniczuk et al. 2010; Bories et al. 2012). The 3xTg-AD mice have been demonstrated to suffer an age-related increase in the levels of Aβ peptides (both soluble $Aβ_{40}$ and insoluble $Aβ_{42}$ forms), amyloid plaques and also of hyperphosphorilated tau protein, in regions such as the hippocampus and the frontal cortex (Oddo et al. 2003, Manaye et al. 2013).

.

In this part of our work, we used synaptosomes from the hippocampus of 3xTg-AD mice and from age-matched wild-type littermates, which were used as a control group. The samples obtained from the cortex were used for immunocytochemistry studies, while those obtained from the hippocampus were used for quantification of APP and secretases densities by Western blot.

4.3.1. APP and Secretases in synaptosomes

4.3.1.1. APP in synaptosomes

The relative abundance of APP in synaptosomes was compared in synaptosomes obtained from 3xTg-AD mice and control mice by Western blot analysis. The immunoreactivity of each band was normalized with β-actin.

The data obtained show that APP tends to be more abundant in the synaptic terminals of 3xTg-AD mice models (70.9% ± 15.2%, n=3) than in the control group (39.6% ± 4.9%, n=3), although the difference is not statistically significant. This is not surprising, since the gene encoding APP in the genome of the transgenic mice has a mutation (APP Swedish Mutation, $APP_{SWE,}$ also known as the Familial Alzheimer's Disease Genetic Mutation), that leads to an overexpression of APP in these animals (Stargardt et al., 2013).

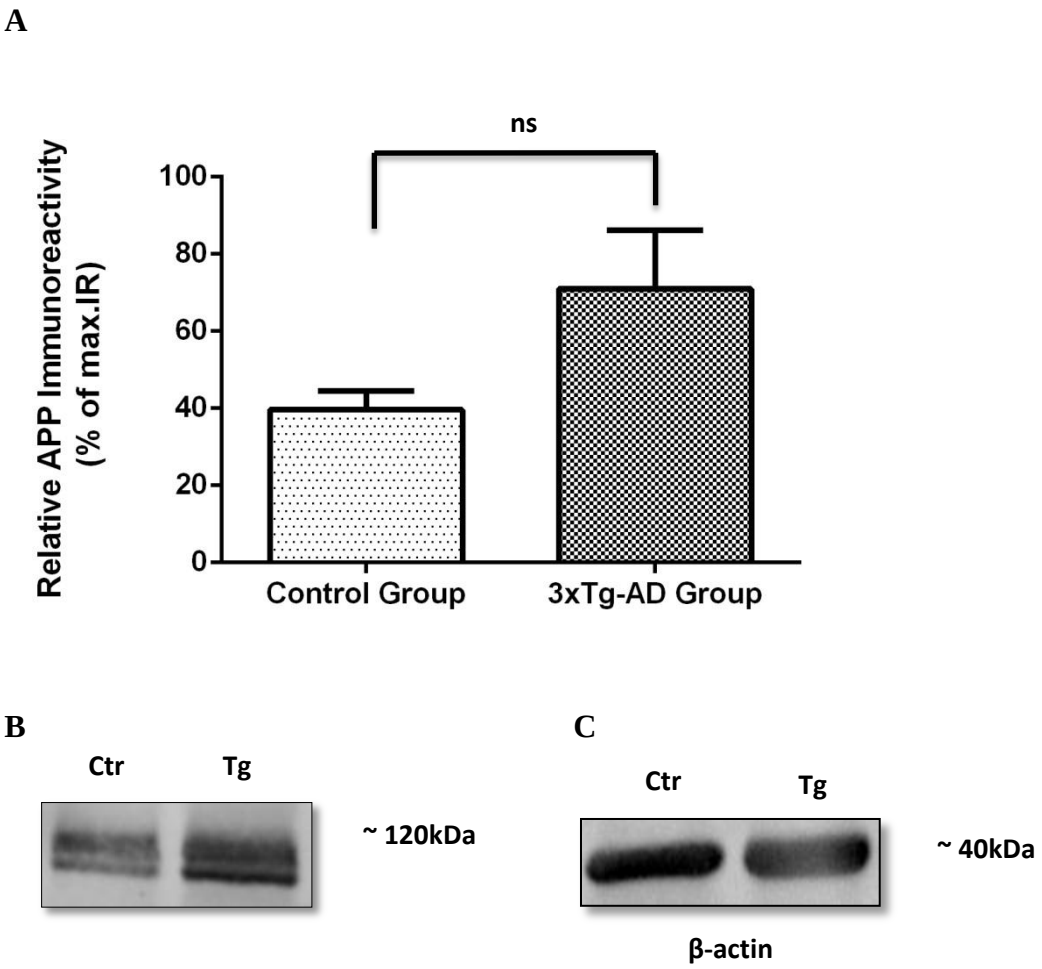

Figure 23. Hippocampal levels of APP in synaptosomes of 3xTg-AD mice in comparison to the control group. The graphic represents the percentage of immunoreactivity for 20 μg of loaded protein, which was calculated considering the maximal immunoreactivity value obtained as 100%. The results are presented as mean ± SEM of 3 independent experiments. **(B)** Representative Western blot of the APP levels in the control group (Ctr) and in the 3xTg-AD group (Tg) of mice. **(C)** Representative Western blot of the β-actin density (control for protein loading).

4.3.1.2.BACE1 in synaptosomes

The density of BACE1 was analyzed, by Western Blot, using hippocampi from both the control and the 3xTg-AD in the same gel. The antibody used recognized a well-defined band with an apparent molecular weight of approximately 70 kDa.

The data obtained show that there is no significant difference in the abundance of BACE1 in the synaptic terminals of 3xTg-AD mice (72.8% ± 13.8%, n=3) in comparison to the control mice group (68.0% ± 11.1%, n=3)

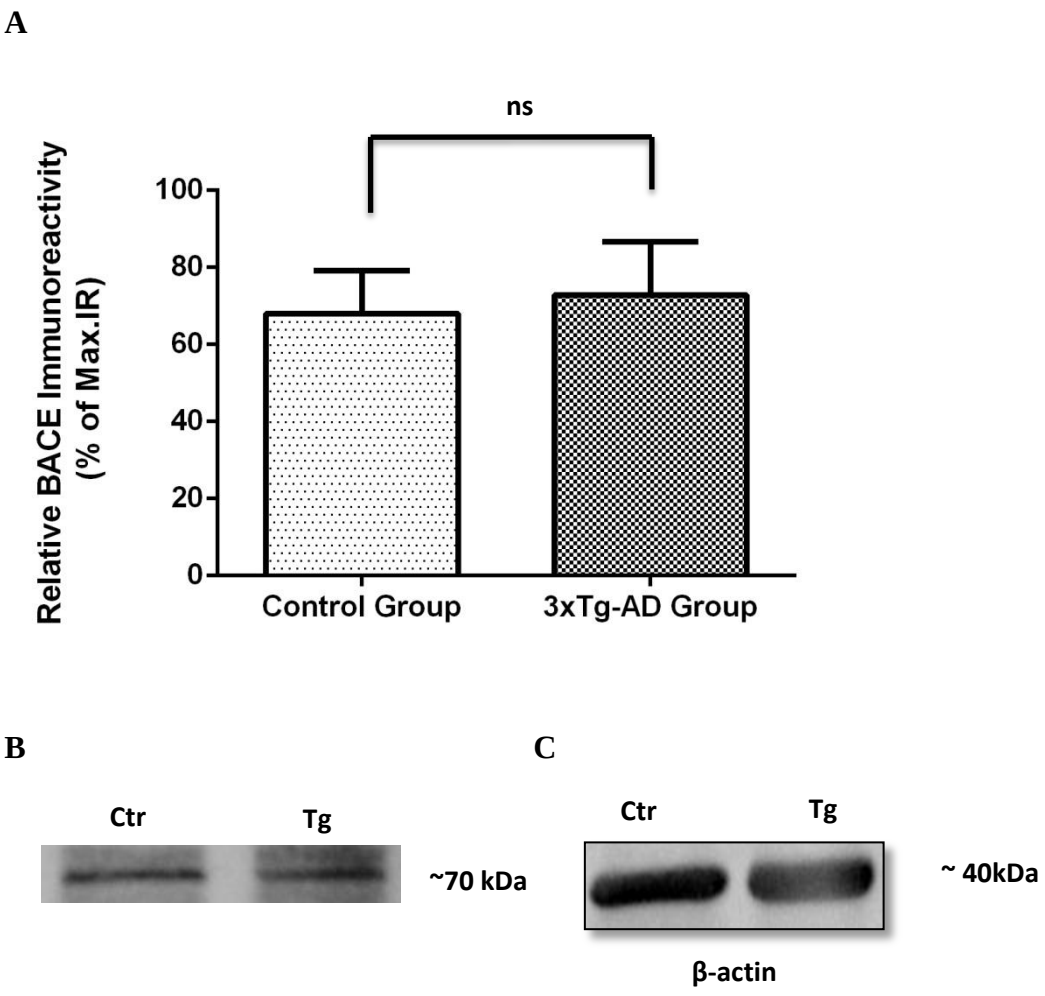

Figure 24. Hippocampal levels of BACE1 in synaptosomes of 3xTg-AD mice in comparison to a control group. The graphic represents the percentage of immunoreactivity for 20 µg of loaded protein, which was calculated considering the maximal immunoreactivity value obtained as 100%. The results are presented as mean ± SEM of 3 independent experiments. The statistical analysis was done using the unpaired t test (ns-non significant) **(B)** Representative Western blot of the BACE1 levels in the control group (Ctr) and in the 3xTg-AD group (Tg) of mice. **(C)** Representative Western blot of the β-actin density

In a recent study, it was shown that the levels of BACE1 increase in 3xTg-AD mice in an age-dependent manner, suggesting a functional role of BACE1 in Aβ overproduction in these AD animal models (Zhang et al., 2012). Others have also demonstrated that oxidative stress, which typically leads to metabolic dysfunction and apoptosis of neurons, is one of the main reasons for the elevated levels of BACE1 in cortical regions of AD mice models (Mouton-Liger et al., 2012).Our data did not reveal difference between BACE 1 densities in 3xTg-AD mice as compared with control animals (wild-type), however we did not check for the possible effects of age in BACE1levels.

The increase in BACE1 levels and activity was also reported in the brains of AD patients, particularly in the temporal cortex, which may be either a reaction to pathology or one of the causes in the sporadic form of AD (Holsinger et al., 2002; Marks and Berg, 2010). It has also been stated that the APP Swedish mutation, present in the AD models used for the study, makes BACE1-mediated cleavage more efficient, because enhances the expression of BACE1 (Wang et al., 2013).

4.3.1.3. ADAM10 in synaptosomes

The levels of ADAM10 in hippocampus of 3xTg-AD mice *versus* control mice were compared by Western blot analysis. The data obtained showed a significant ($p<0.01$) reduction on the levels of ADAM10 in the 3xTg-AD mice (22.83% ± 6.64%, n=3), in comparison to the control group (81.84% ± 9.15%, n=3).

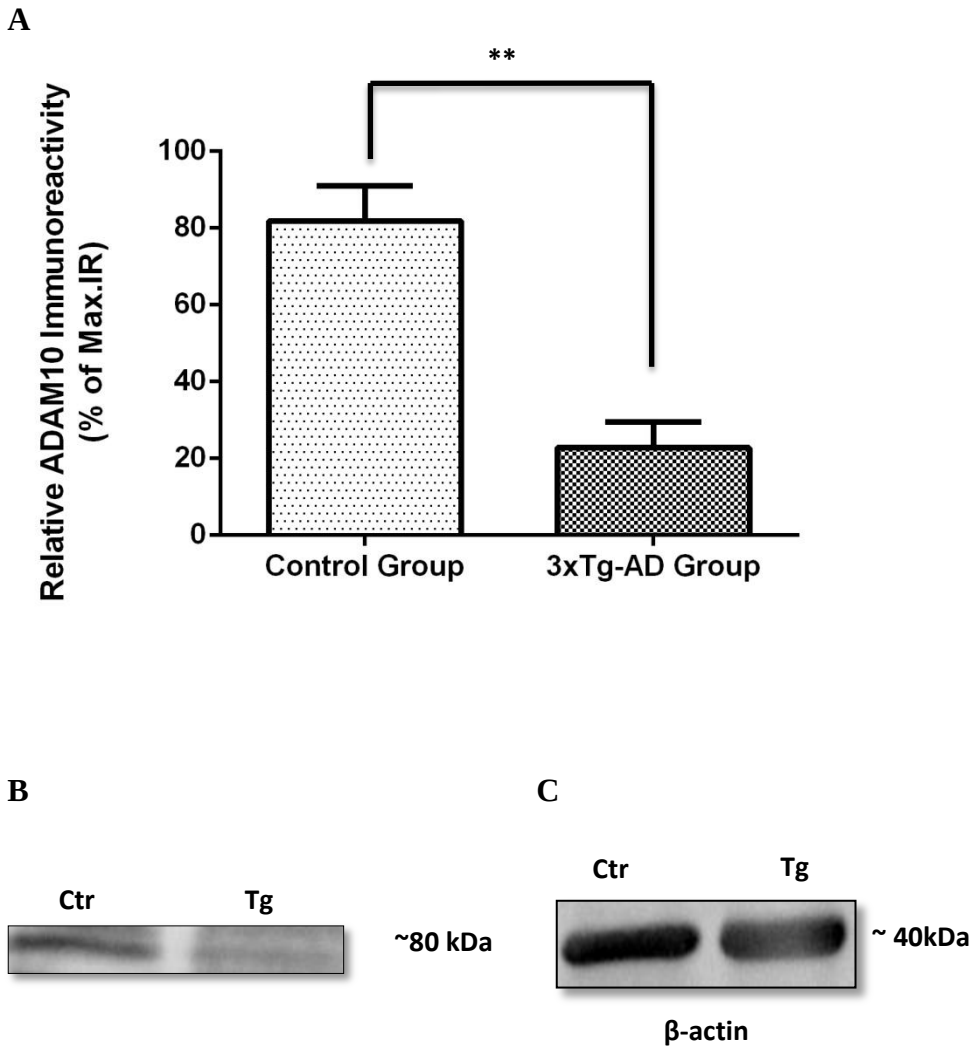

Figure 25. Hippocampal levels of ADAM10 in synaptosomes of 3xTg-AD mice in comparison to a control group. The graphic represents the percentage of immunoreactivity for 20 µg of loaded protein, which was calculated considering the maximal immunoreactivity value obtained as 100%. The results are presented as mean ± SEM of 3 independent experiments. The statistical analysis was done using the unpaired t test (** - $p<0.01$) **(B)** Representative Western blot of the ADAM10 levels in the control group (Ctr) and in the 3xTg-AD group (Tg) of mice. **(C)** Representative Western blot of the β-actin density (protein loading control)

Data from literature concerning ADAM10 expression in pathology-affected brains are controversial. Our data show a significant decrease in ADAM 10 density in the 3xTg-AD mice, as compared with control mice group. A recent study reported ADAM10 mRNA levels are increased in hippocampus of AD patients (Epis, et al, 2012), however this does not necessary implicates an increase in ADAM 10 protein levels.

4.3.2. Presence of APP and secretases in Glutamatergic and GABAergic nerve terminals of 3xTg-AD mice

In this part of the study we aimed to investigate if there was an AD pathology-dependent modification of the distribution of APP and secretases in different types of cortical nerve terminals. This was investigated the 3xTg-AD mice and age-matched (15 months old) wild-type mice (control animals).

First, the density of markers of different types of nerve terminals, namely vGLUT1 and vGAT, was evaluated in control and 3xTg-AD.

As illustrated in Figure 26, in the control group, in the general population of cortex nerve terminals (identified as synaptophysin-immunoreactive elements) we found that 85.5% ± 5.8% (n=3) were glutamatergic. A similar pattern can be observed in the group of transgenic mice, in which glutamatergic terminals represented 85.8% ± 1.8% (n=3) of the synaptophysin-immunopositive elements. Therefore, in 3xTg-AD mice there were not observed significant alterations in the density of glutamatergic terminals (vGLUT1-immunopositive), as compared with age-matched control mice.

A

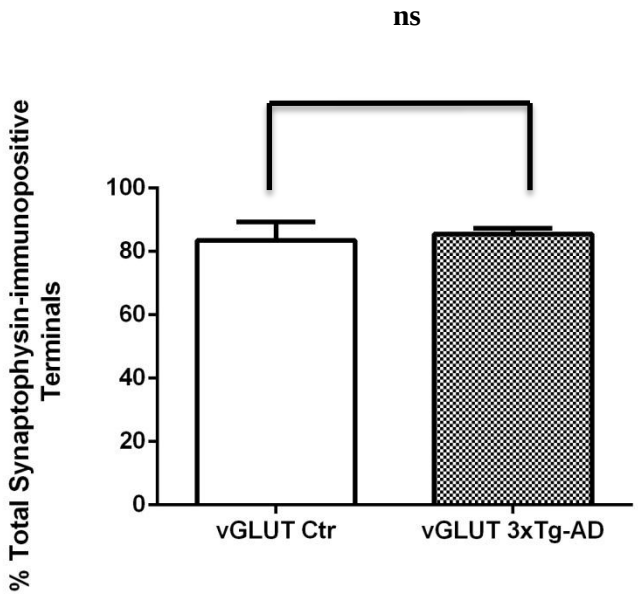

B

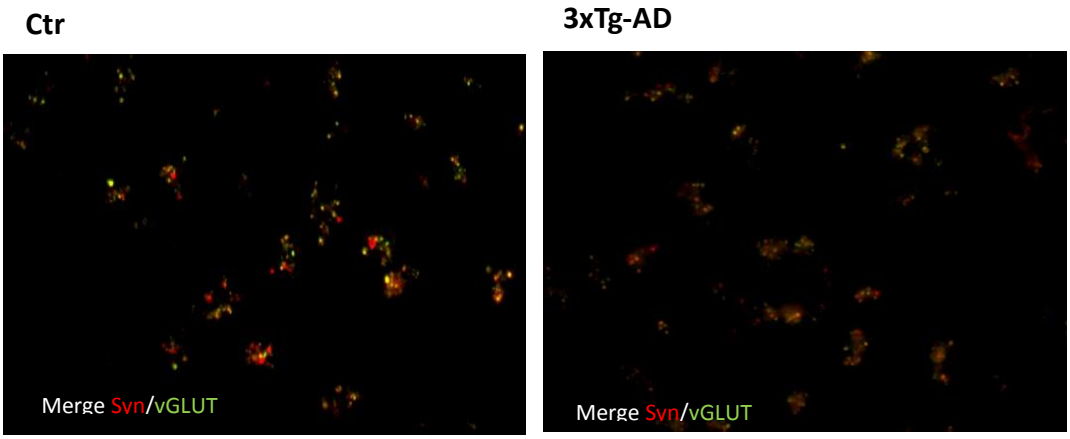

Figure 26. Relative glutamatergic nerve terminals abundance in the plated purified presynaptic nerve terminals of the control group in comparison to the 3xTg-AD group of mice. (A) The graphic represents the percentage of co-localization between markers of glutamatergic (vGLUT) nerve terminals and synaptophysin (Syn)-immunopositive elements. The total population was considered to be the overall number of synaptophysin-immunopositive elements. The results are presented as mean ± SEM of 3 independent experiments. ns – non significant. **(B)** Representative merge images of Synaptophysin-immunopositive elements (Syn, red) and the marker of glutamatergic (vGLUT, green) nerve terminals, in the control group and in the 3xTg-AD group of mice, The yellow labeling correspond to the co-localization between Syn and VGLUT positive elements. The magnification used to obtain the images was 630x.

This result was not expectable, as it has been described by many group, that the glutamatergic system is affected in AD. A decrease in the number of vGLUT1 has already been reported in AD models, as well as in post-mortem studies in AD patients (Masliah et al., 2000; Kirvell et al., 2006). However, others suggest that, similar to what happens with the cholinergic system, some studies suggest that there is an increase of glutamatergic synapses in patients with mild cognitive deficits, indicating a possible compensatory mechanism that becomes less notable with the progression of the disease (Revett et al., 2013). Results from our group also showed that in AD models, resulting from Aβ intracerebroventricular injection, there is loss of glutamatergic terminals, in parallel with memory dysfunction (Cunha et al., 2008). In fact, glutamatergic neurons seem to suffer significant damage in regions such as the hippocampus, the frontal, temporal and parietal cortex, which are severely affected during AD development However, in animal transgenic models of AD, during the early stages of the pathology, it was shown that the cortical glutamatergic and GABAergic terminals become upregulated, mainly the presynaptic bouton populations. This increase has also been reported in AD patients, where an elevation in the number of glutamatergic terminals was observed (for review see Bell et al., 2008).

It was next evaluated if the overall abundance of GABAergic terminals changed in association with AD pathology. In the control group, it was found that 16.8% ± 2.8% (n=3) of the general population of cortex nerve terminals were GABAergic. On the other hand, in the group of 3xTg-AD mice, the abundance of GABAergic terminals suffered a slight increase: 29.2% ± 6.6% (n=3) of synaptophysin immunopositive terminals were enriched in vGAT (Figure 27).

These data are somewhat in contrast with the findings showing that the GABAergic system suffers a significant decrease during normal aging in rat hippocampus (Vela et al., 2003), as well as in AD transgenic mice model (Bell and Cuello, 2006).

The discrepancies between our data , showing no significant alterations in the density of glutamatergic and GABAergic terminals in 3xTgAD mice model (as compared with control mice), and the literature data that in general reported a loss of nerve terminals, could be due to the methodology used to assess the density of nerve terminals. However, we are aware of the necessity of increase the number of animals tested and perform other type of assays to confirm these observations.

A

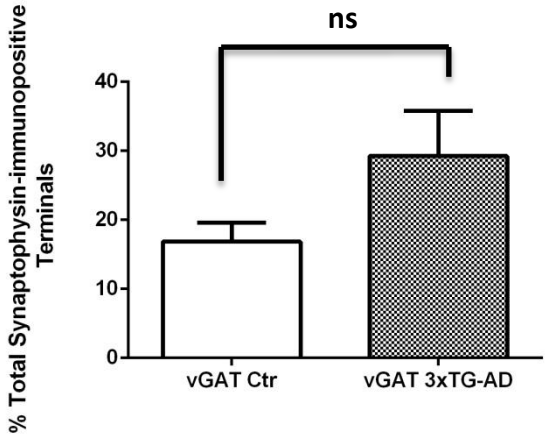

B

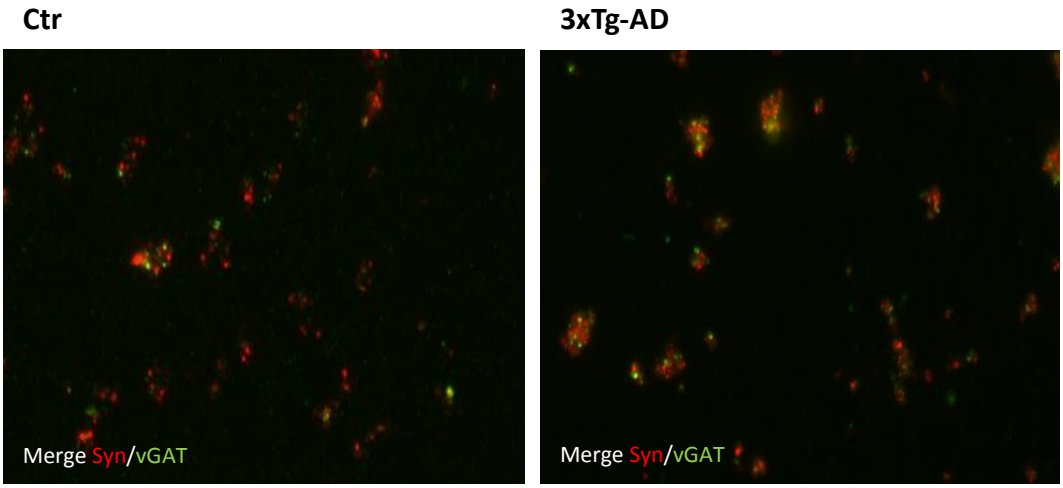

Figure 27. Relative GABAergic nerve terminals abundance in the plated purified presynaptic nerve terminals of the control group in comparison to the 3xTg-AD group of mice. (A) The graphic represents the percentage of co-localization between markers of glutamatergic (vGAT) nerve terminals and synaptophysin-immunopositive (Syn) elements. The total population was considered to be the overall number of synaptophysin-immunopositive elements. The results are presented as mean ± SEM of 3 independent experiments. ns – non significant. **(B)** Representative marge images of Synaptophysin (Syn, red)-immunopositive elements and the marker of GABAergic (vGAT, green) nerve terminals, in the control group and in the 3xTg-AD group of mice. Yellow labeling corresponds to a co-localization of synaptophysin- and vGAT-immunopositive elements. The magnification used to obtain the images was 630x.

The presence of APP in purified synaptosomes of both groups of animals was also assessed. In the whole population of nerve terminals of the control group, identified as synaptophysin-immunopositive elements, 18.3% ± 0.4% (n=3) were endowed with APP. In 3xTg-AD mice, APP-immunopositive terminals represented 37.1% ± 1.1% (n=3) of the general population of cortical nerve terminals. The data presented in Figure 28 show that, although there is an increase in the levels of APP in the 3xTg-AD mice, it is not as elevated as it would be expected.

A

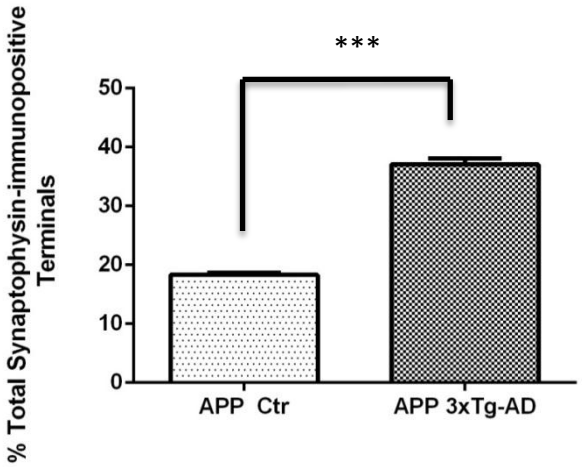

B

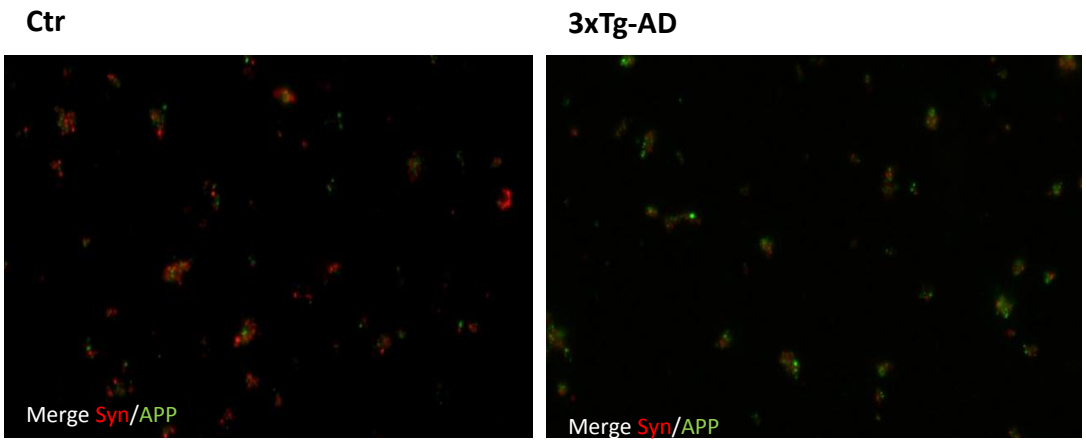

Figure 28. **APP is more abundant in the presynaptic nerve terminals of the 3xTg-AD group of mice. (A)** The graphic represents the percentage of co-localization between APP-immunopositive elements and synaptophysin-immunopositive elements. The total population was considered to be the overall number of synaptophysin-immunopositive elements. The results are presented as mean ± SEM of 3 independent experiments. *** - $p<0.001$. **(B)** Representative merge images obtained for Synaptophysin-immunopositive elements (Syn, red) and APP-immunopositive elements (APP, green), in the control group and in the 3xTg-AD group of mice. Yellow labeling corresponds to a co-localization of synaptophysin- and APP-immunopositive elements. The magnification used to obtain the images was 630x.

The results obtained in the quantification of APP, in synaptosomes, by Western Blot analysis, in the hippocampus of mice of both groups, did not show such evident increase in the levels of APP in 3xTg-AD mice as those obtained by immunocytochemistry analysis. This might be explained by the fact that the hippocampus seems to be the most affected brain region in AD (Wang et al., 2012). It is possible that, in this model, the cortex region was not as affected as the hippocampus by the progression of the pathology. Besides, in another model of AD overexpressing APP (Tg2576), it has been described that, the highest levels of total APP are detected at age of 90 days (Unger et al., 2005).

In order to determine whether the distribution of APP changed with the pathology in glutamatergic terminals, the co-localization of APP with vGLUT1 was also evaluated. As illustrated in Figure 29, in the control group, 23.1% ± 2.4% (n=3) of glutamatergic terminals were enriched with APP, while in the 3xTg-AD mice, 16.6% ± 2.1% (n=3) of the glutamatergic terminals co-localized with APP.

A

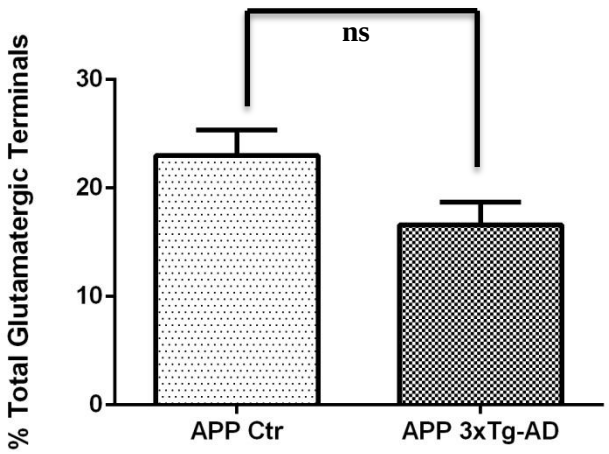

B

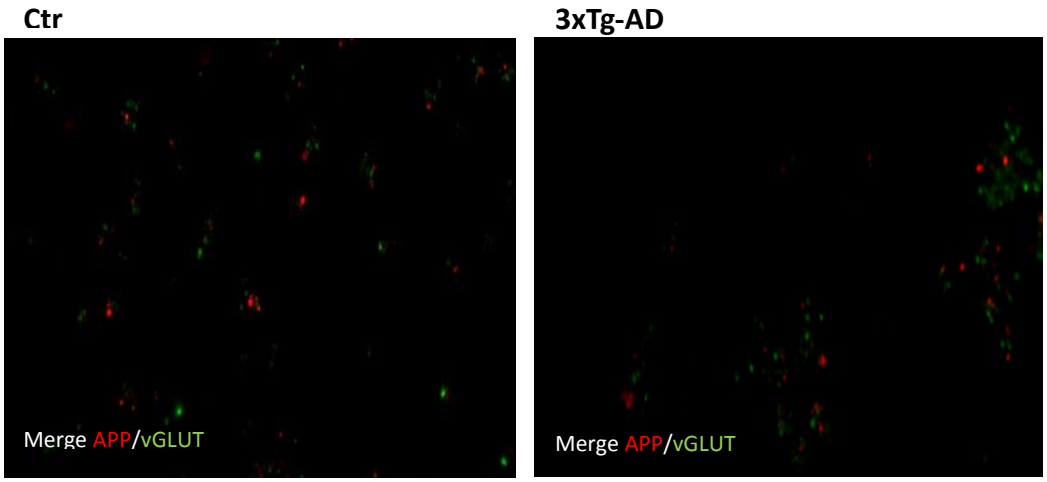

Figure 29. APP distribution in Glutamatergic presynaptic nerve terminals of the control group and of the 3xTg-AD mice. (A) The graphic represents the percentage of co-localization between the marker of Glutamatergic nerve terminals (vGLUT) and APP-immunopositive elements . The total population was considered to be the overall number of vGLUT-immunopositive elements. The results are presented as mean ± SEM of 3 independent experiments. ns – non-significant. **(B)** Representative merge images obtained for APP-immunopositive elements (APP, red) and the marker of glutamatergic (vGLUT, green) nerve terminals, in the control group and in the 3xTg-AD group of mice. Yellow labeling corresponds to a co-localization of APP- and vGLUT-immunopositive elements. The magnification used to obtain the images was 630x.

Then, the presence of BACE1 in nerve terminals in both 3xTg-AD and control mice groups was studied. As illustrated in Figure 30, in the control group, 71.2% ± 4.5% (n=3) of the synaptophysin immunopositive elements were endowed with BACE1 immunoreactivity, while, in the 3xTg-AD mice, 47.5% ± 7.6% (n=3) of the general population of nerve terminals co-localized with BACE1. This results is surprising, as it has already been described that, in AD brains, the levels of BACE1 are elevated approximately twofold in comparison to healthy ones, suggesting its involvement in the development of AD pathogenesis. In addition to that, it has also been reported that the APP Swedish mutation leads to an enhanced APP cleavage by BACE1 (Vassar et al., 2009).

A

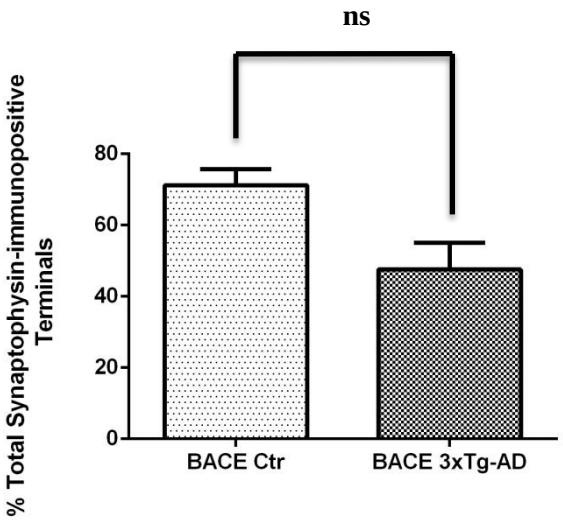

B

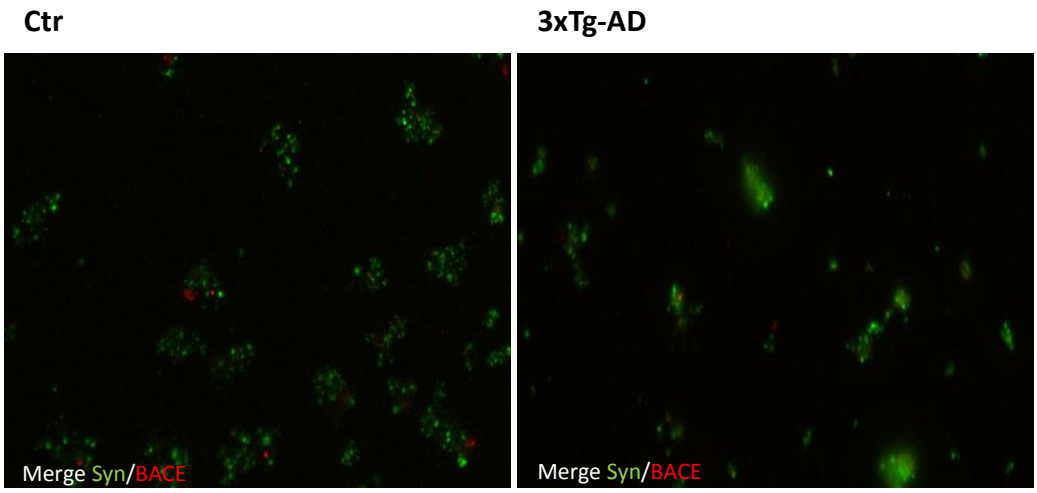

Figure 30. **Distribution of BACE1 in presynaptic nerve terminals of the control group and of the 3xTg-AD group of mice. (A)** The graphic represents the percentage of co-localization between BACE1-immunopositive elements and synaptophysin-immunopositive elements. The total population was considered to be the overall number of synaptophysin-immunopositive elements. The results are presented as mean ± SEM of 3 independent experiments. ns – non significant . **(B)** Representative merge images obtained for Synaptophysin-immunopositive elements (Syn, green) and BACE1-immunopositive elements (BACE, red), in the control group and in the 3xTg-AD group of mice. Yellow labeling corresponds to a co-localization of Syn- and BACE1-immunopositive elements. The magnification used to obtain the images was 630x.

It was also evaluated the relative abundance of ADAM10 in the nerve terminals of 3xTg-AD and control (wild-type) mice groups. As illustrated in Figure 31, in the control group, although it was not abundant, ADAM10 was more present than in the 3xTg-AD mice: in the overall population of nerve terminals, 6.9% ± 0.3% (n=3) were enriched in ADAM10. On the other hand, in the 3xTg-AD mice the presence of ADAM10 was almost inexistent: 0.3% ± 0.2% (n=3).

A

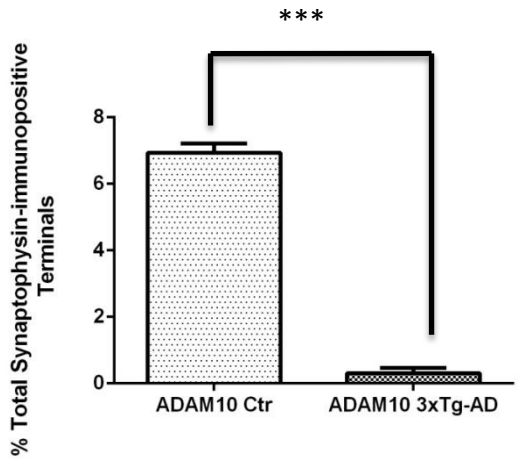

B

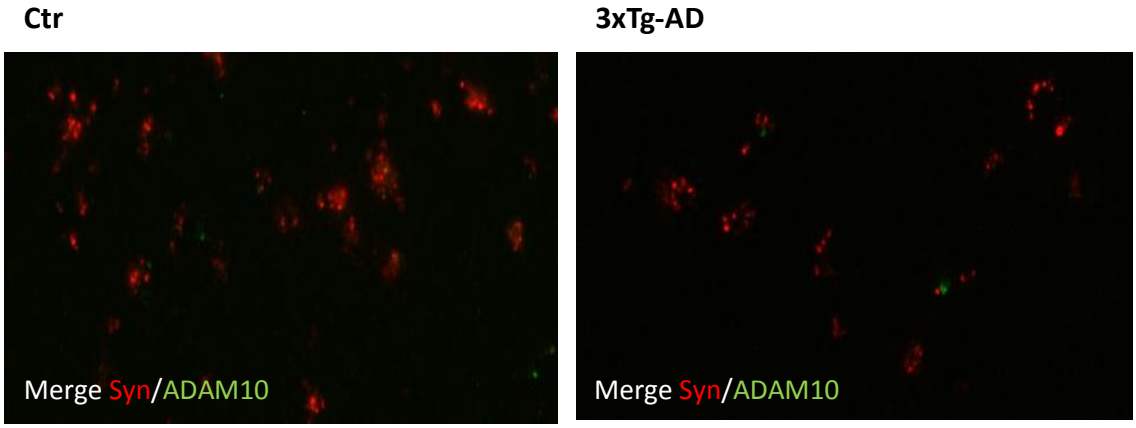

Figure 31. Distribution of ADAM10 in presynaptic nerve terminals of the control group and of the 3xTg-AD group of mice. (A) The graphic represents the percentage of co-localization between ADAM10-immunopositive elements and synaptophysin-immunopositive elements. The total population was considered to be the overall number of synaptophysin-immunopositive elements. The results are presented as mean ± SEM of 3 independent experiments. *** - $p<0.001$ **(B)** Representative merge images obtained for Synaptophysin-immunopositive elements (Syn) and ADAM10-immunopositive elements (ADAM10), in the control group and in the 3xTg-AD group of mice. Yellow labeling corresponds to a co-localization of Syn- and ADAM10-immunopositive elements. The magnification used to obtain the images was 630x.

These contrasting levels of BACE1 and ADAM10 in our preparations might be explained by the fact that these enzymes' activity is highly competitive. Hence, when APP cleavage by one of the secretases is augmented, the other is expected to be diminished (Bekris et al., 2011).

An alternative interpretation of data related to APP protelysis and its involvement in AD pathogenesis is the Presenilin hypothesis, according to which loss or altered PS1 function is suggested to be the causative factor to the onset of the disease (Shen and Kelleher, 2007). Guided by this idea, we decided to investigate the relative abundance of PS1. As it can be observed in Figure 32, the PS1 presence seems to suffer an increase in the 3xTg-AD mice. In the general population of synaptophysin immunopositive elements, in the control group, 0.9% ± 0.6% (n=3) were endowed with PS1, while in the 3xTg-AD mice the number of PS1 immunopositive terminals was higher: 1.7% ± 0.3% (n=3).

A

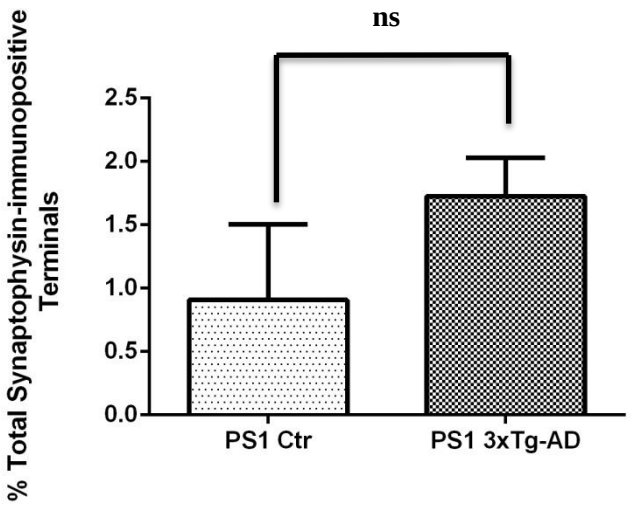

B

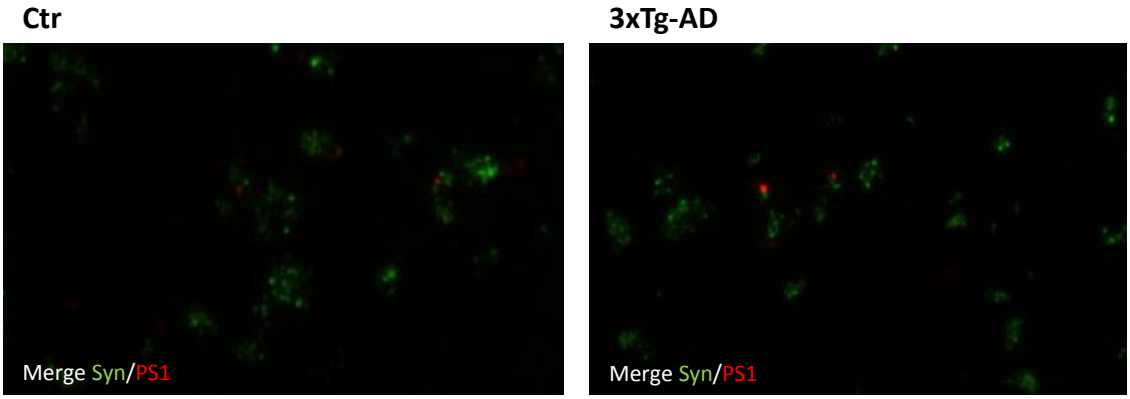

Figure 32. **Distribution of PS1 in presynaptic nerve terminals of the control group and of the 3xTg-AD group of mice. (A)** The graphic represents the percentage of co-localization between PS1-immunopositive elements and synaptophysin-immunopositive elements. The total population was considered to be the overall number of synaptophysin-immunopositive elements. The results are presented as mean ± SEM of 3 independent experiments. ns – non significant. **(B)** Representative merge images obtained for Synaptophysin-immunopositive elements (Syn) and PS1-immunopositive elements (PS1), in the control group and in the 3xTg-AD group of mice. Yellow labeling corresponds to a co-localization of Syn- and PS1-immunopositive elements. The magnification used to obtain the images was 630x.

4.3.3. Co-localization of APP with α- and β-secretases in nerve terminals of 3xTg-AD mice

It was further investigated if APP was co-localized with α-, β- and γ-secretases, in both the control (wild-type) and the 3xTg-AD mice groups.

In our preparations, as it can be observed in Figure 33, the preliminary results suggest a tendency towards a decrease in the co-localization of these proteins. In the control group, 49.5% (n=1) of APP-immunopositive elements were labeled with ADAM10, while in the 3xTg-AD mice group this value suffered a slight decrease: 33.8% (n=1).

A

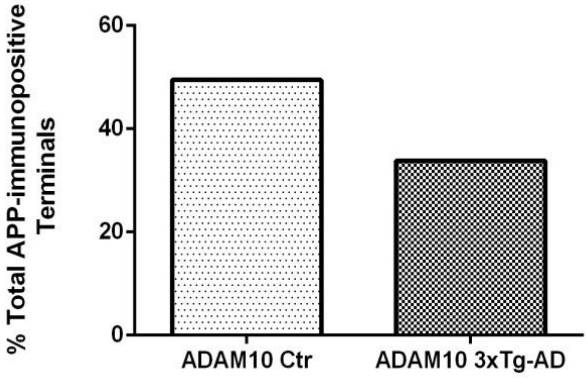

B

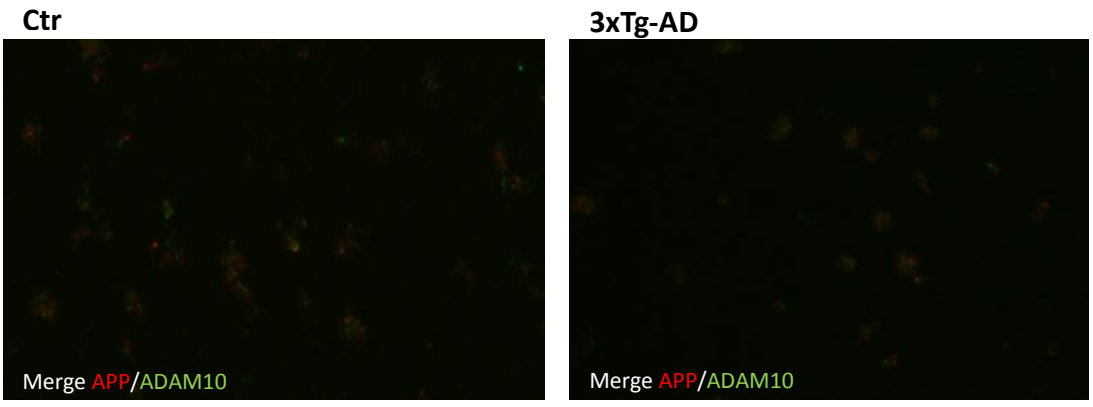

Figure 33. APP and ADAM10 co-localization in the control group and in the 3xTg-AD mice group of mice. Double immunocytochemistry analysis of APP and ADAM10 **(A.1.)** The graphic represents the percentage of co-localization between ADAM10-immunopositive elements and APP-immunopositive elements. The total population was considered to be the overall number of APP-immunopositive elements. **(B)** Representative merge images obtained for APP-immunopositive elements (APP) and ADAM10-immunopositive elements (ADAM10), in the control group and in the 3xTg-AD group of mice. Yellow labeling corresponds to a co-localization of APP- and ADAM10-immunopositive elements. The magnification used to obtain the images was 630x.

Some studies have demonstrated that ADAM10 and APP are co-expressed in human cortical neurons preparations, thereby suggesting that these two proteins are probably co-associated or co-localized (for review see Endres and Fahrenholz, 2010).

The co-immunolabeling of APP and BACE1 platted presynaptic nerve terminals of both control and 3xTg-AD mice was also evaluated. It was found that in the control group 24.9% ± 1.8% (n=3) of APP-immunopositive nerve terminals were also labeled with BACE1, while in the 3xTg-AD mice group this value was lower: 14.4% ± 0.2% (n=3).

A

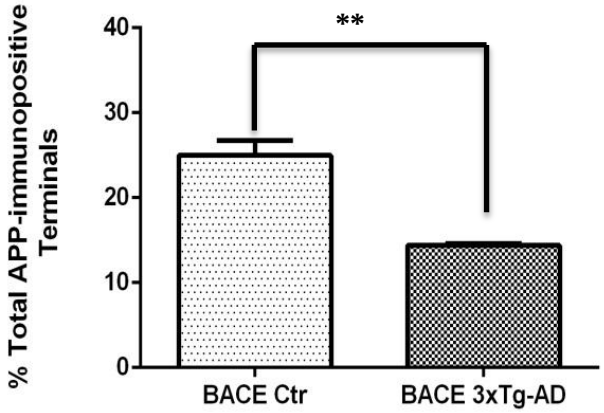

B

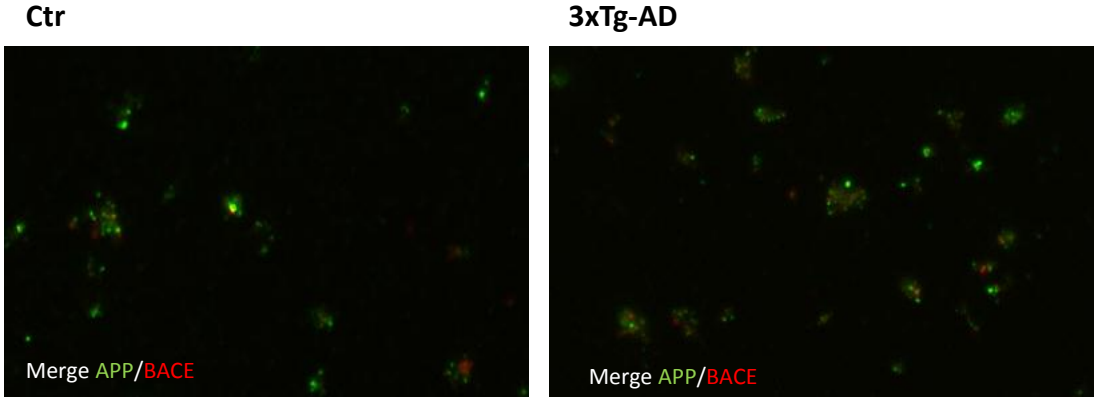

Figure 34. APP and BACE1 co-localization in the control group and in the 3xTg-AD mice group of mice. Double immunocytochemistry analysis of APP and BACE1. **(A)** The graphic represents the percentage of co-localization between BACE1-immunopositive elements and APP-immunopositive elements. The total population was considered to be the overall number of APP-immunopositive elements. The results are presented as mean ± SEM of 3 independent experiments. ** $p<0.01$. **(B)** Representative merge images obtained for APP-immunopositive elements (APP) and BACE1-immunopositive elements (BACE1) in the control group and in the 3xTg-AD group of mice. Yellow labeling corresponds to a co-localization of APP- and BACE1-immunopositive elements. The magnification used to obtain the images was 630x.

This result is somehow surprising, as an increase in BACE1 abundance in the AD model mice was expected, resulting from the increased Aβ deposits found in 3xTg-AD mice model (Oddo et al., 2003; Lefort et al., 2012).

4.4. Age-related changes in APP levels in human cortical brain (preliminary result)

Since the aging brain is generally associated with increased neuronal vulnerability and is, by far, the major risk factor for the development of AD (Schliebs and Arendt, 2011), in this part of the study we performed a comparative analysis of the APP levels present in human brain cortex of individuals with different ages. For this purpose, we used samples from different individuals who suffered a sporadic death (unknown causes) with 21, 41, 60 and 81 years old, in order to compare whether there is an age-related difference in the density of APP (preliminary study).

4.4.1. APP in Cortical Total Extracts

It is known that the Aβ sequence is different among the human and mouse APP sequence. In comparison to human APP, the mouse protein is poorly processed by BACE1, leading to the production of approximately three times lower amounts of Aβ peptides. This phenomenon may be explained by the fact that Aβ peptides seem to be less critical in mice than in humans, although it seems to have a physiological role in rodents (Priller et al., 2006).

As illustrated in Figure 35, in the Western blot performed, the anti-APP antibody used recognized a triple well-defined band with an apparent molecular weight of approximately 120-130 kDa. The immunoreactivity of each band was normalized with β-actin. The presence of more bands than those observable in mice can be explained by the fact that, in humans, APP maturation involves extensive post-translational modifications, like glycosylation, sulfation and phosphorylation (Claeysen et al., 2012).

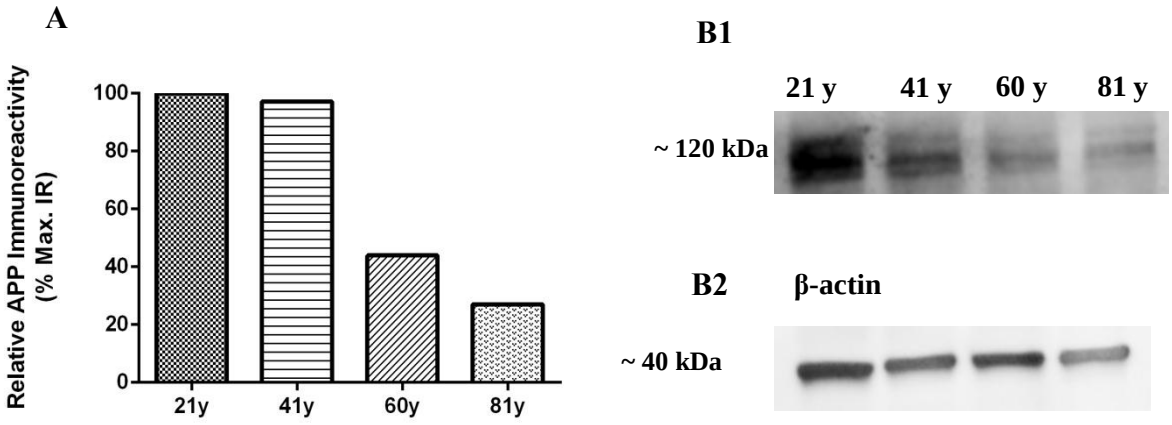

Figure 35. APP levels in total extracts of human cortical samples. The graphic bars (A) represent the percentage of APP immunoreactivity, considering the APP density observed in the 21 years old group as maximal. The immunoreactive APP bands (B1) were quantified and the data were normalized in relation to β-actin density (B2).

The observed results show a clear reduction of the levels of APP in human aged brains. Thus, it might be hypothesized that, in elderly individuals, the proteolysis rate of APP suffers an increase and the amyloidogenic pathway may be potentiated. In fact, it has been reported that during brain aging, the APP processing through the non-amyloidogenic pathway suffers a decrease, thereby enhancing the susceptibility of neurons to cellular stress and contributing to AD neurodegeneration (Kögel et al., 2012). Furthermore, it has also been suggested that there is a loss of physiological APP function , which may be one of the reasons for the reduction of neuronal plasticity and synaptic signaling, as well as enhanced susceptibility of neurons to cellular stress, common in elderly individuals. A downregulation in APP processing related with the ageing was also reported in a human cell line of aging (IMR-90, see Kögel et al., 2012).

5. CONCLUSIONS AND FINAL REMARKS

5.1. Conclusions

- By comparing the levels of APP and secretases in hippocampal synaptosomes (nerve terminals) and total membranes, it was found that APP, β- (BACE1), α- (ADAM10) and γ- (PS1) secretases are present in hippocampal nerve terminals , although they are not enriched in these fractions

- Using subsynaptic fractions of it was observed that APP is mainly located presynaptically. The α-secretase (ADAM10) is distributed pre- and extrasynaptically, whereas β-secretase (BACE1) is mainly present in the extrasynaptic fraction.

- APP is more abundant than secretases, ADAM10, BACE1 and PS1, in purified presynaptic nerve terminals. Both APP and BACE 1 are present in glutamatergic and GABAergic nerve terminals, BACE 1 are present in higher amounts in glutamatergic terminals than in GABAergic terminals

- APP and β-secretase are equally present in both glutamatergic and GABAergic nerve terminals

- APP and β-secretase (BACE1), which are responsible for the formation of Aβ, are co-located in 40% of the nerve terminals

- No significant differences were observed in the relative abundance of APP, α-secretase (ADAM10) and β-secretase (BACE1) in hippocampal nerve terminals of young adult mice (2-3 months old) as compare with adult mice (9 months old).

- In triple transgenic model of AD mice it was observed significant decrease in the ADAM 10 density in synaptosomes as compared with control (wild type) mice animals, but no significant changes were found in the levels of BACE1.

- In human cortical brain regions it seems that APP density decrease with the advance of age (preliminary data).

5.2. Final Remarks

The results presented in our work provide the first comparative analysis of the synaptic and subsynaptic distribution of APP and secretases in cortical brain regions of mice, mainly in hippocampus, as well as of the relative abundance of APP and secretases and their co-localization in glutamatergic and GABAergic presynaptic nerve terminals. Besides, we investigated if there are any age- or AD pathology -related changes in the distribution of these proteins.

However, there are some questions that remain unanswered. One of them is to know whether the distribution of APP and secretases is affected in cholinergic nerve terminals, since the cholinergic system is one of the most affected in AD. It should also be studied if APP and each of the secretases are co-localized in different types of nerve terminals. It would also be of great interest to investigate changes in the distribution and density of these proteins related with age and AD pathology in both humans and mice brain samples.

Nevertheless, our work might contribute to better understanding the reason why only particular synapses suffer intense degeneration at early stages of AD. This is of particular importance, since the information obtained by the experimental strategies proposed would allow a better definition of the molecular targets and neurochemical events that are responsible for synaptic dysfunction in early stages of AD. This will probably be a setting up point for future projects, involving the development of more effective and neuroprotective therapeutical approaches, able to stop the progression of the AD at early phases.

6. REFERENCES

Arendt, T. (2009) Synaptic degeneration in Alzheimer's disease. *Acta neuropathol,* **118:** 167-79.

Bekris, L. M., Galloway, N. M., Millard, S., Lockhart, D., Li, G., Galasko, D. R., Farlow, M. R., Yu, C.E. (2011). Amyloid precursor protein (APP) processing genes and cerebrospinal fluid APP cleavage product levels in Alzheimer's disease. *Neurobiol aging,* **32**

Bell, K.F.S. and Cuello, C. A. (2006) Altered synaptic function in Alzheimer's disease. *Eur J Pharmacol,* **545**: 11-21.

Bell, K.F.S., Zheng, L., Fahrenholz, F., Cuello, C. A. (2008) ADAM-10 over-expression increases cortical synaptogenesis. *Neurobiol Aging,* 29: 554-65.

Белоусов, Ю.Б., Зырянов, С.К., Белоусов, Д.Ю., Бекетов, А.С. (2009) Клинико-экономические аспекты терапии болезни Альцгеймера в России., *Качественная Клиничекая Практика*, **1**.

[Belousov, Yu.B., Zyrianov, S.K., Belousov, D.Yu., Beketov, A.S. (2009) Kliniko-economicheskie aspekty terapii bolezni Alcgeimera v Rossii, *Kachestvennaya Klinicheskaya Praktika,* **1]**[1]

Bories, C., Guitton, M. J., Julien, C., Tremblay, C., Vandal, M., Msaid, M., De Koninck, Y., Calon, F. (2012). Sex-dependent alterations in social behaviour and cortical synaptic activity coincide at different ages in a model of Alzheimer's disease. *PloS one*, **7**

Brunholz, S., Sisodia, S., Lorenzo, A., Deytss, C., Kins, S., Morfini, G. (2012) Axonal transport of APP and the spatial regulation of APP cleavage and function in neuronal cells. *Exp Brain Res,* **217:**353-364

Capell, A., Steiner, H., Willem, M., Kaiser, H., Meyer, C., Walter, J., Lammich, S., Multhaups, G., Haass, C. (2000) Maturation and pro-peptide Cleavage of β-secretase. *J Biol Chem,* **275:** 30849-54

Carroll, R., Lust M., Kim, K., Emmerling M. (1995). An Age-Relate Correlation Between Levels of b-Amyloid Precursor Protein and β-amyloid in Human Cerebrospinal Fluis. *Biochem and Biophys Res Commun,* **210:**345-349

Cay, Y., Zhang, X., Macklin, L., Cai, H., Luo, X., Oddo, S., LaFerla, F., Struble, F., Rose, G., Patrylo, P. (2012). BACE1 elevation is involved in amyloid plaque development in the triple transgenic model of Alzheimer's disease: Differential A-beta antibody labeling of early-onset axon terminal pathology. *Neurotox Res, 21*(2), 160–174. doi:10.1007/s12640-011-9256-9.BACE1

[1] Belousov, Yu.B., Zyrianov, S.K., Belousov, D.Yu., Beketov, A.S. (2009) Clinical and economical aspects of Alzheimer's Therapy in Russia, *Quality Clinical Practice*, **1** [Author's Translation]

Chow, V. W., Mattson, M. P. Wong, P C., Gleichmann, M. (2010). An Overview of APP processing enzymes and products. *Neuromolecular Med*, **12:**1–12.

Claeysen, S., Cochet, M., Donneger, R., Dumuis, A., Bockaert, J., Giannoni, P. (2012). Alzheimer culprits: cellular crossroads and interplay. *Cell Signal*, **24:**1831–40

Cleary, J.P., Walsh D. M., Hofmeister, J.J., Shankar, G.M., Kuskowski M.A., Selkoe D.J., Ashe K.H. (2005) Natural oligomers of the amyloid-β protein specifically disrupt cognitive function. *Nat Neurosci*, **8**:79–84

Cole, S. L. and Vassar, R. (2008) The Role of Amyloid Precursor Protein Processing by BACE1, the β-secretase, in Alzheimer´s Disease Pathophysiology. *J Biol Chem*, **283**: 29621-5

Coleman, P., Federoff, H., Kurlan, R. (2004) A focus on the synapse for neuroprotection in Alzheimer disease and other dementias. *Neurology*, **63:** 1155-62.

Crimins, J. L., Pooler, A., Polydoro, M., Luebke, J. I., Spires-Jones, T. L. (2013). The intersectionof amyloid beta and tau in glutamatergic synaptic dysfunction and collapse in Alzheimer's disease. *Ageing Res Rev*, 1–7

Cunha, R.A. (1998) On slices, synaptosomes and dissociated neurones to study *in vitro* ageing physiology. *Trends Neurosci*, **21:**286

Davis, S., & Laroche, S. (2003). What Can Rodent Models Tell Us About Cognitive Decline in Alzheimer's Disease? *Molecular Neurobiology*, *27*(3), 249–276.

Dunkley, P.R., Jarvie, P.E., Robinson, P.J. (2008) A rapid Percoll gradient procedure for preparation of synaptosomes. *Nature protocols*, **3**: 1718-28.

Endres, K. and Fahrenholz, F. (2010) Upregulation of the α-secretase ADAM10 - risk or reason for hope? *FEBS J*, **277:** 1585-96

Epis, R., Marcello, E., Gardoni, F., Di Luca, M. (2012). Alpha, beta-and gamma-secretases in Alzheimer's disease, *Front Biosci (Schol Ed)*, **42:**1–27

Evin, G., Barakat, A. and Masters, C. L. (2010) BACE: Therapeutic target and potential biomarker for Alzheimer's disease. *Int J Biochem Cell Biol*, **42:** 1923-6

Fraering, P. C. (2007) Structural and Functional Determinants of γ-Secretase , an Intramembrane Protease Implicated in Alzheimer ' s Disease. *Curr Genomics*, **8:** 531-549.

Frykman, S., Hur, J., Aoki, M., Winblad, B., Behbahani, H., Tjernberg, L. (2010) Synaptic and Endosomal Localization of Active γ-Secretase in Rat Brain. *PLoS One*, **5**

Fukumoto, H., Rosene, D. L., Moss, M. B., Raju, S., Hyman, B. T., Irizarry, M. C. (2004). Beta-secretase activity increases with aging in human, monkey, and mouse brain. *AmJ Pathol*, **164:**719–25.

Götz, J., Eckert, A., Matamales, M., Ittner, L. M. and Liu, X. (2011) Modes of Aβ toxicity in Alzheimer's disease. *Cell Mol Life Sci*, **68:** 3359-3375

Gralle, M. and Ferreira, S. T. (2007) Structure and functions of the human amyloid precursor protein: the whole is more than the sum of its parts. *Prog in Neurobiol*, **82:** 11-32

Groemer, T. W., Thiel, C. S., Holt, M., Riedel, D., Hua, Y., Hüve, J., Wilhelm, B. G., Klingauf, J. (2011). Amyloid precursor protein is trafficked and secreted via synaptic vesicles. *PloS One*, **6**

Hardy, J., and Higgins, G. (1992). Alzheimer's disease: the amyloid cascade hypothesis. *Science*, **256:**184–185

Hoe, H., Lee, H., Pak, D. (2012). The Upside of APP at Synapses, *CNS Neurosci Ther*, **18:** 47–56.

Holsinger D., McLean, C.A., Evin, G. (2002) Increased Expression of the Amyloid Precursor β-secretase in Alzheimer's Disease. *Ann Neurol*, **51:**783-786

Huang, Y. and Muche, L. (2012). Alzheimer Mechanisms and Therapeutic Strategies. *Cell*. **148:** 1204-1222

Hunter, S., and Brayne, C. (2012). Relationships between the amyloid precursor protein and its various proteolytic fragments and neuronal systems. *Alzheimers Res Ther*, **4:**10.

Kamenetz, F., Tomita, T., Hsieh, H., Seabrook, G., Borchelt, D., Iwatsubo, T., Sisodia, S., Malinow, R.. (2003). APP Processing and Synaptic Function, *Neuron*, **37**:925–937.

Karran, E., Mercken, M. and Strooper, B. D. (2011) The amyloid cascade hypothesis for Alzheimer's disease: an appraisal for the development of therapeutics. *Nature reviews. Drug discovery*, **10:** 698-712

Kedikian, G., Heredia, F., Salvador, V. R., Raimunda, D., Isoardi, N., Heredia, L., Lorenzo, A. (2010). Secreted amyloid precursor protein and holo-APP bind amyloid beta through distinct domains eliciting different toxic responses on hippocampal neurons. *J Neurosci Res*, **88:**1795–1803

Kim, T. W., Wu, K., Xu, J. L., McAuliffe, G., Tanzi, R. E., Wasco, W., Black, I. B. (1995). Selective localization of amyloid precursor-like protein 1 in the cerebral cortex postsynaptic density. *Brain Res Mol Brain Res*, **32:**36–44

Kirazov, E., Kirazov, L., Bigl, V., Schliebs, R. (2001). Ontogenetic changes in protein level of amyloid precursor protein (APP) in growth cones and synaptosomes from rat brain and prenatal expression pattern of APP mRNA isoforms in developing rat embryo. *Int J Dev Neurosci*, **19:**287–96.

Kirvell, S.L., Esiri, M., Francis, P. (2006) Down-regulation of vesicular glutamate transporters precedes cell loss and pathology in Alzheimer's disease. *J Neurochem.* **98:** 939-950

Kögel, D., Deller, T., Behl, C. (2012). Roles of amyloid precursor protein family members in neuroprotection, stress signaling and aging. *Exp Brain Res*, **217:**471–9

Laudon, H., Winblad, B. and Näslund, J. (2007) The Alzheimer's disease-associated γ-secretase complex: Functional domains in the presenilin 1 protein. *Physiol & Beha*, **92:**115-20

Lazarov, O., Morfini, G. a, Lee, E. B., Farah, M. H., Szodorai, A., DeBoer, S. R., Koliatsos, V. E., Kins, S., Lee, VM., Wong, PC., Price D.L., Brady, S.T., Sisodia, S.S. (2005). Axonal transport, amyloid precursor protein, kinesin-1, and the processing apparatus: revisited. *J Neurosci*, **25:**2386–95

Lefort, R., Pozueta, J., Shelanski, M. (2012) Cross-linking of Cell Surface APP Leads to Increased Aβ Production in Hippocampal Neurons: Implications for Alzheimer's Disease. *J Neurosci,* **32:**10674-10685

Lichtenthaler, S. F. (2011) Alpha-secretase in Alzheimer's disease: molecular identity, regulation and therapeutic potential. *J Neurochem*, **116:**10-21

Manaye, K. F., Mouton, P. R., Xu, G., Drew, A., Lei, D.-L., Sharma, Y., Rebeck, G. W., Turner, S. (2013). Age-related loss of noradrenergic neurons in the brains of triple transgenic mice. *Age*, **35:**139–47

Mangialasche, F., Solomon, A., Winblad, B., Mecocci, P. and Kivipelto, M. (2010) Alzheimer's disease: clinical trials and drug development. *Lancet Neurol*, **9:** 702-16

Marcello, E., Epis, R., Di Luca, M. (2008). Amyloid flirting with synaptic failure: towards a comprehensive view of Alzheimer's disease pathogenesis. *European journal of pharmacology*, *585*(1), 109–18. doi:10.1016/j.ejphar.2007.11.083

Marcello, E., Gardoni, F., Mauceri, D., Romorini, S., Jeromin, A., Epis, R., Borroni, B., et al. (2007). Synapse-associated protein-97 mediates alpha-secretase ADAM10 trafficking and promotes its activity. *J Neurosci*, **27:**1682–91.

Marcello, E., Saraceno, C., Musardo, S., Vara, H., Guzman, A., Fuente, D., Pelucchi, S., Di MAriono, D., Borroni, B., Tramontano, A., Pérez-Otano, I., Padovani, A., Giustetto, M., Gardoni, F., Di Luca, M. (2013). Endocytosis of synaptic ADAM10 in neuronal plasticity and Alzheimer's disease. *J Clin Invest*

Marks, N. and Berg, M. (2009) BACE and γ-secretase Characterization and Their Sorting as Therapeutic Targets to Reduce Amyloidogenesis. *Neurochem Res*, **35:**181-210

Masliah, E., Alford, M., Mallory, M., Rockenstein, E., Moechars, D., Leuven, F.. (2000) Abnormal Glutamate Tranport Function in Mutant Amyloid Precursor protein Transgenic Mice. *Exp Neurol*. **163:**381-386

McIntire, S.L., Reimer, R.J., Schuske, K., Edwards, R.H., Jorgensen, E.M. (1997) Identification and characterization of the vesicular BAGA transporter. *Nature,* **389:**870-6

Mouton-Liger, F., Paquet, C., Dumurgier, J., Bouras, C., Pradier, L., Gray, F., & Hugon, J. (2012). Oxidative stress increases BACE1 protein levels through activation of the PKR-eIF2α pathway. *Biochimica et biophysica acta*, *1822*(6), 885–96. doi:10.1016/j.bbadis.2012.01.009

Mustafiz, T., Portelius, E., Gustavsson, M. K., Hölttä, M., Zetterberg, H., Blennow, K., Nordberg, A., Lithner, C.U. (2011). Characterization of the brain β-amyloid isoform pattern at different ages of Tg2576 mice. *Neurodegener Dis*, **8:**352–63.

Nadezhdin, K.D., Bocharova O.V., Bocharov, E.V., Arseniev, A.S. (2011). Structural and Dynamic Study of the Transmembrane Domain of the Amyloid Precursor Protein. *Acta Naturae,* **8:**69-76

Nalivaeva, N., and Turner, A. J. (2013). The amyloid precursor protein: A biochemical enigma in brain development, function and disease. *FEBS Lett*

O'Brien, R.J. and Wong, P.C. (2011) Amyloid Precursor Protein Processing and Alzheimer's Disease. *Annu Rev Neurosci,* **34:**185-204

Obregon, D., Hou, H., Den, ***8***g, J., Giunta, B., Tian, J., Darlington, D., Shahaduzzaman, M., Tan, J. (2012). Soluble amyloid precursor protein-α modulates β-secretase activity and amyloid-β generation. *Nature Commun*, **3:**777.

Octave, J., Pierrot, N., Santos, S. F., Nalivaeva, N., Turner, A. (2013). From synaptic spines to nuclear signaling: nuclear and synaptic actions of the amyloid precursor protein. *J Neurochem,* 1-8

Oddo, S., Caccamo, A., Shepherd, J. D., Murphy, M. P., Golde, T. E., Kayed, R., Metherate, R., LaFerla, F.M. (2003). Triple-Transgenic Model of Alzheimer's Disease with Plaques and Tangles:Intracellular Aβ ᴺᴸ and Synaptic Dysfunction. *Neuron,* **39**:409–421.

Palop, J.J. and Mucke, L. (2010). Amyloid-β Induced Neuronal Dysfunction in Alzheimer's Disease : From Synapses toward Neural Networks. *Nat Neurosci* **13:**812–818.

Phillips, G. R., Huang, J. K., Wang, Y., Tanaka, H., Shapiro, L., Zhang, W., Shan, W. S., Arndt, K., Frank, M., Gordon, R.E., Gawinowicz, M.A., Zhao, Y., Colman, D.R. (2001). The presynaptic particle web: ultrastructure, composition, dissolution, and reconstitution. *Neuron*, **32:**63–77

Priller, C., Bauer, T., Mitteregger, G., Krebs, B., Kretzschmar, H. a, Herms, J. (2006). Synapse formation and function is modulated by the amyloid precursor protein. *J Neurosci,* **26:**7212–7221

Prox, J., Rittger, A., Saftig, P. (2012). Physiological functions of the amyloid precursor protein secretases ADAM10, BACE1, and presenilin. *Exp Brain Res*, **217**:331–41.

Rebola, N.,Canas, P.M., Oliveira, C.R., Cunha, R.A. (2005) Different synaptic and subsynaptic localization of adenosine A2A receptors in the hippocampus and striatum of the rat. *Neuroscience*, **132**:893-903.

Reddy, P.H., Manczak, M., Mao, P., Calkins, M.J., Reddy, A.P., Schirendeb, U. (2010) Amyloid-beta and mitochondria in aging and Alzheimer's disease: implications for synaptic damage and cognitive decline. *J Alzheimers Dis*, **20:**499-512

Reiss, K., Maretzky, T., Ludwig, A., Tousseyn, T., De Strooper, B., Hartmann, D., Saftig, P. (2005). ADAM10 cleavage of N-cadherin and regulation of cell-cell adhesion and beta-catenin nuclear signalling. *EMBO J*, **24:**742–752.

Revett, T. J., Baker, G. B., Jhamandas, J., Kar, S. (2013). Glutamate system, amyloid ß peptides and tau protein: functional interrelationships and relevance to Alzheimer disease pathology. *J Psychiatry Neurosci*, **38**:6–23

Ribaut-Barassin, C., Moussaoui, S., Brugg, B., Haerberle, A., uber, G., Imperato, A., Delhaye-Bouchaud, N., Mariani, J., Bailly, Y. (2000) Hemisynaptic Distribution Patterns of Presenilins and β-APP isoforms in the Rodent Cerebellum and Hippocampus. *Synapse*, **35:**96-110

Rodrigues, R.J., Alfaro, T.M., Rebola, N., Oliveira, C.R., Cunha, R.A. (2005) Co-localization and functional interaction between adenosine A(2A) and metabotropic group 5 receptors in glutamatergic nerve terminals of the rat striatum. *J Neurochem*, **92:** 433-41.

Sahara, N., Yahagi, Y., Takagi, H., Kondo, T., Okochi, M., Usami, M., Shirasawa, T., Mori, H. (1996) Identification and characterization of presenilin I-467, I-463 and I-374. *FEBS Lett*, **38:**7-11

Sandbrink, R., Monning, U., Masters, C., Beyreuther, K. (1997). Expression of the APP Gene Family in Brain Cells, Brain Development and Aging. *Gerontology*, *43*, 119–131.

Schliebs, R., and Arendt, T. (2011). The cholinergic system in aging and neuronal degeneration. *Behav Brain Res*, **221:**555–63

Walsh, D.M., Klyubin I., Fadeeva, J.V., Cullen, W., K., Anwyl, R., Wolfe, M.S., Rowan, M.J., Selkoe, D.J. (2002) Naturally secreted oligomers of amyloid β protein potently inhibit hippocampal long-term potetiation *in vivo*. *Nature*, **416:**535-9

Shen, J., and Keller. (2007). The presenilin hypothesis of Alzheimer ' s disease : Evidence for a loss-of-function pathogenic mechanism, **104:**403–409.

Smolarkiewicz, M., Skrzypczak, T., Wojtaszek, P. (2013). The very many faces of presenilins and the γ-secretase complex. *Protoplasma*.

Stargardt, A., Gillis, J., Kamphuis, W., Wiemhoefer, A., Kooijman, L., Raspe, M., Benckhuijsen, W., Reits, E. (2013). Reduced Amyloid β degradation in early Alzheimer's disease but not in the APPswePS1dE9 and 3xTg-AD mouse models. *Aging cell,* **12**

Sterniczuk, R., Antle, M. C., Laferla, F. M., Dyck, R. H. (2010). Characterization of the 3xTg-AD mouse model of Alzheimer's disease: part 2. Behavioral and cognitive changes. *Brain Res,* **1348:**149–55

Stockley, J. H., and O'Neill, C. (2007). The proteins BACE1 and BACE2 and beta-secretase activity in normal and Alzheimer's disease brain. *Biochem Soc Trans*, **35:** 574–6

Tabaton, M. and Tamagno, E. (2007) The molecular link between β- and γ-secretase activity on the amyloid beta precursor protein. *Cell Mol Life Sci,* **64:**2211-8

Takamori, S., Rhee, J. Rosenmund, C., Jahn, R. (2000) Identification of a vesicular glutamate transporter that defines a glutamatergic phenotype in neurons. *Nature,* **407:** 189-194

Tan, J. and Evin, G. (2011) BACE1 Trafficking and Alzheimer's Disease Pathogenesis. *J Neurochem*, **61**

Thinakaran, G., and Koo, E. H. (2008) Amyloid precursor protein trafficking, processing, and function. *J Biol Chem*, **283:** 29615-9

Turner, P. R., O'Connor, K., Tate, W. P., and Abraham, W. C. (2003) Roles of amyloid precursor protein and its fragments in regulating neural activity, plasticity and memory. *Prog Neurobiol*, **70:**1-32

Unger, C., Hedberg, M. M., Mustafiz, T., Svedberg, M. M., Nordberg, A. (2005). Early changes in Abeta levels in the brain of APPswe transgenic mice--implication on synaptic density, alpha7 neuronal nicotinic acetylcholine- and N-methyl-D-aspartate receptor levels. *Moll Cell Neurosci*, **30:**218–27.

Vassar, R. (1999). Beta-Secretase Cleavage of Alzheimer's Amyloid Precursor Protein by the Transmembrane Aspartic Protease BACE. *Science*, **286:**735–741.

Vassar, R. (2004) BACE1:The β-Secretase Enzyme in Alzheimer's Disease. *J Molr Neurosci,* **23:**105-113.

Vassar, Robert, Kovacs, D. M., Yan, R., & Wong, P. C. (2009). The beta-secretase enzyme BACE in health and Alzheimer's disease: regulation, cell biology, function, and therapeutic potential. *J Neurosci.* **29:**12787–94.

Vela, J., Gutierrez, A., Vitorica, J., & Ruano, D. (2003). Rat hippocampal GABAergic molecular markers are differentially affected by ageing. *J Neurochem*, **85:**368–377

Vingtdeux, V., and Marambaud, P. (2012). Identification and biology of α-secretase. *J Neurochem,* **120**:34–45

Wang, H., Li, R., Shen, Y. (2013). β-Secretase: its biology as a therapeutic target in diseases. *Trends Pharmacol Sci*, **34:**215–225.

Wang, H, Megill, A., He, K., Kirkwood, A., Lee, H.K. (2012). Consequences of inhibiting amyloid precursor protein processing enzymes on synaptic function and plasticity. *Neural Plast*, 1-24

Wang, P., Yang, G., Mosier, D. R., Chang, P., Zaidi, T., Gong, Y.-D., Zhao, N.-M., Dominguez, B., Lee, K., Gan, W., Zheng, H. (2005). Defective Neuromuscular Synapses in Mice Lacking Amyloid Precursor Protein (APP) and APP-Like protein 2. *J Neurosci*, **25:**1219–25.

Wimo, A., Jonsson, L., Bond, J., Prince, M., Winblad, B. (2013) The worldwide economic impact of dementia 2010. *Alzheimers Dement*, **9:** 1-11

Yang, L., Wang Z., Wang, B., Justice, N., Zheng, H. (2010). Amyloid Precursor Protein Regulates Cav 1.2 L-type Calcium Channel Levels and Function to Influence GABAergic Short-term Plasticity. *J Neurosci*, **29:** 15660–15668.

[Yaxno, N. N. and Preobrazhenskaya, I.S. (2006) Bolezn' Alcgeimera: klinika, patogenez, lechenie, *Russkij Medicinskij Zhurnal.* **641**] [2]

Яхно Н.Н., и Преображенская И.С. (2006) Болезнь Альцгеймера: клиника, патогенез, лечение. *Русский медицинский журнал*, **641**

Zhang, Y., Thompson, R., Zhang, H. Xu, H. (2011) APP processing in Alzheimer's disease. *Mol brain*, **4:**3

Zheng, H. and Koo, E. H. (2011) Biology and pathophysiology of the amyloid precursor protein. *Molecular Neurodeg*, **6:** 27

[2] Yaxno, N.N. and Preobrazhenskaya, I.S. (2006) Alzheimer's Disease: clinical, pathogenesis, treatment. *Russian Medicinal Journal,* **641** [Author's Translation]